



Carbon-modified plastic materials for food packaging

Dissertation Thesis

Study programme: P2301 Mechanical Engineering

Study branch: Materials engineering

Author: **mgr inž Michal Szczypinski**

Thesis Supervisor: prof. RNDr. Stanislav Mitura, DrSc.
Department of Material Science



Declaration

I hereby certify, I, myself, have written my dissertation as an original and primary work using the literature listed below and consulting it with my thesis supervisor and my thesis counsellor.

I acknowledge that my bachelor dissertation is fully governed by Act No. 121/2000 Coll., the Copyright Act, in particular Article 60 – School Work.

I acknowledge that the Technical University of Liberec does not infringe my copyrights by using my dissertation for internal purposes of the Technical University of Liberec.

I am aware of my obligation to inform the Technical University of Liberec on having used or granted license to use the results of my dissertation; in such a case the Technical University of Liberec may require reimbursement of the costs incurred for creating the result up to their actual amount.

At the same time, I honestly declare that the text of the printed version of my dissertation is identical with the text of the electronic version uploaded into the IS/STAG.

I acknowledge that the Technical University of Liberec will make my dissertation public in accordance with paragraph 47b of Act No. 111/1998 Coll., on Higher Education Institutions and on Amendment to Other Acts (the Higher Education Act), as amended.

I am aware of the consequences which may under the Higher Education Act result from a breach of this declaration.

January 24, 2021

mgr inž Michal Szczypinski

Acknowledgment

I would like to thank the following people who have helped me undertake this research and contributed to this work:

My supervisor prof. Stanisław Mitura, for his enthusiasm for the research, encouragement and tremendous patience. For watching over my doctorate throughout my studies, for insightful comments and valuable tips. For all interesting scientific discussions and disputes. I am eternally grateful for introducing me to the world of nanoscience and to familiarize with the academic community from all over the world.

The head of the Department of Material Science prof. Petr Louda, for his consistent support, for the possibility of conducting research in the department, for involving me in many interesting projects and for the assistance in matters related to my stay and work in the foreign country – Czech Republic.

My colleagues dr. Totka Bakalová and dr. Lukáš Voleský for their wonderful collaboration. For irreplaceable help in conducting experiments, analyzing the results and creative approach in finding solutions to problems. For devoting their time to me.

My parents, who always encouraged me to work and always believed in me.

Michał Marek Szczypiński

Anotace

Téma: Uhlíkové modifikace polymerních materiálů pro balení potravin

Abstrakt: Práce se zaměřuje na vývoj nanodiamantových/polymerních povlaků na plastových obalových fóliích s antioxidačním účinkem, který inhibuje žluknutí tuků. Teoretická část se zabývá aspekty povrchového inženýrství týkající se filmotvorných materiálů, stabilitou koloidních suspenzí, smáčivostí povrchů a jejich adhezí. Dále se věnuje vlastnostmi nanodiamantů a tribologií polymerních filmů. Experimentální část zahrnuje aktivaci povrchu polymerních fólií plazmovou technologií ke zlepšení adheze, přípravu suspenzí tvořících film, modifikací plastových fólií antioxidačními vrstvami a odléváním suspenzí na jejich povrch, mikroskopická analýza získaných povlaků a vyhodnocení jejich tribologických a antioxidačních vlastností. Vytváření řízeného rancidifikačního lněného oleje na filmu potaženém vyvinutými nanodiamantovými/polymerními povlaky potvrdilo jejich vysokou účinnost.

Klíčová slova: nanodiamant, balení potravin, povrchová aktivace, antioxidační povlak, tribologické vlastnosti polymerních povlaků

Annotation

Topic: Carbon-modified plastic materials for food packaging

Abstract: The work focuses on the development of nanodiamond/polymer coatings on plastic packaging films with an antioxidant effect that inhibits the rancidity of fats. The theoretical part deals with aspects of surface science related with film-forming materials, colloidal suspensions stability, surface wettability and adhesion. In addition, it also covers topics such as nanodiamond properties and plastic films tribology. The experimental part involves the plastic films surface activation with plasma technology to improve adhesion, preparation of film-forming suspensions, coating plastic films with antioxidant layers by casting suspensions on their surface, microscopic analysis of the obtained coatings and evaluation of their tribological and antioxidant properties. Conducting a controlled rancidification linseed oil spread on the film coated with the developed nanodiamond/polymer coatings confirmed their high efficiency.

Key words: nanodiamond, food packaging, surface activation, antioxidant coating, tribological properties of polymer coatings

Table of Contents

List of abbreviations, signs and symbols.....	7
1 Introduction.....	8
2 Objectives of dissertation.....	9
3 Theoretical part.....	10
3.1 Colloid and Surface Chemistry.....	10
3.1.1 Terminology.....	10
3.1.2 Stability of dispersion systems.....	11
3.1.3 <i>Film-forming materials</i>	16
3.1.4 <i>Wettability</i>	17
3.1.5 Surface treatment.....	19
3.2 Properties of functionalized nanodiamond.....	20
3.2.1 Nanodiamond surface functionalization.....	20
3.2.2 Nanodiamond aqueous suspensions.....	22
3.2.3 Nanodiamond–polymer composites.....	23
3.2.4 Antioxidant behaviour of nanodiamond.....	24
3.3 Tribology of packaging films.....	26
3.3.1 Coefficient of friction.....	26
3.3.2 Adhesion aspect.....	26
4 Experimental part.....	28
4.1 Used materials.....	28
4.1.1 Plastic substrate.....	28
4.1.2 Polymer matrix.....	30
4.1.3 Nanodiamond particles (ND).....	32
4.1.4 Lewis acid catalyst.....	33
4.2 Preparation of test samples.....	33
4.2.1 Film-forming suspension preparation.....	34
4.2.2 Substrate surface activation by plasma treatment.....	36
4.2.3 Suspension casting.....	37
4.2.4 Incorporation of NDP to polymer matrix via chemical bonding.....	37
4.3 Characterization of suspensions containing NDP.....	39
4.3.1 pH and suspensions stability.....	39
4.3.2 Surface tension.....	42
4.4 Characterization of PVA/NDP and PAA/NDP composite films.....	45
4.4.1 Infrared spectral analysis of samples subjected to esterification.....	45
4.4.2 Surface <i>morphology</i>	56
4.5 Characterization of coated plastics.....	60
4.5.1 Free surface energy and wettability of plastic substrate.....	60
4.5.2 Films adhesion.....	65
4.5.3 Coefficient of friction.....	67
4.5.4 Antioxidant properties.....	69
5 Summary and conclusion.....	76
References.....	80
List of Figures.....	85
List of Tables.....	87

List of abbreviations, signs and symbols

AC	Alternating Current
AFM	Atomic Force Microscopy
AM	Amplitude Modulated
ATR	Attenuated Total Reflectance
c	Concentration
CoF	Coefficient of Friction
COOH	Carboxyl group (carboxylic group)
CVD	Chemical Vapour Deposition
DSC	Differential Scanning Calorimetry
EDL	Electrical Double Layer
EN	European Standard
FSE	Free Surface Energy
FTIR	Fourier-Transform Infrared Spectroscopy
IR	Infrared
ISO	International Organization for Standardization
IUPAC	International Union of Pure and Applied Chemistry
L_c	Critical Load
LDPE	Low-Density Polyethylene
m	Mass
M	Molecular mass
ND	Nanodiamond
ND-N	Carboxylated nanodiamond with negative Zeta potential
ND-P	Hydroxylated nanodiamond with positive Zeta potential
OH	Hydroxyl group (hydroxylic group)
OWRK	Owens, Wendt, Rabel and Kaelble (OWRK)
PAA	Poly(acrylic acid), Polyacrylic acid
PE	Polyethylene
PV	Peroxide Value
PVA	Poly(vinyl alcohol), Polyvinyl alcohol
R	Alkyl group
ROS	Reactive Oxygen Species
Sa	Arithmetical mean height
Sz	Maximum height
U	Potential energy
UV	Ultraviolet
V	Volume
W_a	Work of adhesion
W_c	Work of cohesion
γ	Interfacial energy
ζ	Electrokinetic potential, Zeta potential
θ	Contact angle
σ	Surface tension

1 Introduction

The shelf life is a very important property for food products. Too short shelf life makes it difficult to distribute the product to the market and thus more difficult to reach the customer. Another problem related to the short shelf life is the issue of wasting food that has not been consumed. Research carried out on the Italian market shows that there is a relationship between the short shelf life and food waste – the shorter the period, the more often the food product is thrown out by stores [1]. This promotes overproduction of food, which has a negative impact on the environment [2]. It is estimated that 1/3 of food produced worldwide is wasted. This phenomenon is becoming a global problem, occurring primarily in developed countries [3].

This problem can be remedied by the use of appropriate packaging that will extend the shelf life of food products stored in them. The so-called active packaging can prevent the physical and chemical processes that cause spoilage of stored food [4,5]. One method of preventing food spoilage is the use of antioxidants in the packaging material [5-8]. A particularly interesting solution is the use of nanodiamonds for this purpose [8-10]. Due to their atomic structure, nanodiamonds exhibit antioxidant properties [10-14]. Moreover, it has been shown that nanodiamonds with the surface functionalized as a result of oxidation inhibit the process of fat rancidity [8,15].

So far, no easy-to-implement and effective solution has been developed that would allow the immobilization of nanodiamond particles on the surface of the packaging film, thereby maintaining their antioxidant properties.

In this work, attempts were made to develop coatings adherent to polyolefin films containing functionalized nanodiamond particles on their surface, which show antioxidant properties against high-fat food products that undergo rancidity. This solution must not adversely affect the quality of the stored food, must be durable and must be made of materials that do not endanger health and are friendly to humans and the environment.

2 Objectives of dissertation

The purpose of the work is to develop a polymer coating applied to commercially available polyolefin packaging films, which has antioxidant properties and is particularly useful in the protection of high-fat products. This coating should meet the following requirements: be completely non-toxic, have no smell or color, do not change the taste of food, do not delaminate and do not contaminate stored food.

The objectives of the dissertation work were specified during the doctoral studies based on the newly acquired knowledge during the literature review, in cooperation with other research institutions and in active participation in domestic and international conferences. Objectives of the work include:

- Development of a polymer film-forming suspension, containing nanodiamond particles, capable of forming a coherent coating on a polyolefin material.
- Assessment of the stability of the prepared film-forming suspensions.
- Preparation of the substrate (commercially available polyolefin packaging film) for the application of the developed coating by plasma surface activation.
- Application of a film-forming medium to obtain an antioxidant coating.
- Developing a method of immobilizing nanodiamond particles having antioxidant effects with the polymer matrix of the coating.
- Verification of mechanical properties having a significant impact on the usability of the materials obtained, i.e. adhesion to the substrate and tribological properties of cast coatings.
- Assessment of antioxidant properties.

The idea was to develop a technology that would be easy to implement in industry, while the process would be completely harmless to humans and not adversely affecting the environment.

3 Theoretical part

In the theoretical part, the thesis deals with research in the field of surface science covering topics such as surface wettability, adhesion, contact angle, surface tension and surface free energy. In addition, the topic of colloid chemistry and the related issue of their stability was discussed. The theoretical part also describes the properties and behavior of functionalized nanodiamonds in water suspensions, which play a major role in this research. The thesis deals also with physics and chemistry of film-forming suspensions and finally, methods of coatings' tribological properties evaluation, which are significant in packaging application.

3.1 Colloid and Surface Chemistry

3.1.1 Terminology

Due to large discrepancies in the terminology applied to colloid chemistry in common parlance or in the scientific literature [16-19], which are mutually exclusive, the following terms, defined by IUPAC and officially valid [20,21], have been used in this thesis:

Solution – A liquid or solid phase containing more than one substance, when for convenience one (or more) substance, which is called the solvent, is treated differently from the other substances, which are called solutes.

Dispersion – Material comprising more than one phase where at least one of the phases consists of finely divided phase domains, often in the colloidal size range, distributed throughout a continuous phase domain.

Colloidal – The term refers to a state of subdivision, implying that the molecules or polymolecular particles dispersed in a medium have at least in one direction a dimension roughly between 1 nm and 1 μm , or that in a system discontinuities are found at distances of that order.

Colloid – A short synonym for colloidal system.

Colloidal dispersion – A system in which particles of colloidal size of any nature (e.g. solid, liquid or gas) are dispersed in a continuous phase of a different composition (or state).

Suspension – A liquid in which solid particles are dispersed.

Colloidal suspension – A suspension in which the size of the particles lies in the colloidal range.

Sol / Colloidal sol – Fluid colloidal system of two or more components.

Thus, an aqueous suspension of fully deagglomerated monodispersed 5 nm nanodiamond, which is used in this research, may also be called a colloid, a colloidal suspension, a dispersion and a colloidal dispersion as it meets all these definitions. The prepared during the research aqueous mixtures of dissolved polymers and fully deagglomerated nanodiamond can also be referred to as suspensions, colloids, colloidal suspensions, dispersion, colloidal dispersion or even sols. Therefore, these terms will be used interchangeably with the above-mentioned materials.

In the theoretical part of this work, the above-defined terms mainly refer to the system in which the dispersing phase is a liquid and the dispersed phase is nanometric solid particle. The used term depends on the source on which the certain paragraph is based.

3.1.2 Stability of dispersion systems

Dispersion systems are in many cases thermodynamically unstable and only the kinetic aspect determines the time after which the particles of the dispersed phase will fuse to form larger phases. If the forces of attraction in the system are dominant, the particles undergo aggregation processes. If the repulsive forces are dominant, the particles move freely. Then the system is more or less permanent. A particle of the dispersed phase has a defined interface. Near the phase boundary between the particle of the dispersed phase and the continuous phase, there is a distribution of electrostatic potential caused by the distribution of charges in the subsurface layer, associated ions or dipoles. Dispersion systems are in many cases thermodynamically unstable and only the kinetic aspect determines the time after which the particles of the dispersed phase will fuse to form larger phases. If the forces of attraction in the system are dominant, the particles undergo aggregation processes. If the repulsive forces are dominant, the particles move freely. Then the system is more or less permanent. For instance, a positively charged surface placed in an electrolyte containing neutral ions will repel the cations and the anions will be attracted to the interface. In this case, to achieve electroneutrality, the electrolyte layer near the interface must have a net negative charge equal to the surface charge of the solid material. Charged particles are

found in most dispersion systems and this may be the result of the dissociation of the ionic groups of the molecules located on the particle surface or the adsorption of ions or dipoles on the interface from the outer phase. It can also often result from adsorption of ionic surfactants on hydrophobic particle surfaces, as well as ion exchange between the outer and inner phases of the system. Fig. 3.1 shows the diagram the structures of the particles of the dispersed phase and the diagram of the potential distribution resulting from the distribution of charges near their surface. This is the so-called electrical double layer (EDL). The EDL is characterized by a potential decrease at the solid/liquid interface, which depends on the concentration and nature of the ionic species. [22-24]

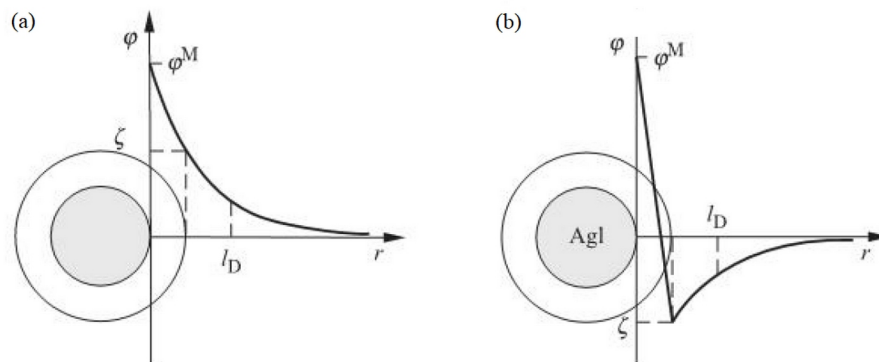


Fig. 3.1: Schemes of the dispersed phase particles: (a) positively charged particle of the hydrophobic system in the electrolyte solution; (b) an AgI particle in a KI solution (excess). In (a) and (b) the potential distribution (φ) as a function of distance (r) is presented. φ^M – potential at the surface of the particle nucleus, ζ – potential at the boundary of the Helmholtz-Stern layer, l_D – Debye length. [22]

The electrical double layer consists of two parts. The first part, the Helmholtz-Stern layer, adheres to the solid phase. It is the size of ions and the counter-ions accumulated close to the charged particle form a compact layer. In this layer, the potential changes linearly with the distance from the interface and reaches the value of ζ (Zeta) at the interface. Zeta is the electrokinetic potential. The other part of the EDL is the diffusion layer. Due to the Brownian motion, the potential change in this part of the double layer is non-linear. EDL has a double charged layer. One part is on the particle surface and the other part is the diffusion area, extending into the solution. The thickness of the diffusion layer depends on the concentration and type of ions in the solution. Its thickness has a dramatic effect on the durability of the dispersion system.

However, the stability of the dispersion system depends not only on the Coulomb force induced electrostatic interactions between the charged particles. Short-range Van der Waals interactions and higher-order electrostatic interactions such as dipole-dipole also have a significant influence. The sum of these interactions gives the net value of the energy which determines whether the dispersed particles will attract or repel each other (see Fig. 3.2). To maintain the dispersion system stability, the repulsion forces have to be stronger than the attraction ones. [22,25]

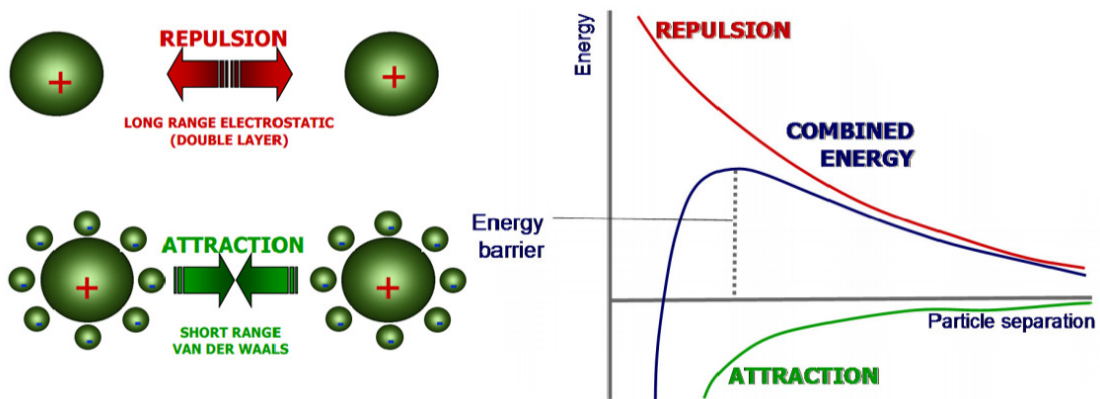


Fig. 3.2: Long range electrostatic repulsion forces and short range van der Waals attraction forces. [25]

In typical dispersion systems, the particle sizes and distances between them are usually larger than the extent of their mutual interactions. It is assumed, according to the DLVO theory, that the total energy of the system U_C is the sum of the components of the electrostatic energy U_E and the dispersive energy U_D . [22,26]

$$U_C = U_E + U_D \quad (3.1)$$

At the smallest distances between particles, it is also necessary to take into account the short-range repulsive interactions, which are not directly taken into account in the DLVO theory. The superposition of these energies gives the total value of the energy of interactions between particles in the dispersed phase (Fig. 3.3). When the particles are far enough apart, the interaction energy is 0. As the distance decreases, U_C passes through a shallow minimum (*secondary minimum*), increases to a maximum of U_{max} , and then rapidly decreases. As the particles come close to near direct contact, short-range Born repulsion occurs, preventing further approach (*primary minimum*). The behavior of the particles in the dispersion system can be explained as a result of the superposition of all the effects

mentioned here. The most important for durability is the height of the U_{\max} barrier. If this barrier is not high, irreversible aggregation (coagulation) of the dispersed phase particles is easy and the system is unstable. In addition to coagulation, it is also possible to aggregate particles in a second (much shallower) minimum, i.e. flocculation. In addition, the stability of the system is favored by: low I_D value (resulting from the low concentration of ions in the solution) and high ζ potential. The addition of electrolytes reduces the U_{\max} value. When U_{\max} approaches 0, the electrolyte concentration at which this occurs is called the Critical Coagulation Concentration. Then the potential ζ of particles decreases below the critical value, which depends on the type of colloid. [22]

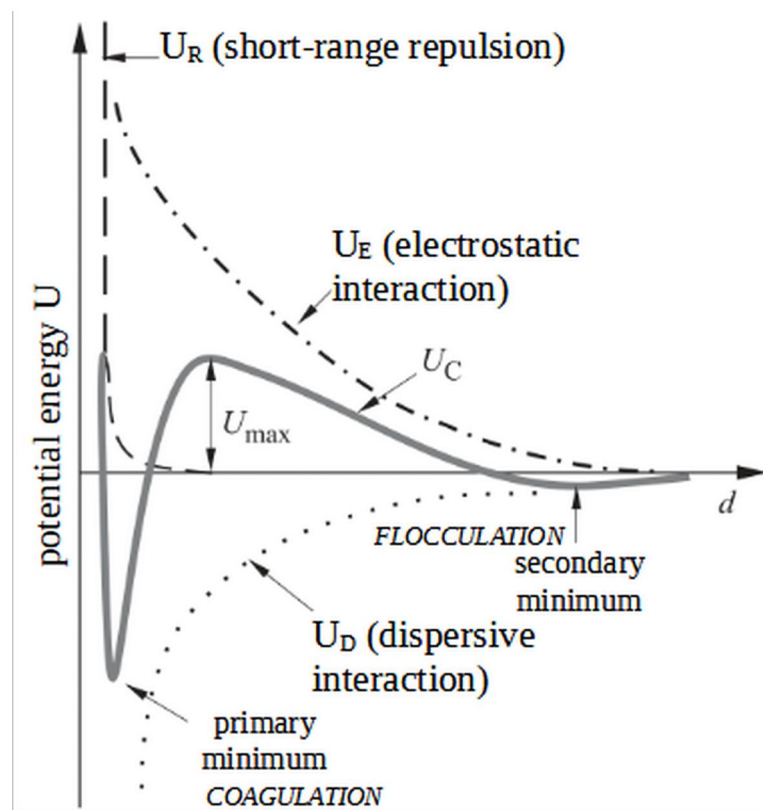


Fig. 3.3: The potential energy of interactions between two particles of the dispersed phase. [22]

The potential at the extremity of the Helmholtz-Stern layer (slipping plane) is called the zeta potential (ζ) or electrokinetic potential. This boundary is the surface separating that part of the interfacial space containing the ions immobilized on the surface of the solid phase and in its immediate vicinity from the rest of it. The existence of the potential ζ causes the occurrence of electrokinetic phenomena. When the two phases of the dispersed phase-electrolyte solution, bound by electrostatic interactions, move or can move relative

to each other, electrokinetic effects are observed. The mutual phase displacement takes place on the slipping plane inside the liquid, near the surface of the solid. The slipping plane separates the solution containing the ions strongly attracted by the surface from the diffuse layer (Fig. 3.4). [27-32]

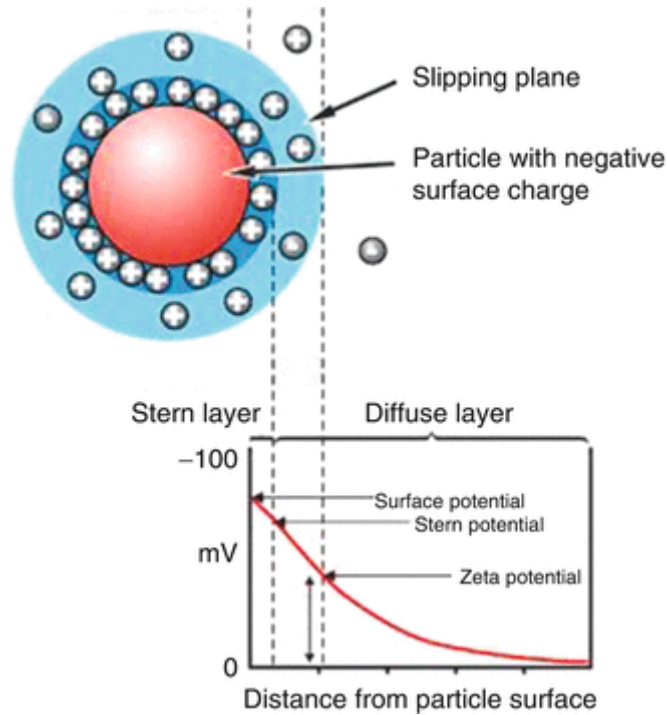


Fig. 3.4: Diagram showing the ionic concentration and potential difference. [30]

The electrokinetic potential of the various dispersed phases depends largely on the concentration of hydrogen ions. For various colloid systems, there is a pH value at which the electrokinetic potential is zero (isoelectric point) and electrostatic repulsion does not prevent colloid coagulation. The dependence of the zeta potential on pH and on the concentration of other ions differs for different types of dispersed phases. [28,33]

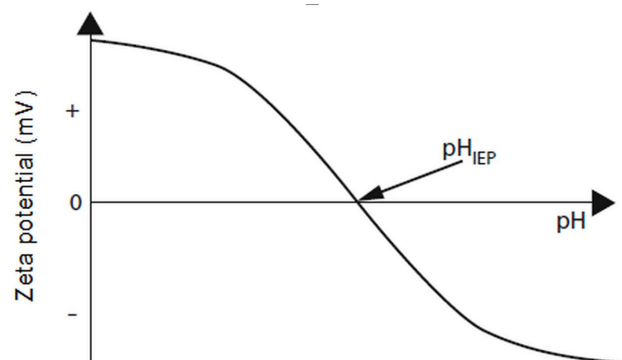


Fig. 3.5: The dependence of the Zeta potential on pH. [28]

The zeta potential value is essential for the stability of colloidal particles and for electrokinetic phenomena. Table 3.1 shows how a given potential value influences the dispersion behavior [34].

Tab. 3.1: Stability behaviour of a colloid depending on zeta potential. [34]

Zeta potential (mV)	Stability behavior
0 to ± 5	Rapid coagulation or flocculation
± 10 to ± 30	Incipient instability
± 30 to ± 40	Moderate stability
± 40 to ± 60	Good stability
> 61	Excellent stability

3.1.3 Film-forming materials

A film-forming material is a substance that is capable of forming a film when applied to a solid surface. Film-forming materials are most often used as solutions in organic solvents, aqueous solutions or dispersions. They are applied by various methods. Film-forming materials that are not reactive form films as a result of solvent evaporation, while chemical changes (e.g. polymerization, condensation, cross-linking) occur in the case of reactive materials. Film-forming materials should:

- exhibit good wetting of the surface to be coated and the dispersed particles;
- bind the particles into the film firmly;
- dry rapidly in a thin layer;
- have good adhesion to the surface being covered.

In many cases, these properties are obtained by combining two or more film-forming materials, as well as by the introduction of certain additives. [35,36]

Several polymers can function as film-forming materials, including those that are soluble in water. Such polymers include, inter alia, poly(acrylic acid) (PAA) and poly(vinyl alcohol) (PVA). Both polymers form thin films when the solvent – water evaporates after casting on the surface their solutions. These polymers in solid state have a consistent semi-crystalline structure in which individual polymer chains are linked with each other by

hydrogen bonds. In solutions, at a lower concentration the macromolecules are mainly present on the surface and acting as a surfactant, which reduces the surface tension. Moreover, these polymers are polyelectrolytes and have been successfully used to disperse carbon nanoparticles in water. The legitimacy of their use as dispersants depends on their protonation, which is pH-dependent and affects the degree of hydrolysis of the resulting films. In case of PAA, the best dispersion conditions were achieved at pH 5, which is a value close to the pK_a of PAA. [37-38]

3.1.4 Wettability

In the case of film-forming materials, an important aspect is the wettability of the surface they cover. In this regard, the wetting of the solid surface by the liquid is essential. The tendency of a liquid to wet a solid is determined by:

- the work of adhesion – represents the work necessary to detach a liquid from a unitary solid surface while simultaneously creating two new surfaces of the same size: a liquid-gas surface and a solid-gas surface;
- the work of cohesion – represents the work of breaking a column of liquid with a unit cross-section to create two free surfaces of the same size. [22]

According to Young's Law and Young-Dupré equation [39,40], the Work of adhesion is given by the following equation:

$$W_a = \gamma_{lv} + \gamma_{sv} - \gamma_{ls} \quad , \quad (3.2)$$

while the Work of cohesion is given as follows:

$$W_c = 2 \gamma_{lv} \quad , \quad (3.3)$$

where

γ_{lv} is the surface tension of the liquid,

γ_{sv} is the solid–vapor interfacial energy

γ_{sl} is the solid–liquid interfacial energy. [41]

Figure 3.6 shows the situation that exists on the surface of a solid partially wetted by a liquid. The liquid droplet is in mechanical equilibrium on the solid surface. Its shape and the associated contact angle θ_e depend on the type of liquid and the type of solid phase.

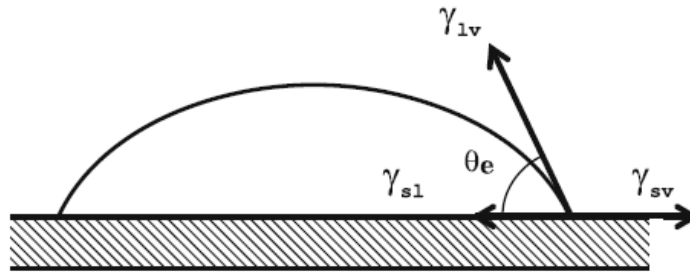


Fig. 3.6: Young's force balance giving the equilibrium contact angle. [41]

Considering, in accordance with the aforementioned Young's law, the forces acting in this system, we obtain the equilibrium condition of these forces:

$$\cos(\theta_e) = \frac{\gamma_{sv} - \gamma_{sl}}{\gamma_{lv}}, \quad (3.4)$$

which can be converted to the form:

$$W_a = \gamma_{lv}(1 + \cos(\theta_e)) = \frac{1}{2} W_c (1 + \cos(\theta_e)) \quad . [22,41] \quad (3.5)$$

If the interaction between liquid and solid molecules is at least as strong as the interaction of molecules in the liquid ($W_a \geq W_c$), then, $\theta_e = 0^\circ$ and the liquid perfectly wets the solid. If, on the contrary, $W_a < W_c$, then the angle θ_e assumes the appropriate value in the range $0-180^\circ$. In the limit case $W_a = 0$, $\theta = 180^\circ$, the liquid forms a spherical drop on the surface of the solid. In fact, there is always interaction between the liquid and the solid phase, hence the angle θ_e is always less than 180° . The surface tension of a solution is typically different from that of a pure solvent. Aqueous solutions of strong inorganic electrolytes, with low anions and cations, show a surface tension greater than that of pure water. In case of strong electrolytes dissociating into large ions, such as sulfonate and phosphate ions, the surface tension decreases. This applies in particular to solutions of organic compounds, the molecules of which contain polar groups, such as alcohols, acids and their salts, esters, etc. Substances that lower the surface tension of a solvent are called surfactants. [22]

The behavior of colloidal dispersions, adhesion, and friction is influenced by surface and interface tension. It should be borne in mind that the force of attraction of one molecule to

another depends on the structure of those molecules. A substance with a high surface energy attracts other substances. This attraction is mainly due to the electrostatic interactions resulting from the charges of the molecules. Mutual attraction of positive and negative charges causes the formation of temporary dipoles within a given atom due to the change in electron density and results in an interaction between the formed temporary dipoles. These interactions are called dispersive forces and exist between all atoms regardless of their structure. Large molecules having a large electron cloud will show stronger dispersive forces than smaller molecules. However, the interactions are relatively weak and the influence on the magnitude of the dispersion forces is small. The polar forces are a much stronger influence. They are closely related to the structure and composition of molecules and are related to the electronegativity of the atoms they contain. The presence of an electronegative atom in the molecule deforms the density of the electron cloud and causes it to concentrate around these atoms to form a constant dipole. The polar forces are related to the interactions between these constant dipoles. Polar interactions can be up to 100 times stronger than dispersion interactions. Polar liquids (e.g. water) have contact angles that are respond strongly to the polar component of surface energy. This happens because the polar part of a liquid only interacts with the polar part of a surface, while the dispersive part of a liquid only interacts with the dispersive part of a surface. [42]

3.1.5 Surface treatment

In polymeric materials, interatomic covalent bonds can be polarized to varying degrees, which depends on the difference in the electronegativity of the atoms forming the bond. Polar polymers are those in which the macromolecules contain atoms that form hydrogen bonds. Examples of polar polymers are aliphatic polyamides which contain strongly polar carbon-nitrogen bonds as well as strongly polar -NH-, -(C=O)- groups. Non-polar polymers are for instance polyethylene (PE). In polyethylene, there is no electronegativity difference between the carbon atoms that form the main chain, and the negligibly small dipole moments between the carbon and hydrogen atoms cancel out as a result of their spatial symmetry. As a result, PE is non-polar and hydrophobic. [43]

In order to increase the wettability of non-polar polymers with polar liquids, surface activation (surface treatment) has to be performed. This treatment consists in generating a cold plasma discharge under atmospheric pressure and “sweeping” the surface with it. The

emitted electrons collide with electrons and molecules in the atmosphere causing excitation, dissociation, and ionization. Electrons are also emitted from ionized atoms and molecules which additionally speeds up the entire reaction occurring repeatedly. Oxygen radicals and ozone are generated by ionization and dissociation of oxygen molecules in the air. High-energy electrons reaching the surface of the polymeric material separate the polymer chains (main and side chains). The cleaved surface polymer layer gets into a radical state. The oxygen radicals and the ozone layer in the gas phase recombine with the main chain and side chains to form polar functional groups such as hydroxyl and carbonyl groups (Fig. 3.7). This makes the surface hydrophilic. [44]

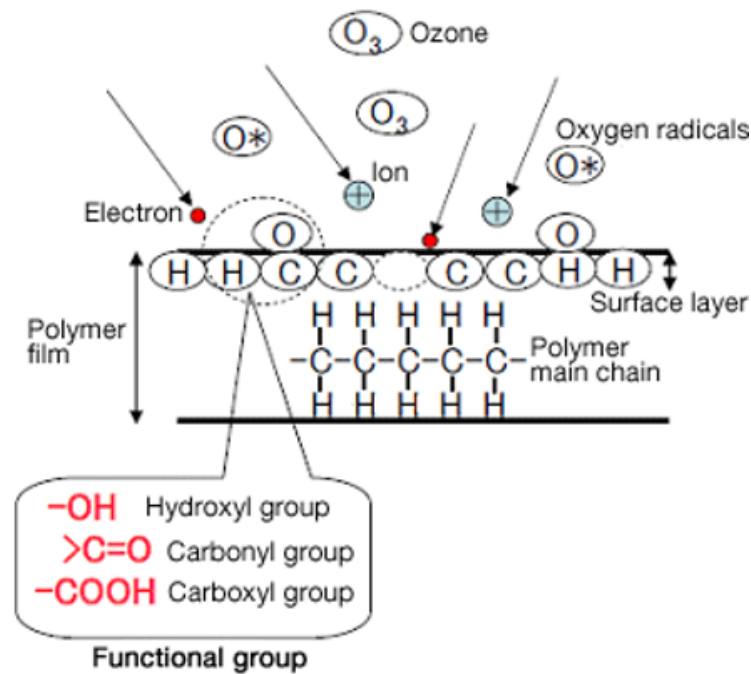


Fig. 3.7: Introduction of polar functional groups into polymer chain in surface layer of polymeric material.

3.2 Properties of functionalized nanodiamond

3.2.1 Nanodiamond surface functionalization

Nanodiamonds (NDs) due to their core/shell layer structure associated with the presence of sp^2 and sp^3 hybridization carbon atoms can be subjected to chemical functionalization of their structures by attaching functional groups [45-48]. This distinguishes nanodiamonds in this matter, for example, from nanotubes. The modification of the nanodiamond with functional groups does not affect the structure of the diamond core and the properties

related to it. The most popular starting point for further modification of the nanodiamond surface is its preliminary carboxylation. This is made by air oxidation or ozone treatment during purification process. The rich chemistry of carboxyl groups allows for their replacement or attachment of other compounds (Fig. 3.8). [49,50]

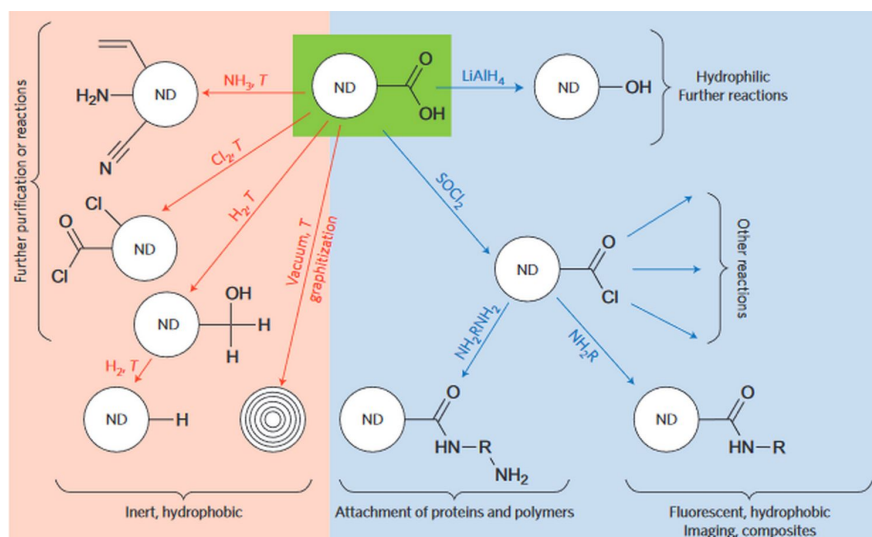


Fig. 3.8: Paths of chemical functionalization of nanodiamond surface. [49]

The carboxyl groups of the nanodiamond can be completely reduced using a microwave CVD plasma treatment in hydrogen at high temperature, completely removing the oxygen from the surface of the nanodiamond. The use of strong reducing agents such as lithium aluminum hydride allows the replacement of carboxyl groups with hydroxyl groups. Such finished nanodiamond surface can be used in esterification with acyl chlorides, which will enable the attachment of long carbon chains to the ND surface. Another possibility of hydroxylated ND is silanization. The COCl functional groups are the reactive derivative of the carboxyl ones. They are obtained by nucleophilic substitution with thionyl chloride. The reactivity of the resulting acyl chloride allows for further attachment of chemical compounds, including amine derivatives such as amino acids. In turn, heating the carboxylated ND in ammonia results in the formation of a variety of different surface groups including NH_2 , C-O-H , $\text{C}\equiv\text{N}$ or groups containing C=N . ND graphitic shells can be functionalized in Diels-Adler and addition reactions due to the presence of double bonds between the carbon atoms. In Fig. 3.9 are shown the functionalization schemes of carboxyl and hydroxyl groups [49-51].

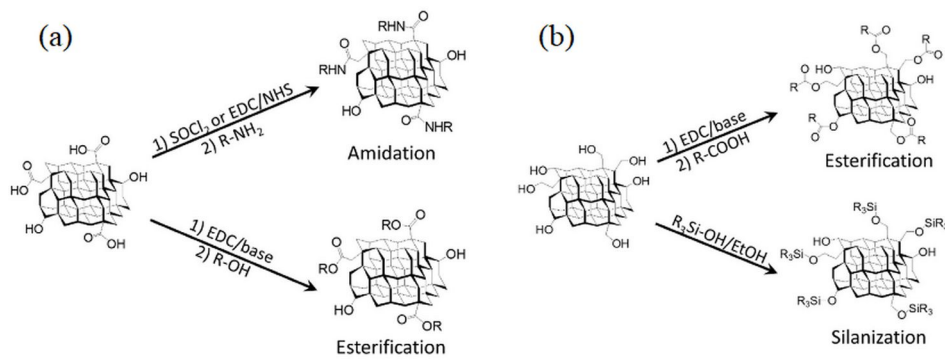


Fig. 3.9: Functionalization of: (a) carboxyl and (b) hydroxyl groups on NDs. [51]

3.2.2 Nanodiamond aqueous suspensions

Obtaining aqueous colloidal suspensions (hydrosols) of individual diamond particles with diameters of 4–5 nm is a complex process. Nanodiamond particles tend to aggregate. Deaggregation is carried out by milling the previously purified ND in suspension with ceramic microbeads or using ultrasonification. To prevent re-aggregation, the functionalization of the ND surface must be performed. As a result of functionalization, an electric charge will be obtained which will cause the repulsion of the single-sign charge nanoparticles. Relatively stable hydrosols have a ND content of up to 10 wt%. It is important that the stability of nanodiamond colloids depends on the pH. The pH influences the electrokinetic potential (Zeta potential) of the electric double layer of dispersed nanodiamond particles and this in turn determines whether the particles repel or attract each other to form aggregates. Fig. 3.10 Figure 3.10 shows a titration curve of colloidal suspensions with nanodiamonds showing the change in Zeta potential from the pH of the suspension. The nanodiamond particles with a positive Zeta potential were modified by oxidizing their surface with a strong oxidant (chromium oxide in sulfuric acid), and those with negative Zeta potential were oxidized with molecular oxygen in the presence of diboron oxide or singlet oxygen in sodium hydroxide. [49,52,53]

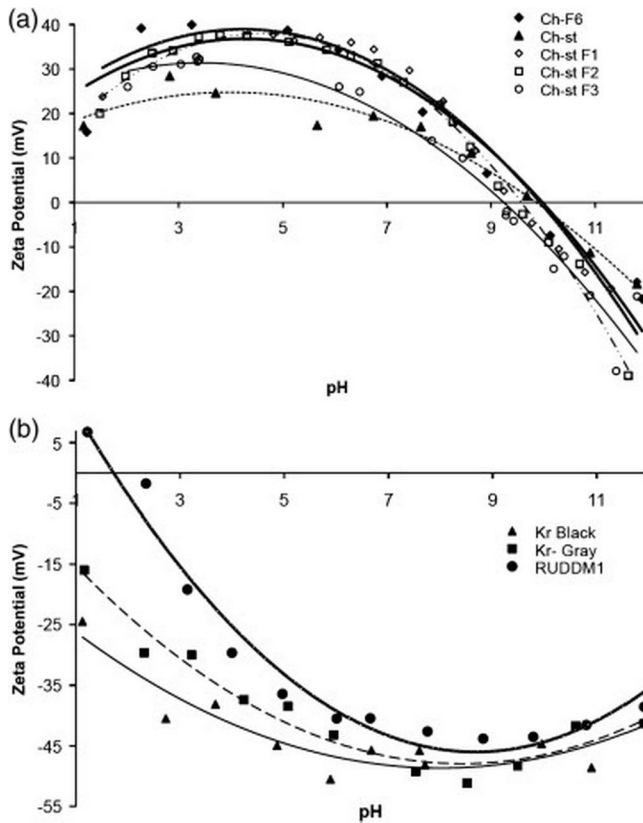


Fig. 3.10: The dependence of the Zeta potential on the pH of the ND colloidal suspension in the case of: (a) Positive Zeta potential; (b) Negative Zeta potential. [53]

The change in pH (and also in the Zeta potential) in the titrated suspensions was associated with a color change resulting from Rayleigh scattering as a result of the formation of larger aggregates. Larger aggregates (occurring by lower absolute values of Zeta potential) begin to sediment faster, making the slurry less stable. The use of additives or dispersants must be very careful and within a specific pH window for maintain stable dispersion. [52,53]

3.2.3 Nanodiamond–polymer composites

Due to their thermal stability, high Young's modulus, strong hardness, high specific surface area combined with active surface functional groups, nanodiamonds are used as reinforcement in polymer materials. Moreover, they have large and accessible external surface which maximizes interactions with the polymer matrix and exert the strong influence on polymer properties. Active functional groups on the surface of the nanodiamond make it possible to bind it covalently with the polymer chain by carrying out chemical reactions. ND particles can thus be used as a cross-linking agent.[50,54,55]

Nanodiamond has also been used as a component in thin PVA films without the effect of its aggregation. The PVA/ND nanocomposites were prepared by simple casting method from aqueous medium maintaining high dispersibility of ND in the PVA matrices. In this case,

ND was not covalently bound to the polymer, but through spectroscopically confirmed hydrogen bonds. Fig. 3.11 shows possible configurations of hydrogen interactions in a PVA/ND system, in which ND was functionalized with polar groups on its surface. [56]

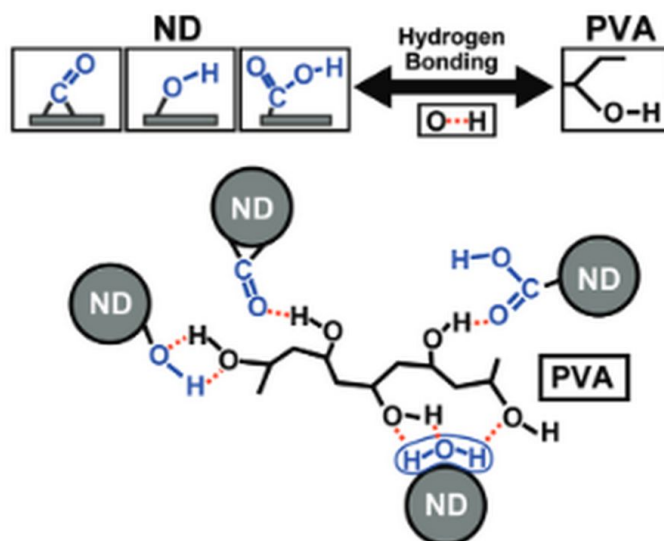


Fig. 3.11: Schemes of the hydrogen bonding interaction between PVA and ND particles. [56]

3.2.4 Antioxidant behaviour of nanodiamond

As mentioned in the introduction, nanodiamonds exhibit antioxidant properties, including inhibiting the rancidity of fats [8-10,15]. Rancidification (fat oxidation) occurs through auto-oxidation. It is a radical chain reaction in which oxygen molecules are the generating free radicals in the form of reactive oxygen species (ROS). It is favored by increased temperature and the presence of sunlight (catalyzed by UV radiation). Oxidation primarily occurs with unsaturated fats. Via a free radical process, the double bonds of an unsaturated fatty acid can undergo cleavage (Fig. 3.12), releasing volatile aldehydes and ketones. Free radical scavengers can terminate this chain reaction by reducing the ROS or donating the electrons to neutralize free radicals [57-60].

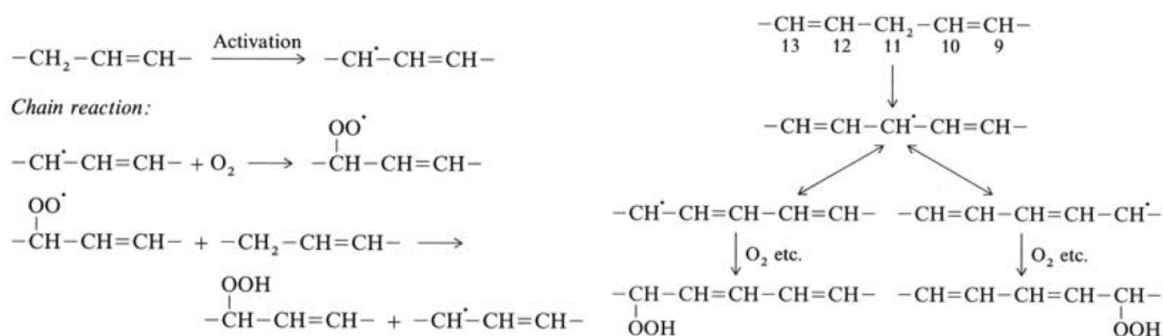


Fig. 3.12: Scheme of chain reaction occurring during oxidative rancidification – oxidation of double bonds. [60]

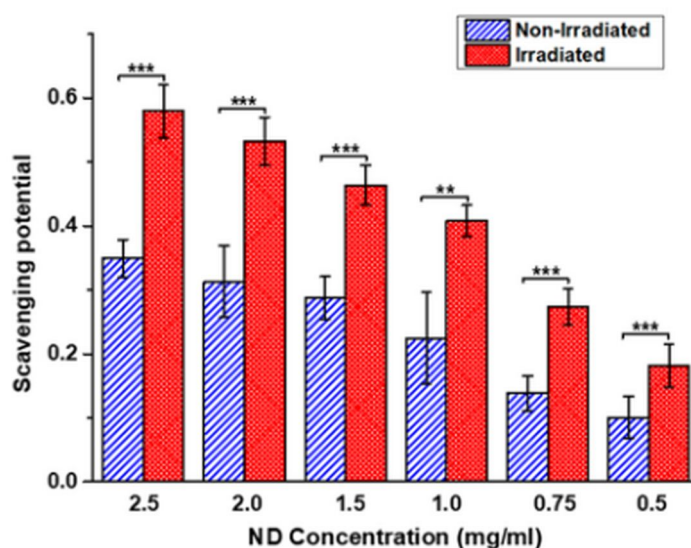


Fig. 3.13: Graphs comparing the scavenging potentials of aqueous suspensions of the ND in comparison to * $p < 0.05$, ** $p < 0.01$, *** $p < 0.001$ M DPPH. Aqueous suspension of the ND exhibits an increased scavenging potential after being exposed to irradiation. [61]

Oxygenated ND was found to exhibit the greatest electrochemical activity. The ND surface exhibits delocalised π character due to unsaturated bonding of surface atoms and extensive oxidation occurring with C=O bond formation. Moreover, a nanodiamond is photostable UV filter. It can absorb UV rays which contribute to the ROS formation, thus increasing its scavenging potential (Fig. 3.13). The delocalized sp^2 nature on the nanocarbon surfaces can stabilize radicals and prevent the degradation of antioxidant ability, therefore the nanodiamond can be used long-lasting antioxidant. [61,62]

3.3 Tribology of packaging films

3.3.1 Coefficient of friction

Friction is a force that enables or hinders the movement of two contact surfaces. The coefficient of friction (CoF) of the packaging film indicates its frictional characteristic. CoF is determined by dividing the force needed to move one surface across another by the force perpendicular to the surfaces. Controlling CoF enables processors to optimize line performance and avoid problems with forming, sealing, transporting and storing packages.

In horizontal form fill and seal packaging systems too much friction in the sealant side of the film can lead to dragging or sticking of the film while moving on metal plates, and in vertical form fill and seal packaging systems this can cause poor film feeding over metal forming collars. In both of these systems, too much friction in the sealant side of the film can result in sideways skid, leading to poor seals and associated leakage. Other problems associated with too high CoF are: pull belt slippage, excessive pull belt wear, reduction in packaging speed and film tracking problems. [63,64]

CoF values range from 0 to 1 – low CoF indicates lesser resistance and high CoF higher resistance to sliding (higher slip). CoF less than 0.25 is considered low (high slip), while CoF greater than 0.45 is considered high (no slip). The CoF can be controlled by adding lubricants and slip agents to a film resin. CoF can be affected by many factors like antiblock additives, surface treatment, antistats, inks, varnishes or adhesives. [64]

3.3.2 Adhesion aspect

Multi-layer polymer films are widely used in the food packaging industry. This is especially the case with active packages as they are usually composed of many layers, each with a different function. Films can be designed through the use of different layers to provide a variety of properties. Strength, flexibility, barrier, ease of heat sealing properties are among the essential properties that are subject to stringent requirements. Moreover, each layer shall maintain its integrity and adhesion to the surrounding layers, even under high strain and stress. Failure between different layers in a multi-layer film will lead to failures in the required function. Delamination completely destroys the usefulness of such a film. Adhesion results from intermolecular interactions of the contacting substances. The most common adhesion theories are based on the phenomenon of adsorption, simple

mechanical tacking, diffusion, electrostatic interactions and the concept of weak boundary layers [67]. A concept has been proposed that the adhesion of the coating to the substrate can be expressed in two forms: fundamental adhesion and practical adhesion [68]. Fundamental adhesion would be the resultant of all interfacial intermolecular interactions, while practical adhesion would result from measurements. As can be expected, the values of these two forms do not overlap with each other. However, the practical adhesion depend on the fundamental one, but is also influenced by many other factors. The measurement methods used may also differ in the obtained results, because the result is affected by the parameters of adhesion measurement technique as well as environmental conditions. Currently, the most commonly used multi-layer plastic film adhesion tests are: peel-tests and scratch-tests. The peel-tests consist in fixing the sample film on a rigid plate and the pulling off layers to be tested in the reverse direction. The angle at which the layers are peeled off varies depending on the strength of adhesion and the test methodology used. Another popular method of testing the bond strength of the coating to the substrate is the scratch test. The scratch resistance test allows to check whether the coatings applied to the substrate are sufficiently strongly attached to it. The principle of the test is to drag an indenter of known geometry over a surface with a constant or increasing load. Increasing load causes damage at some point, which is observed through an optical microscope or by a change in the friction force, acoustic emission or a change in the penetration depth of the indenter. Performing a scratch-test allows for making an analysis of scratch-induced damages in multi-layer packaging film. [65,66]

4 Experimental part

4.1 Used materials

4.1.1 Plastic substrate

As part of this research, commercially available packaging film was used as the substrate for the antioxidant coating. The film is 110 microns thick and is used to produce dry dog food packaging. The appearance of the film is shown in Fig. 4.1.

Differential scanning calorimetry was used to identify the polymer from which the packaging is made. Mettler Toledo DSC 1 (Switzerland) device was used for testing. Knowing the phase transition temperatures of popular polymer materials used in the production of packaging films, it was decided to conduct a test in the temperature range from 25°C to 280°C. The test was carried out in 3 stages way: heating-cooling-heating with 10°C/min heating rate. The 3-stages was designed to eliminate the impact of the plastic processing history and get rid of low-molecular additives. The results were evaluated using STARe Software provided by Mettler Toledo. The obtained DSC curves are presented in Fig. 4.2a-c.

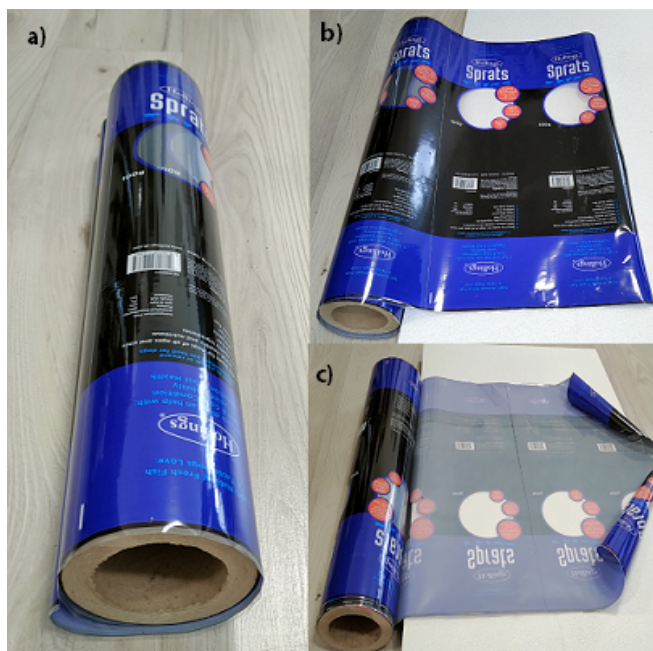


Fig. 4.1: Packaging film used in experiments (made by Plastmoroz, Poland): (a) Packaging film roll; (b) outer side; (c) inner side. Source: photograph by author

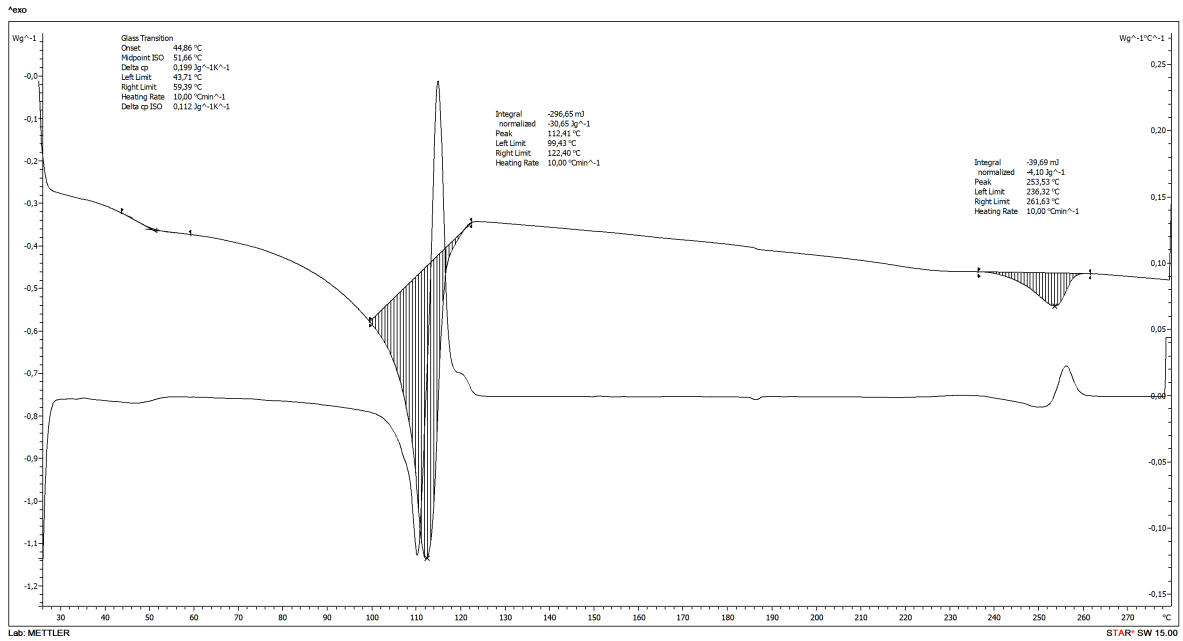


Fig. 4.2a: DSC curve of first heating stage.

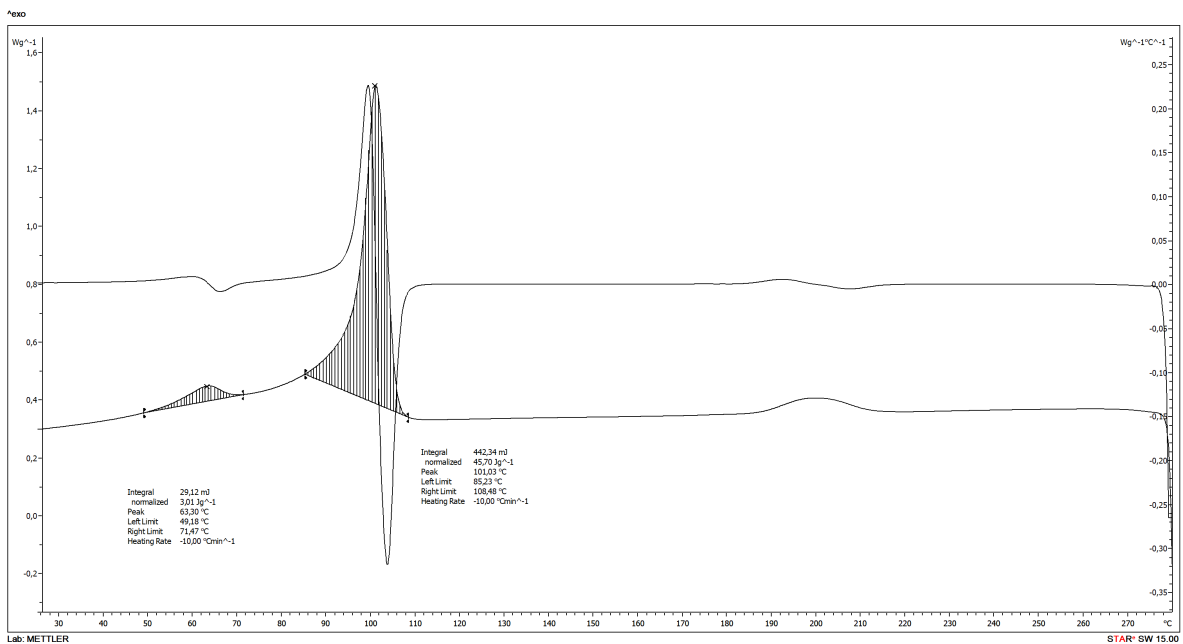


Fig. 4.2b: DSC curve of cooling stage.

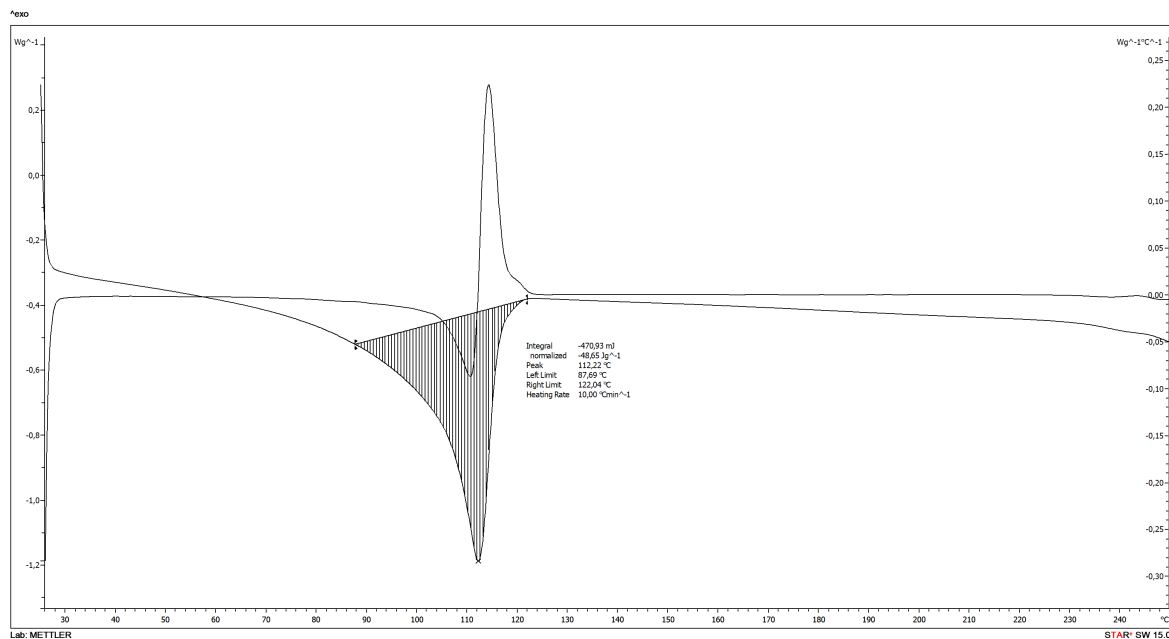


Fig. 4.2c: DSC curve of second heating stage.

Analysis of the obtained results showed that the temperatures of phase transitions are about 112°C in the case of heating and about 101°C in the case of cooling.

Differential scanning calorimetry showed that the film is predominantly made of low-density polyethylene (LDPE) [69]. LDPE is a thermoplastic commonly used in the production of packaging materials. It has excellent resistance to acids, bases and esters, and good resistance to vegetable oils [70].

4.1.2 Polymer matrix

An important aspect in the selection of the polymer matrix is not only the properties of a given polymer after the formation of the coating, but also its film-forming ability as well as its characteristics in the form of a solution or suspension containing nanoparticles. The prepared mixtures must be a long-term stable dispersions and doesn't consist of toxic and environmentally harmful ingredients.

In this work, it was decided to use two polymers that are effective in film-forming: poly(vinyl alcohol) (PVA) and poly(acrylic acid) (PAA). Both are soluble in water. They have no color and no odor and aren't toxic. Due to their polarity, they are resistant to grease, oils and most organic solvents. The polymer raw materials used in the research are presented in Table 4.1.

Tab. 4.1: Specification of used polymer compounds.

Compound	Product name	Manufacturer	Acronym
Poly(acrylic acid)	Poly(acrylic acid), 25% soln. in water [Mw ~345,000]	Polysciences, Inc.(USA)	PAA
Poly(vinyl alcohol)	Poly(vinyl alcohol), MW 25000, 88% hydrolyzed (PVA 25K 88%)		PVA

Poly(acrylic acid) with an average molecular weight of 345,000 and poly(vinyl alcohol) with an average molecular weight of 25,000 were used in the research. Poly(acrylic acid) was purchased in the form of 25%_{wt.} aqueous solution, but poly(vinyl alcohol) in the form of the 88% hydrolyzed powder. The parameters of the polymers used were selected so that it was possible to obtain low-viscosity aqueous solutions. A high molecular weight increases the viscosity of the material. An aqueous solution of poly(vinyl alcohol) with a higher molecular weight would have such a high viscosity that it would be difficult to disperse the nanodiamond in it. Moreover, the water solubility primarily depends upon degree of hydrolysis of poly(vinyl alcohol). Resins of lower hydrolysis grade can be dissolved at progressively lower temperatures. 88% hydrolyzed PVA have high degree of solubility, even in cold water, but for the complete dissolution heating is required. Higher hydrolysis grade products require progressively more energy to dissolve because of their greater degree of crystallinity. 4-5% solutions of both polymers with mentioned molecular weight have similar viscosity (see Fig. 4.3).

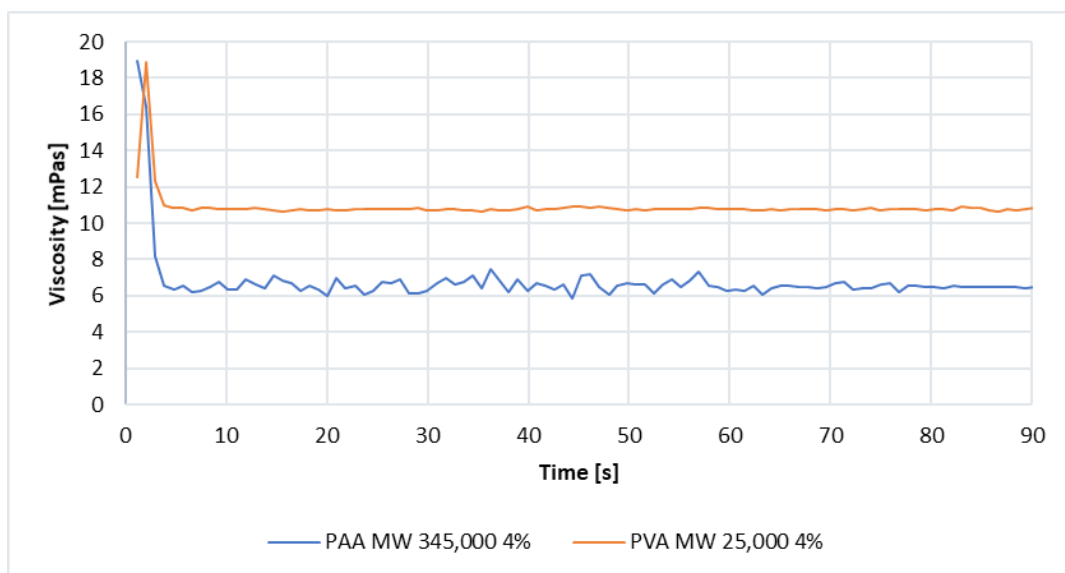


Fig. 4.3: Results of the viscosity measurement carried out on a rotational viscometer at a defined share rate of 1000 s^{-1} at room temperature of 4% aqueous solutions: polyacrylic acid with a molecular weight of 345,000 (blue) and polyvinyl alcohol with a molecular weight of 25,000 (orange).

4.1.3 Nanodiamond particles (ND)

As mentioned in the theoretical part, nanodiamonds with a properly functionalized surface exhibit antioxidant properties. They are a key component of the film-forming suspension, because they are the active ingredient and ensure the functionality of the coating, which is the subject of this work. The functionalizing the nanodiamond surface is also necessary to obtain a stable dispersion, since unmodified diamond aggregates. For the purposes of the research, it was decided to choose aqueous nanodiamond suspensions having a high absolute value of Zeta potential. Two types of aqueous nanodiamond suspensions were used: one with a positive (ND-P) and the other with a negative Zeta potential (ND-N). The ND-P has protonated hydroxyl groups on its surface, while the ND-N has deprotonated carboxylic groups on its surface. These colloidal suspensions provide fully deagglomerated monodispersed 4-5 nm nanodiamonds. The specification of used ND suspensions is shown in Tab 4.2.

Tab. 4.2: Specification of used nanodiamond suspensions.

Product name	Avg. particle size	Additional information	Manufacturer
ND5nmNH2O	4-5 nm	zeta potential -35mV, carboxylated, 10 mg/mL slurry in DI water	Adamas Nanotechnologies (USA)
ND5nmPH2O		zeta potential +35mV, hydroxylated, 10 mg/mL slurry in DI water	

Nanodiamond powders obtained after the water evaporation from the suspensions were subjected to Raman spectroscopy. Spectra were obtained using an inVia confocal Raman microscope (Renishaw, UK) equipped with two excitation diode lasers at 532 nm and 785 nm. The obtained spectra were characterized by high signal noise (due to the small size of the nanodiamond core – few nanometers), therefore they were smoothed and the baseline correction was performed. The spectra after processing are shown in Fig. 4.4.

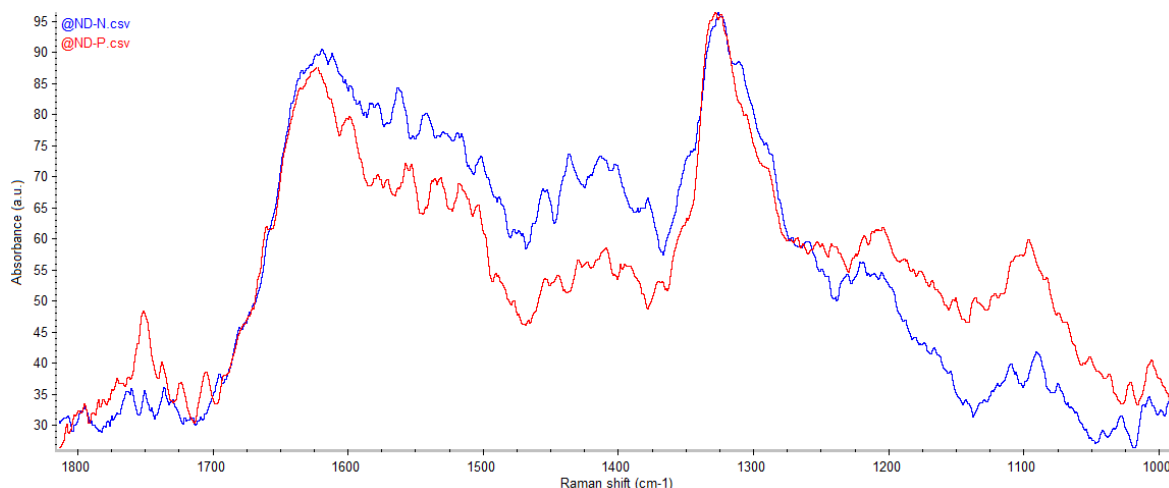


Fig. 4.4: Raman spectra of carboxylated (ND-N, blue) and hydroxylated (ND-P, red) nanodiamond powders formed after evaporation of water from suspensions.

The Raman spectra of both ND powders show a sharp diamond peak at 1327 cm^{-1} . Moreover, the both ND powders exhibit the characteristic Raman features of graphitic carbon: the G-band at $\sim 1560\text{ cm}^{-1}$ and the disorder-induced D-band at $\sim 1350\text{ cm}^{-1}$. The $\sim 1620\text{ cm}^{-1}$ peak could be assigned to O–H stretching vibrations of the groups formed as a result of oxidizing process.

4.1.4 Lewis acid catalyst

The Lewis acid-catalyzed esterification was carried out for nanodiamonds covalent incorporation into polymer matrix. Zinc chloride was used as a Lewis acid catalyst. Zinc chloride Puriss. p.a., ACS Reagent, Reag. ISO, Reag. Ph. Eur., $\geq 98\%$ was purchased from Honeywell Fluka™ (USA).

4.2 Preparation of test samples

Two types of water-soluble polymers (PVA and PAA) and two types of aqueous suspensions of nanodiamond particles with a size of 5 nm (protonated and deprotonated) were planned for the preparation of samples of film-forming polymer suspensions containing nanodiamonds. The prepared suspensions were to have a variant with a lower and higher nanoparticle content (10 mg ND per 1 g of polymer and 100 mg ND per 1 g of polymer respectively). The polymer concentration in all dispersion samples was to be 1 g/100 ml. Thus, 8 types of suspensions were prepared for the production of a thin films (coatings) on the plastic substrate of packaging film. Details of the samples of suspensions are presented in Table 4.3.

Tab. 4.3: List of prepared samples of film-forming suspensions.

Sample name	Polymer solution	Polymer conc. [mg/100 ml]	ND type	ND conc. [mg/100 ml]
ND-P/PVA 10 S	Poly(vinyl alcohol)	1000	ND-P	10
ND-P/PVA 100 S				100
ND-N/PVA 10 S			ND-N	10
ND-N/PVA 100 S				100
ND-P/PAA 10 S	Poly(acrylic acid)		ND-P	10
ND-P/PAA 100 S				100
ND-N/PAA 10 S			ND-N	10
ND-N/PAA 100 S				100

The produced thin films (coatings), regardless of the surface on which they were cast, were marked as shown in Table 4.4. This table also provides information on the nanodiamond content of each film (coating).

Tab. 4.4: List of prepared samples of polymer-nanodiamond composite coatings.

Sample name	Polymer matrix	ND type	ND/Polymer mass ratio	ND conc. (mass fraction)	ND conc. (volume fraction)
ND-P/PVA 10 F	Poly(vinyl alcohol)	ND-P	1:100	0,99%	0,36%
ND-P/PVA 100 F			1:10	9,09%	3,48%
ND-N/PVA 10 F		ND-N	1:100	0,99%	0,36%
ND-N/PVA 100 F			1:10	9,09%	3,48%
ND-P/PAA 10 F	Poly(acrylic acid)	ND-P	1:100	0,99%	0,43%
ND-P/PAA 100 F			1:10	9,09%	4,18%
ND-N/PAA 10 F		ND-N	1:100	0,99%	0,43%
ND-N/PAA 100 F			1:10	9,09%	4,18%

4.2.1 Film-forming suspension preparation

Nanodiamond suspensions based on a poly(vinyl alcohol) solution:

1 L of DI-water in Erlenmeyer flask was heated to 90°C on a hot plate magnetic stirrer equipped with temperature probe. Then the 40 g of poly(vinyl alcohol) powder was added lightly and slowly into the water while stirring continuously allowing each pinch to

dissolve completely otherwise the viscous mass of wet polymer could stick together and clings to the wall of the flask. The procedure for dissolving 40 g of polymer took about 20 minutes. 25 ml of the prepared solution was transferred with pipette to a 100 ml volumetric flask with a plastic stopper, 1 or 10 ml of the appropriate nanodiamond suspension was added depending on the assumed final concentration, and the flask was filled up to 100 ml with DI-water. The closed flask was thoroughly mixed by rotating it several times. The contents of the flask were poured into a 100 ml beaker and subjected to 5 minutes of sonication using an ultrasonic homogenizer equipped with a sonotrode with a diameter of 5 mm. 1 liter of the prepared 4% (w/v) PVA aqueous solution was sufficient for prepare all the planned film-forming suspensions.

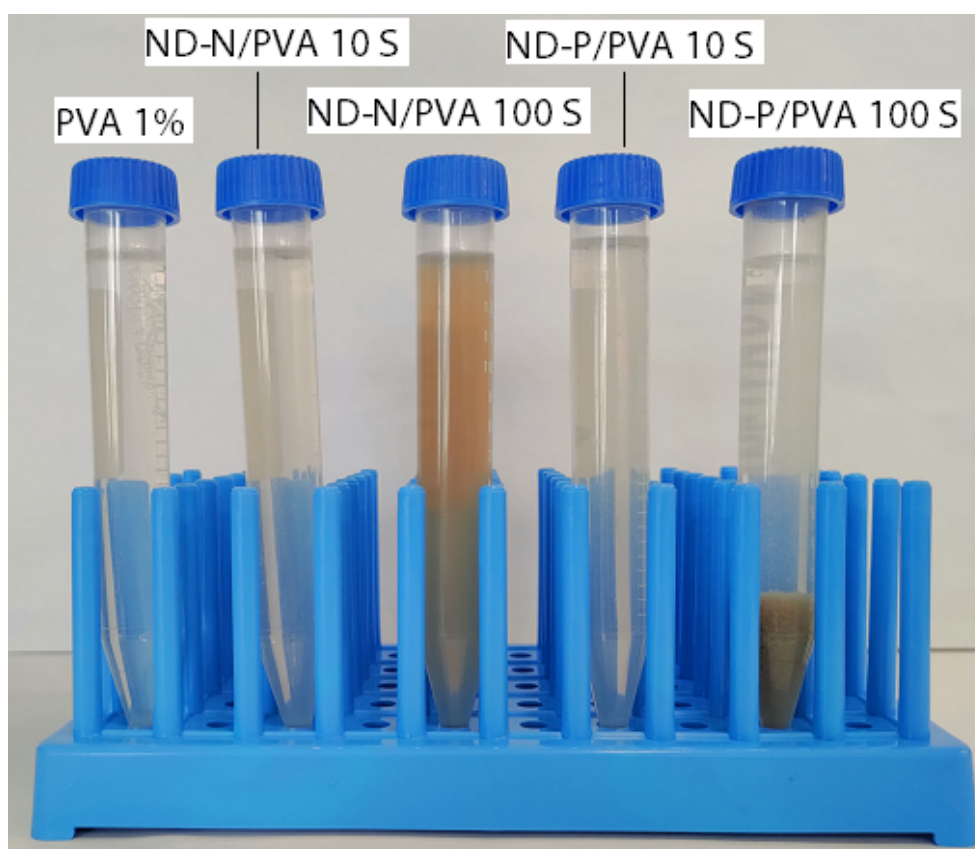


Fig. 4.5: Prepared PVA-based suspensions.

Nanodiamond suspensions based on a poly(acrylic acid) solution:

4 g of 25% (w/w) poly(acrylic acid) aqueous solution and 1 or 10 ml of the appropriate nanodiamond suspension (depending on the assumed final concentration) were added to a 100 ml volumetric flask with a plastic stopper. Then, the flask was filled up to 100 ml with DI-water. The closed flask was thoroughly mixed by rotating it several times. The contents

of the flask were poured into a 100 ml beaker and subjected to 5 minutes of sonication using an ultrasonic homogenizer equipped with a sonotrode with a diameter of 5 mm.

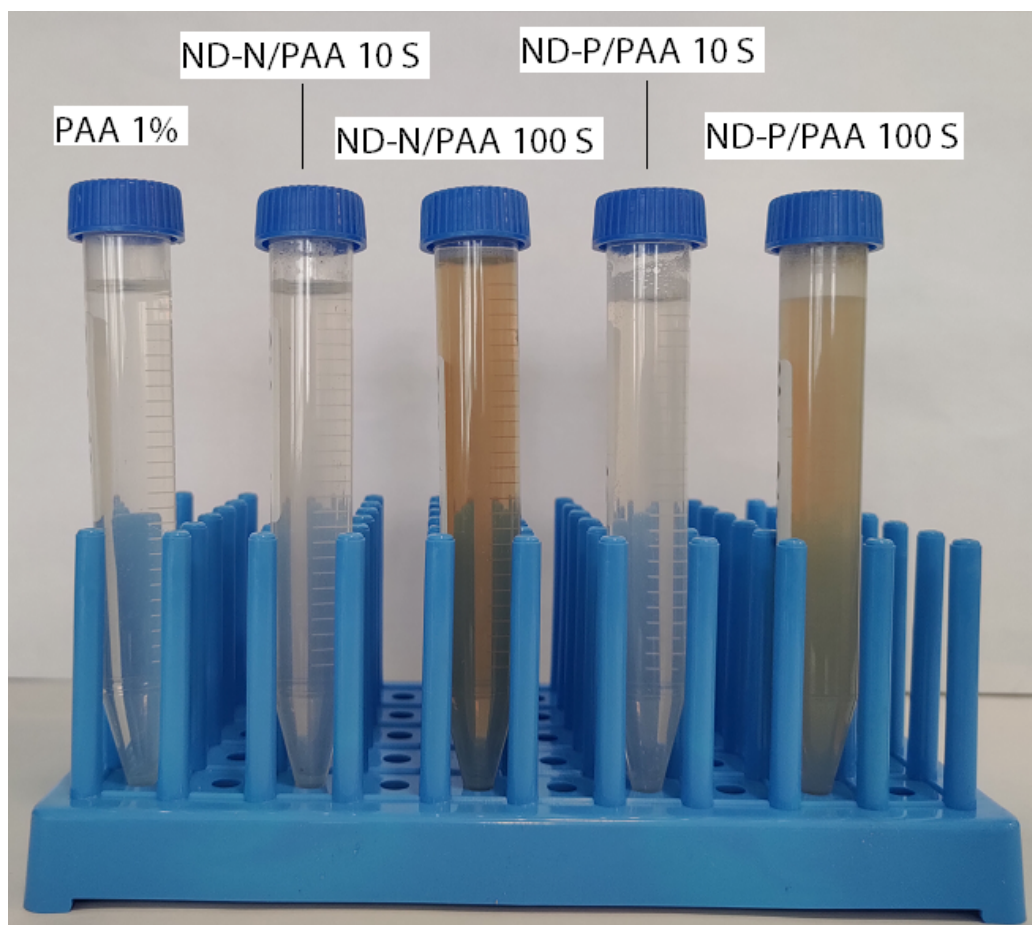


Fig.4.6: Prepared PAA-based suspensions.

4.2.2 Substrate surface activation by plasma treatment

In order to increase the wettability of the plastic substrate surface by aqueous suspensions, which in turn will increase the adhesion of the formed thin films, the plasma treatment was performed. A handheld Piezobrush PZ2 device (relyon plasma GmbH, Germany) was used for this task. It is equipped with cold atmospheric plasma generator – CeraPlas™, which is made of piezoelectric material based on a hard lead zirconium titanate with co-fired copper electrodes. The working parameters of piezoelectric component responsible for plasma discharge are shown Table 4.5.

Tab. 4.5: Operating parameters of plasma generator.

Operating voltage	12 to 24 V _{pp}
Operating frequency	~ 50 kHz
Output voltage	Up to 15 kV
Transferred power	10 W (max.)
Plasma temperature	<50°C
Processing gas	Air
Ozone generation rate	20 ppm (at 8 W)

Immediately before casting the suspension onto a piece of plastic material, which was stuck to HDPE plate, the plasma generated from the device was swept over its surface, moving the device at a speed of approx. 15 mm/s, keeping the nozzle of the device at a height of approx. 5 mm, in a manner of making 1 cm wide “stripes” side by side of the entire material surface.

4.2.3 Suspension casting

The production of thin films (coatings) consisted in casting the suspension. The suspensions were cast on a section of the previously plasma-activated plastic packaging film stuck to the glass microscope slide or directly on the slide, depending on the test performed. 500 µl of the freshly prepared suspension was poured onto a surface with dimensions of 76×26 mm. A thin plastic rod was used to spread evenly the liquid over the entire surface. The sample prepared in this way was placed in a drying chamber with natural convection at a temperature of 105°C for 10 minutes. As a result, after evaporation of the water, which is the dispersion medium for the suspension, a polymer coating adhering permanently to the substrate was obtained.

4.2.4 Incorporation of NDP to polymer matrix via chemical bonding

An attempt was made to carry out an esterification reaction which leads to covalent incorporation of functionalized nanodiamond into a polymer network. Carboxylated and hydroxylated nanodiamonds with poly(vinyl alcohol) and poly(acrylic acid), respectively, were reacted. Figure 4.7 shows schemes of planned chemical reactions whereby the functional groups on the nanodiamond surface are bound to the polymer chain in the acid catalyzed esterification. The diagrams have been simplified for greater clarity – there is

much more than one functional group on the surface of the nanodiamond particle. Tables 4.6 and 4.7 show the detailed composition of the suspensions with catalyst (zinc chloride, $ZnCl_2$) and the coatings obtained therefrom.

Tab. 4.6: List of prepared samples of film-forming suspensions containing catalyst ($ZnCl_2$).

Sample name	Polymer solution	Polymer conc. [mg/100 ml]	ND type	ND conc. [mg/100 ml]	Catalyst conc. [mg/100 ml]
ND-N/PVA 10 CAT S	Poly(vinyl alcohol)	1000	ND-N	10	10
ND-P/PAA 10 CAT S	Poly(acrylic acid)		ND-P		

Tab. 4.7: List of prepared samples of polymer-nanodiamond composite coatings made of suspensions containing catalyst ($ZnCl_2$).

Sample name	Polymer matrix	ND type	ND/Polymer mass ratio	ND conc. (mass fraction)	Catalyst conc. (mass fraction)
ND-N/PVA 10 CAT F	Poly(vinyl alcohol)	ND-N	1:100	0,98%	0,98%
ND-P/PAA 10 CAT F	Poly(acrylic acid)	ND-P			

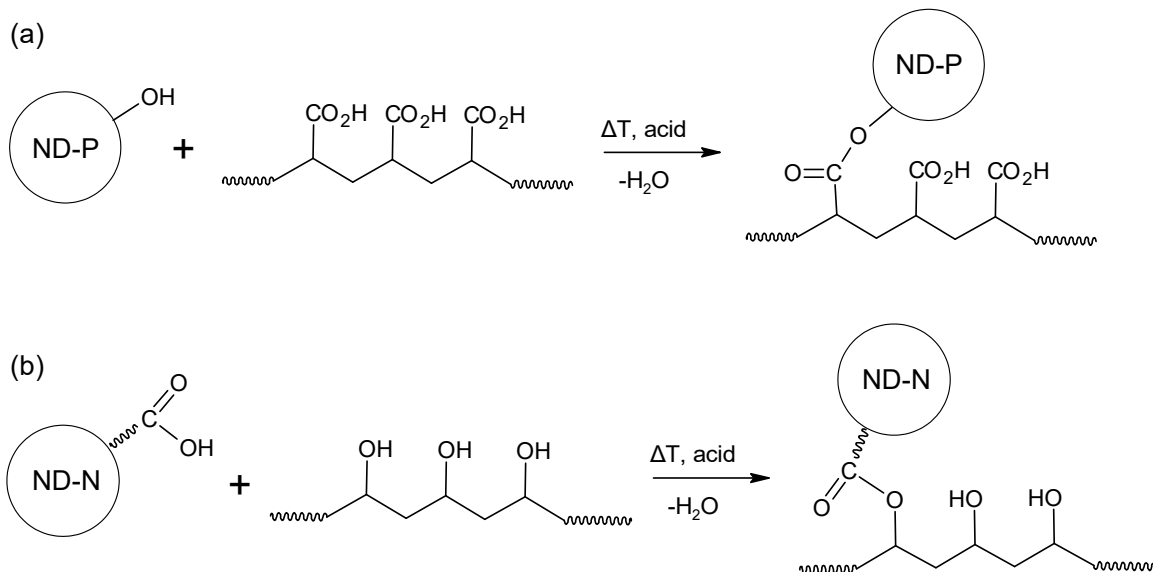


Fig. 4.7: Reaction schemes for esterification of: (a) hydroxylated nanodiamond (ND-P) with poly(acrylic acid); (b) carboxylated nanodiamond (ND-N) with poly(vinyl alcohol).

4.3 Characterization of suspensions containing NDP

4.3.1 pH and suspensions stability

The pH of the prepared film-forming suspensions was measured and their stability was determined. In addition, the pH of pure PVA and PAA solutions as well as the pH of the initial, concentrated carboxylated and hydroxylated nanodiamond suspensions were checked. The pH measurements were carried out using a laboratory pH meter Mettler-Toledo FiveEasy F20-Standard equipped with LE438 electrode. Before the tests, a 2-point calibration with pH 6.86 and pH 4.01 buffer solutions was performed. The instrument's pH measuring resolution was 0.01 pH and the limits of error were ± 0.01 pH. Tests were performed three times for each sample. The results are presented in Tables 4.8 and 4.9.

Tab. 4.8: pH values of used initial nanodiamond suspensions.

Nanodiamond suspension	pH				
	Measurement No.			Mean value	Std Dev
	1	2	3		
ND5nmPH2O	5.09	5.11	5.15	5.12	0.02
ND5nmNH2O	7.35	7.45	7.39	7.40	0.03

Tab. 4.9: pH values of prepared film-forming suspensions/solutions.

Sample			pH				
Polymer (1% w/v aq. solution)	Nanodiamond	Nanodiamond conc. [mg ND/g Polymer]	Measurement No.			Mean value	Std Dev
			1	2	3		
PVA	-	-	5.75	5.58	5.65	5.66	0.05
	ND-P	10	6.60	6.55	6.71	6.62	0.05
		100	6.91	6.81	7.02	6.91	0.06
	ND-N	10	7.26	7.28	7.30	7.28	0.01
		100	7.47	7.48	7.49	7.48	0.01
PAA	-	-	3.50	3.49	3.49	3.49	0.00
	ND-P	10	2.89	2.82	2.63	2.78	0.08
		100	2.61	2.51	2.75	2.62	0.07
	ND-N	10	2.95	3.01	2.88	2.95	0.04
		100	3.45	3.33	3.41	3.40	0.04

PAA and PVA polymer solutions are acidic – PAA stronger (pH 3.49) than PVA (pH 5.66). In the case of adding nanodiamond to the PVA solution, the pH increased, with the addition of ND-N causing a greater increase than the addition of ND-P. A completely different situation was observed in the case of adding nanodiamonds to the PAA solution. The addition of positively charged nanodiamond particles caused a significant decrease in pH, while the addition of more nanodiamond particles caused a greater decrease. The suspension containing 100 mg of ND-N per 1 g of PAA has the same pH as the PAA solution without the addition of nanodiamond, but the pH of the suspension containing 10 mg of ND-N per 1 g of PAA is visibly lower.

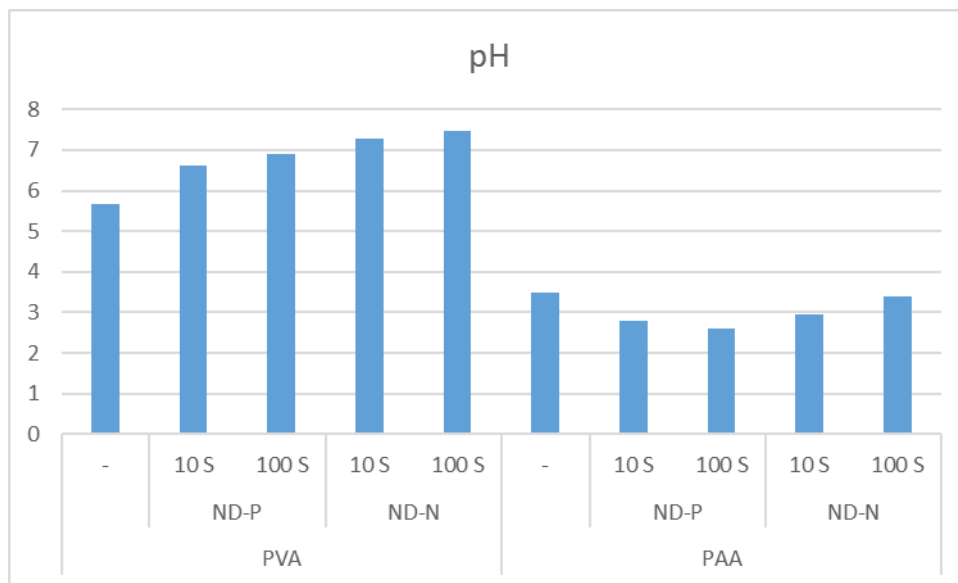


Fig. 4.8: pH values of prepared film-forming suspensions/solutions.

The stability of the suspensions depends on their Zeta potential, which in turn depends on the pH. That is why pH control is so important to maintain the required stability. The pH of the initial high-concentrated suspensions was selected so that their absolute value of zeta potential was over 35 mV, then they achieve the highest stability and there is no aggregation of particles and their sedimentation. Due to specific surface groups on nanodiamonds, they are deprotonated (negatively charged, ND-N) or protonated (positively charged, ND-P) when dispersed in deionized water. The suspension of hydroxylated nanodiamond with a positive Zeta potential has the highest stability at moderate acidic pH, while the suspension of carboxylated nanodiamond with a negative Zeta potential at slightly alkaline pH.

Table 4.10 shows the actual stability of the suspensions prepared in this study. All PAA-based polymer-nanodiamond suspensions are stable. No polymer precipitation or nanoparticle aggregation and sedimentation were observed over a longer period (one month). The situation is different in the case of PVA-based suspensions. The PVA suspension with a higher content of ND-P (100 mg / 1 g of polymer) turned out to be highly unstable. Within a few minutes after preparation of the suspension, the polymer flocculates together with large, aggregated nanodiamond particles and sinks to the bottom. A similar phenomenon is observed in the case of the PVA suspension with ND-N (100 mg / 1 g of polymer), but here the process begins only after 2 days and is much slower. It can be concluded that a situation occurs here when the colloidal stability of nanoparticles is to some extent independent of pH, whereas stability is based upon their electrostatic repulsion between charged particles such as nanodiamonds. Upon addition of ions or locally charged groups/dipols (like hydroxyl groups in PVA) they electrostatically interact with surface groups of NDs and this degrades the colloidal stability. At the increased pH resulting from the addition of NDs, the PVA hydroxyl groups are deprotonated, wherefore the polymer molecules are probably adsorbed on positively charged NDs. They do not repulse each other anymore and this cause aggregation.

Tab. 4.10: Stability of verified suspensions/solutions and their pH.

Polymer \ ND	ND						
	None	ND5nmP H2O 10mg/mL	ND5nmN H2O 10mg/mL	ND5nmP 10mg / 1g of polymer	ND5nmP 100mg / 1g of polymer	ND5nmN 10mg / 1g of polymer	ND5nmN 100mg / 1g of polymer
None	-	5.12 ✓	7.40 ✓	-	-	-	-
PAA in DI-water 1 g / 100 ml	3.49 ✓	-	-	2,78 ✓	2.62 ✓	2.95 ✓	3.40 ✓
PVA in DI-water 1 g / 100 ml	5.66 ✓	-	-	6.62 ✓	6.91 ✗	7.28 ✓	7.48 ○

✓ - stable solution/suspension

○ - moderately stable suspension

✗ - unstable suspension

It should be mentioned that the range of stability of the carboxylated nanodiamond to the pH of the suspension is significantly greater than that of the hydroxylated nanodiamond. Thus, in the case of ND-N this is a moderate acidic to moderate alkaline pH range, while in the case of ND-P high stability is only achieved with a moderate to slightly acidic pH.

4.3.2 Surface tension

Measurements of the surface tension of the prepared suspensions were carried out using two methods: Du Noüy ring method (according to ISO 1409:1995(E) standard) and Pendant drop method (according to ISO 19403-1:2017(E) and ISO 19403-3:2017(E) standards). The purpose of carrying out tests using these two very different techniques was to confront them and compare the obtained results. It should be taken into account that the Pendant drop test is a much newer method which uses advanced imaging equipment with the state of the art analytical software.

Du Noüy ring method:

The method described in ISO 1409 standard is suitable, valid for the determination of the surface tension of polymer dispersions and rubber latices (natural and synthetic) with a viscosity less than 200 mPa·s. It consists in connecting a suspended thin wire ring to a du Nouy tensiometer and immersing it in the tested liquid, and then slowly pulling it out. Just before the ring is detached from the liquid surface, the required force is reached its maximum. This force is measured with a measuring device (inductive sensor). In the tests, a platinum ring with a nominal circumference of 60 mm made of wire with a nominal radius of 0.185 mm was used. Before starting the measurements, the ring was cleaned by rinsing with water and burning in the oxidizing part of the Bunsen burner. The tensiometer has been calibrated according to reference liquid – distilled water. The 50 cm³ cup with the test liquid was thermostated to 23°C. The vessel was then placed on the movable stand of the device below the tensiometer ring. The stand was lifted until the liquid touched the ring and then the ring was immersed to a depth of 5 mm. The ring was then pulled at a speed of 0.1 mm/s by lowering the stand and the maximum tension was recorded in millinewtons per meter. Tests were performed three times for each sample. The results are shown in Table 4.11.

Tab. 4.11: Surface tension of suspensions/solutions determined by Du Noüy ring method.

Sample			Surface tension [mN/m]				
Polymer (1% _w aq. solution)	Nanodiamond	Nanodiamond conc. [mg ND/ g Polymer]	Measurement No.			Mean value	Std Dev
			1	2	3		
PVA	-	-	46.7626	46.6594	46.5483	46.6568	0.0619
	ND-P	10	46.3052	46.1942	46.0911	46.1968	0.0618
		100	47.3087	47.1817	47.0785	47.1896	0.0618
	ND-N	10	46.6100	46.5148	46.4197	47.1896	0.0666
		100	48.2716	48.6456	48.6297	48.5156	0.1221
PAA	-	-	65.0905	65.2300	65.6313	65.2273	0.0782
	ND-P	10	55.6195	55.7647	55.9100	55.7648	0.0839
		100	54.2157	54.1675	54.0308	54.1380	0.0554
	ND-N	10	57.0794	57.2817	57.2169	57.1927	0.0596
		100	61.1299	61.0728	61.0484	61.0837	0.0241

Pendant drop method:

The Pendant drop method described in the mentioned ISO 19403-3 standards can be applied for the characterization of liquid coating materials with non-Newtonian rheology. This method consists in calculation the surface tension from the shape of the pendant drop of the tested liquid in accordance with the Young-Laplace equation. The drop to be tested is captured hanging from a needle. Measurements were performed on an OCA 200 instrument made by DataPhysics Instruments GmbH (Germany). The dedicated SCA Software provided by the manufacturer was used to operate the instrument and process the obtained data. The tested liquid was introduced into the dosing unit consisting of graduated micro syringe and needle with the nominal outer diameter of 0.51 mm. Then a preferably large pendant drop was produced. The image was zoomed, focused and length calibrated in order to determinate the scale. The image of drop with its contour was captured. The software adapted the mathematical model, which is the basis of the evaluation, to the drop contour. The drop contour must be axially symmetrical. Otherwise the correct evaluation is not possible. Moreover, the fit error (Err), which describes the quality of adaptation, should be less than 1 μm . During the performed tests, each measurement met this condition. Tests were performed six times for each sample. The results are shown in Table 4.12.

Tab. 4.12: Surface tension of suspensions/solutions determined by the pendant drop method.

Sample			Surface tension [mN/m]							
Polymer (1% _w t aq. solution)	ND	ND conc. [mg ND/ g Polymer]	Measurement No.						Mean value	Std Dev
			1	2	3	4	5	6		
PVA	-	-	49.994	51.064	49.670	51.220	51.108	49.325	50.397	0.340
	ND-P	10/1	39.091	38.903	38.972	38.992	38.617	38.786	38.894	0.069
		100/1	47.628	48.675	51.298	49.065	49.414	48.218	49.050	0.518
	ND-N	10/1	51.008	50.500	51.002	50.897	51.004	50.290	50.783	0.127
		100/1	49.325	50.783	50.513	50.545	50.338	52.433	50.656	0.411
PAA	-	-	69.716	69.721	69.593	69.706	70.033	69.652	69.737	0.062
	ND-P	10/1	65.585	65.978	65.871	65.815	65.348	64.451	65.508	0.231
		100/1	65.110	63.960	64.382	64.554	65.050	65.167	64.704	0.198
	ND-N	10/1	51.472	51.599	50.586	50.987	51.032	51.354	51.172	0.153
		100/1	68.291	69.378	69.361	69.148	68.978	69.002	69.026	0.163

To better visualize the differences, the graph in Fig. 4.9 summarizes the measurement results obtained with the two methods. There are slight differences between the results determined by different methods. In most cases, higher surface tension values were determined using the hanging drop method. Although the Du Noüy ring method is a technique that was developed in the past and is greater error burdened, the results obtained from it seem to be more reliable and fall into place. Therefore, further analyzes will be based on the results obtained by the Du Noüy ring method.

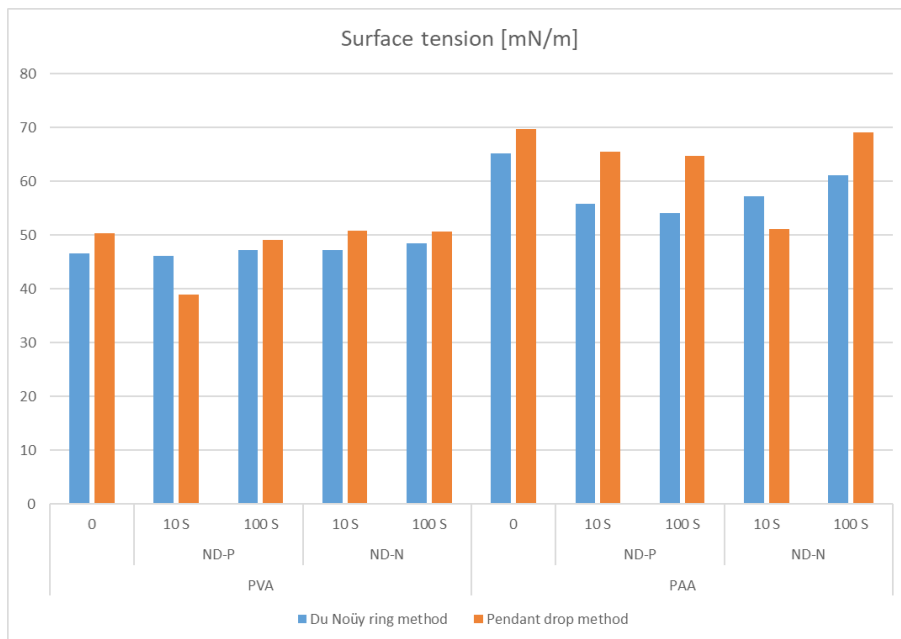


Fig. 4.9: Mean values of suspensions/solutions surface tension determined by Du Noüy ring method (blue) and Pendant drop method (orange).

A 1% solution of poly(acrylic acid) is characterized by about 40% higher surface tension than a 1% solution of poly(vinyl alcohol). Nanodiamond suspensions based on these solutions show a similar trend. In the case of suspensions based on the PVA solution, the addition of nanodiamonds does not change their surface tension (in the case of the sample with the addition of 10 mg ND-P per 1 g of polymer tested by the pendant drop method, such an outlier result may be the cause of high kinetic instability of the suspension). The addition of nanodiamond particles to the PAA solution results in a maximum reduction of the surface tension of the liquid by several percent. In the case of the sample with the addition of 10 mg of ND-P per 1 g of polymer tested by the pendant drop method, an outlier was not observed during the ring method test.

In the case of PVA-based suspensions, the surface tension is approx. 50 mN/m, regardless of the addition or concentration of the nanodiamond. Also the type of nanodiamond used (ND-P or ND-N) has no effect. In turn, in the case of PAA-based suspensions, the addition of nanodiamond particles causes a slight decrease in surface tension. The decrease is more noticeable with the addition of nanodiamonds with positive Zeta potential (ND-P).

Although surface-functionalized nanodiamonds appear to behave like surfactants, their effect is only visible with a medium with high surface tension (PAA-based suspensions). In the case where the aqueous suspension was prepared on the basis of a surfactant (such as PVA), its surface tension is already relatively low, so the effect of reducing the surface tension is practically imperceptible.

4.4 Characterization of PVA/NDP and PAA/NDP composite films

4.4.1 Infrared spectral analysis of samples subjected to esterification

In order to verify whether the nanodiamond was covalently bound to the polymer matrix as a result of Lewis acid catalyzed esterification reaction, IR spectra of the samples were made. This allowed the analysis of the characteristic bands derived from the functional groups of esters and carboxylic acids. The spectra were made with the ATR technique on a zinc selenide crystal using the SHIMADZU IRTracer-100 instrument.

Figs. 4.10a-c are the FTIR spectra of the PVA-based films, and Figs. 4.11a-c are the FTIR spectra of the PAA-based films. The recorded spectra in Figs. 4.10a and 4.10b are

characteristic spectra of polyvinyl alcohol and no significant differences were observed between them [71,72]. Polyvinyl alcohol has a characteristic absorption associated with stretching vibration of both the O-H and C-O groups. When the spectrum is recorded in the form of a thin film, the O-H stretching vibration of the polyvinyl alcohol appears in the region of 3500-3200 cm^{-1} as a very intense and wide band and C-O stretching vibrations appear in the region of 1260-1050 cm^{-1} . O-H stretching bands at 3319 cm^{-1} and C-O stretching bands at 1140 and 1090 cm^{-1} were observed for the tested PVA films. Moreover, the spectrum shows the C-H stretching band at 2940 cm^{-1} .

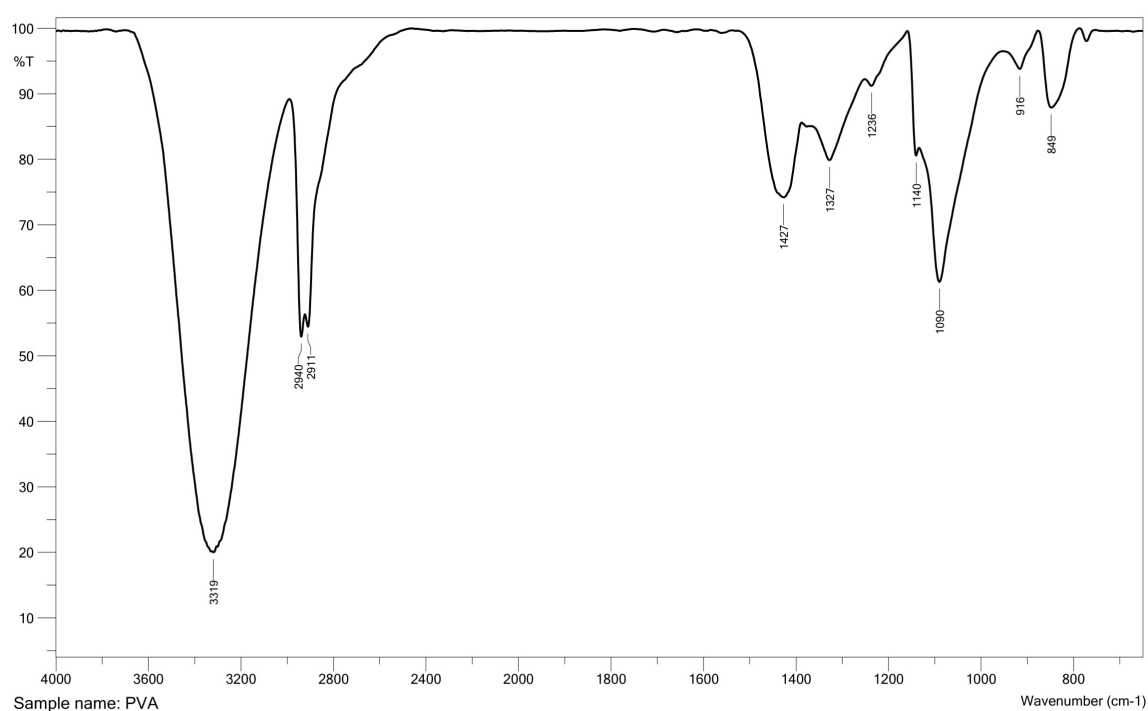


Fig. 4.10a: FTIR spectrum of pure PVA film (without ND, without catalyst).

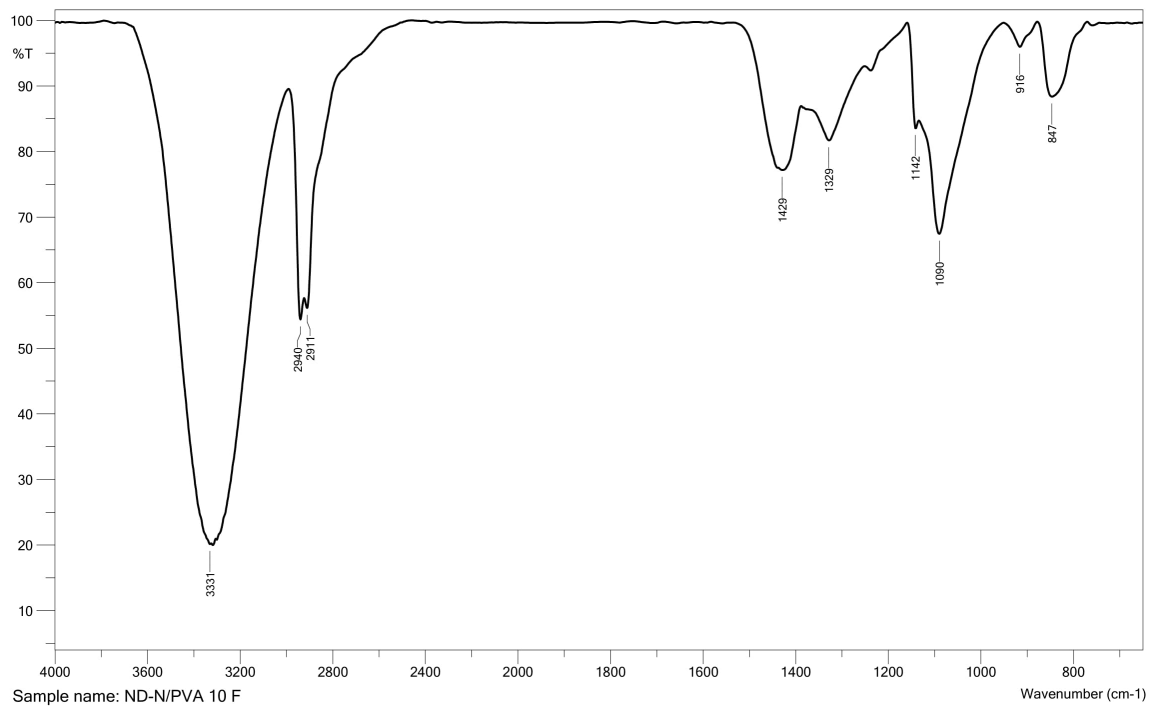


Fig. 4.10b: FTIR spectrum of ND-N/PVA 10 F film (with ND, without catalyst).

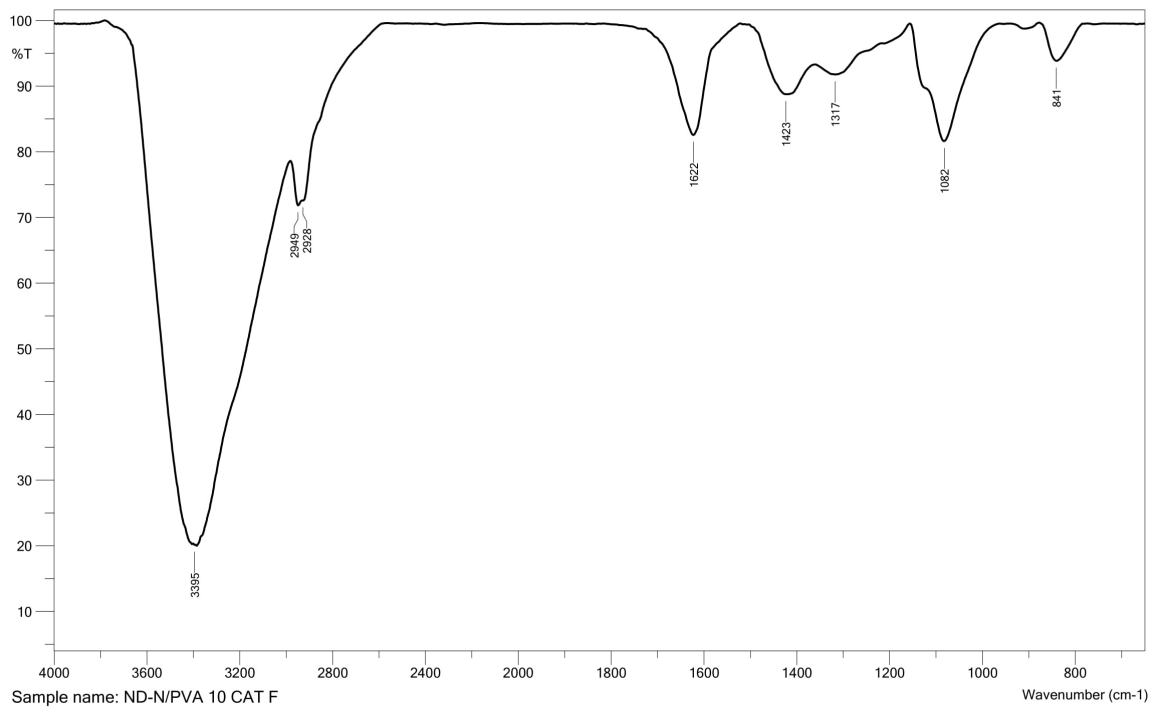


Fig. 4.10c: FTIR spectrum of ND-N/PVA 10 CAT F film (with ND and catalyst).

Figs. 4.11a and 4.11b show the spectra of pure PAA film and PAA film with nanodiamond, respectively. In Fig. 4.11a, polyacrylic acid shows a very wide band of O–H stretching vibrations, similar to polyvinyl alcohol. This band appears in the range of $3400\text{--}2600\text{ cm}^{-1}$, with a maximum at 3103 cm^{-1} . The O–H band in the mentioned range is superimposed on

the C–H stretching vibrations bands, however it is clearly visible at 2940 cm^{-1} . A strong, narrow band of the C=O stretching vibrations appears at 1699 cm^{-1} , and the C–O stretching band at 1229 cm^{-1} . In the range of $1450\text{--}1400\text{ cm}^{-1}$, O–H bending bands appear. The spectrum in Fig. 4.11b differs only in the range of $1450\text{--}1400\text{ cm}^{-1}$ which is related to the O–H bending vibration, but it is a very important band range in the context of the performed esterification reactions in this research.

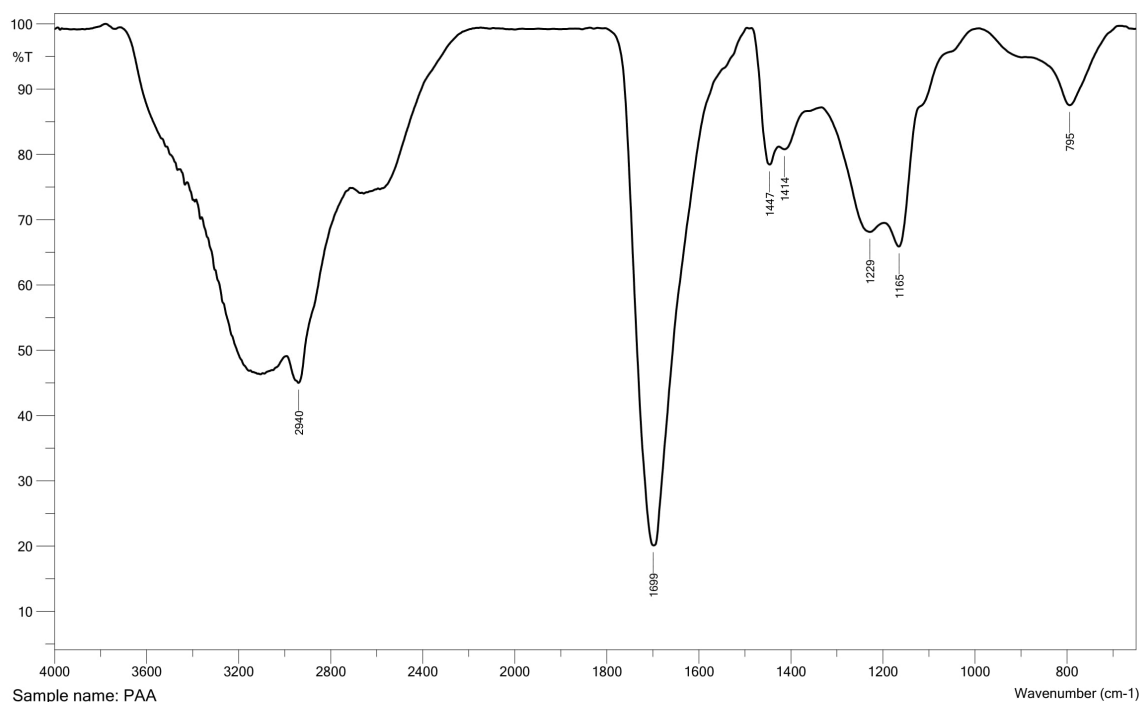


Fig. 4.11a: FTIR spectrum of pure PAA film (without ND, without catalyst).

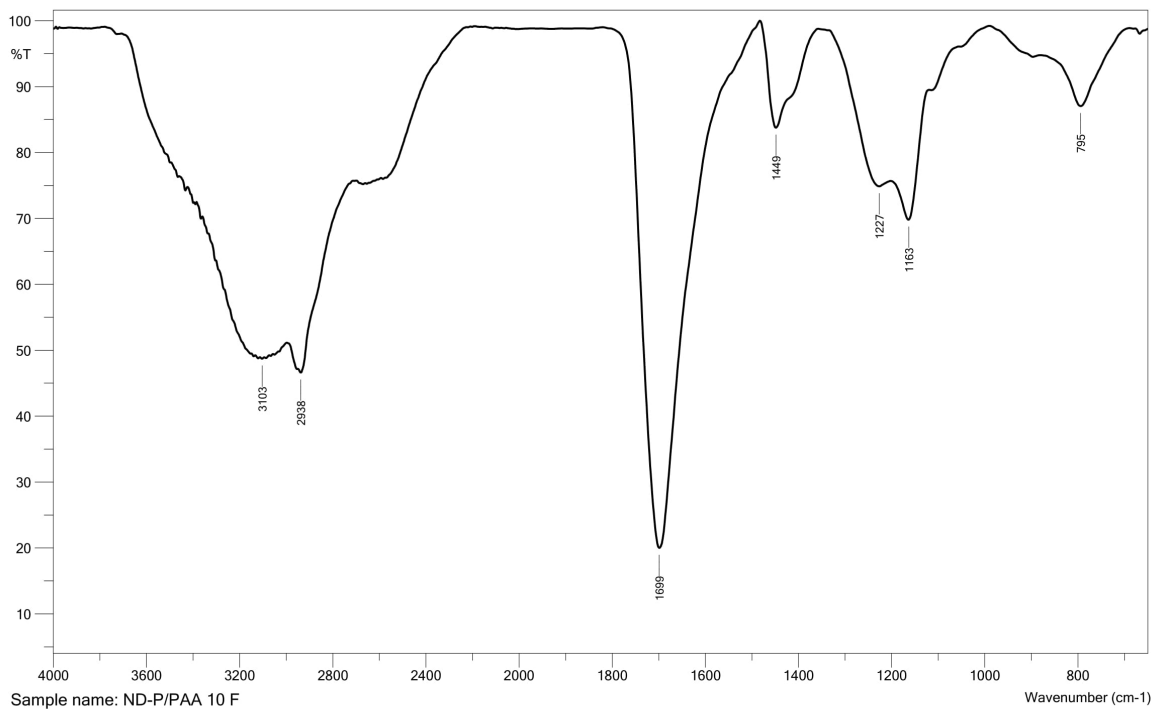


Fig. 4.11b: FTIR spectrum of ND-P/PAA 10 F film (with ND, without catalyst).

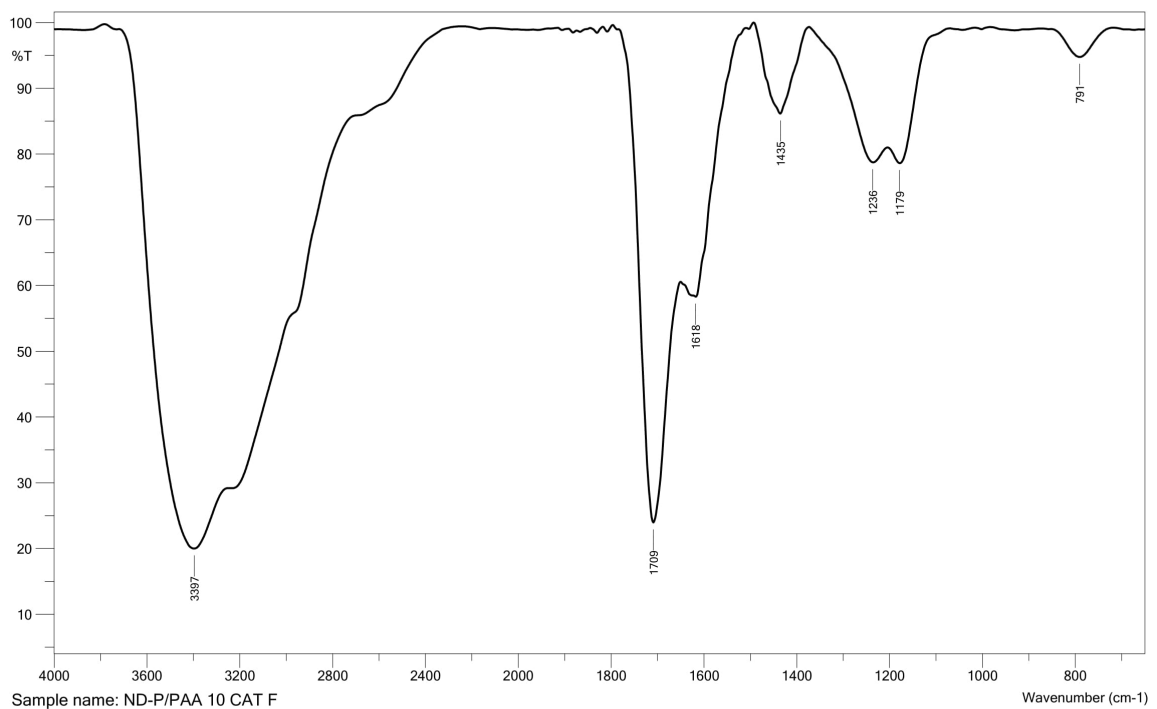


Fig. 4.11c: FTIR spectrum of ND-P/PAA 10 CAT F film (with ND and catalyst).

In the spectra of the samples containing the catalyst (Fig. 4.10c and Fig. 4.11c), very strong bands are visible: the O-H stretching band in the range of 3600-3000 cm⁻¹ and the H-O-H bending vibration at 1620 cm⁻¹. Both indicate the presence of water molecules. This is because the zinc chloride used as a catalyst is a hygroscopic substance and even drying at a

temperature above 100°C is not able to completely remove them from the reaction medium, especially since water is also a product of the esterification that must be constantly removed to ensure the progress of the reaction. The strong bands coming from the water make the remaining bands much weaker. This makes it difficult to compare the spectrum of the sample with the catalyst to those without the catalyst.

For the aforementioned reason, the absorbance of the spectra was normalized by aligning the bands within the fingerprint region (from about 1500 to 500 cm^{-1}). The normalized spectra of the PVA/ND-N films are shown in Fig. 4.12, and the normalized spectra of the PAA/ND-P films in Fig. 4.13.

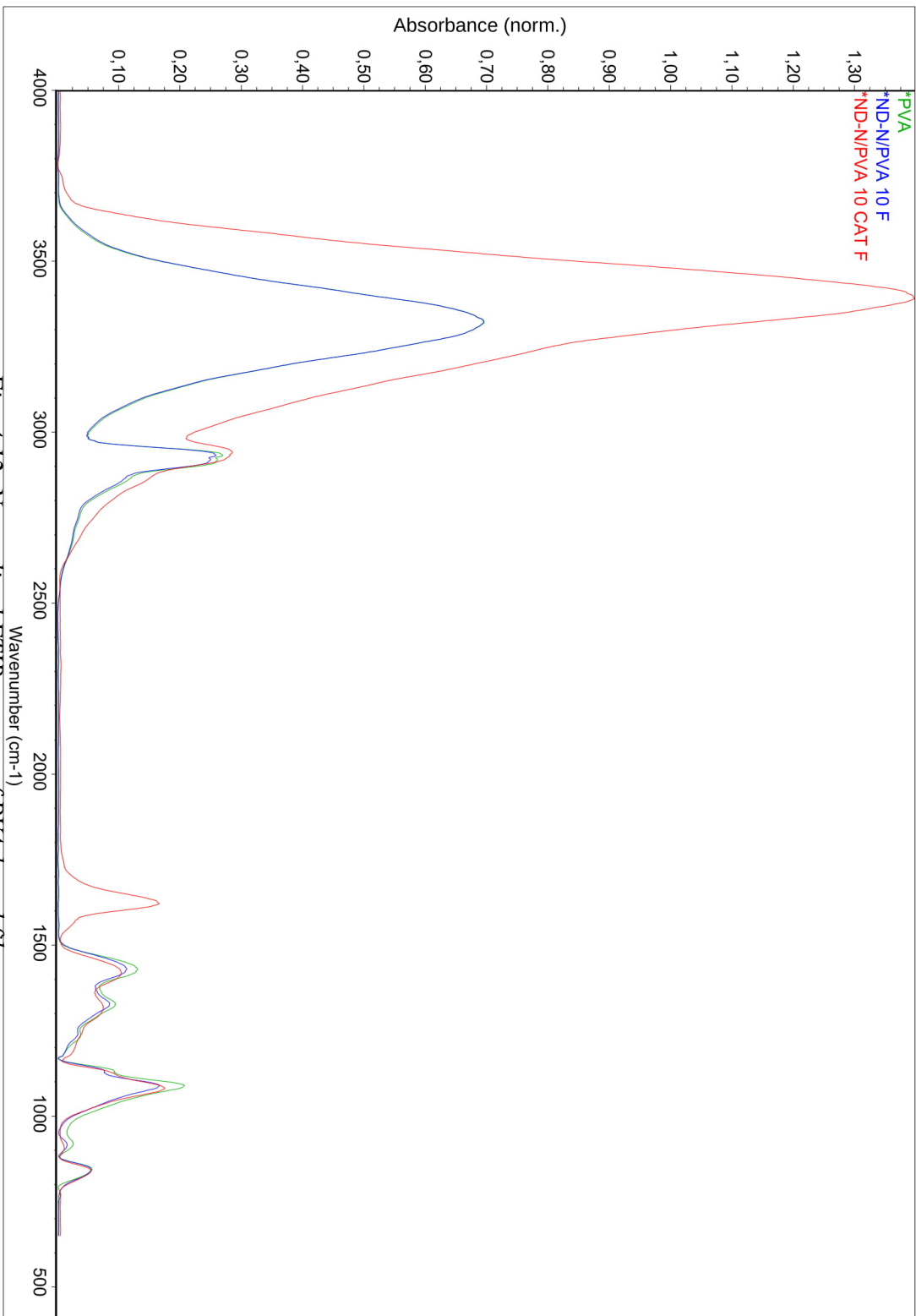


Fig. 4.12: Normalized FTIR spectra of PVA-based films.

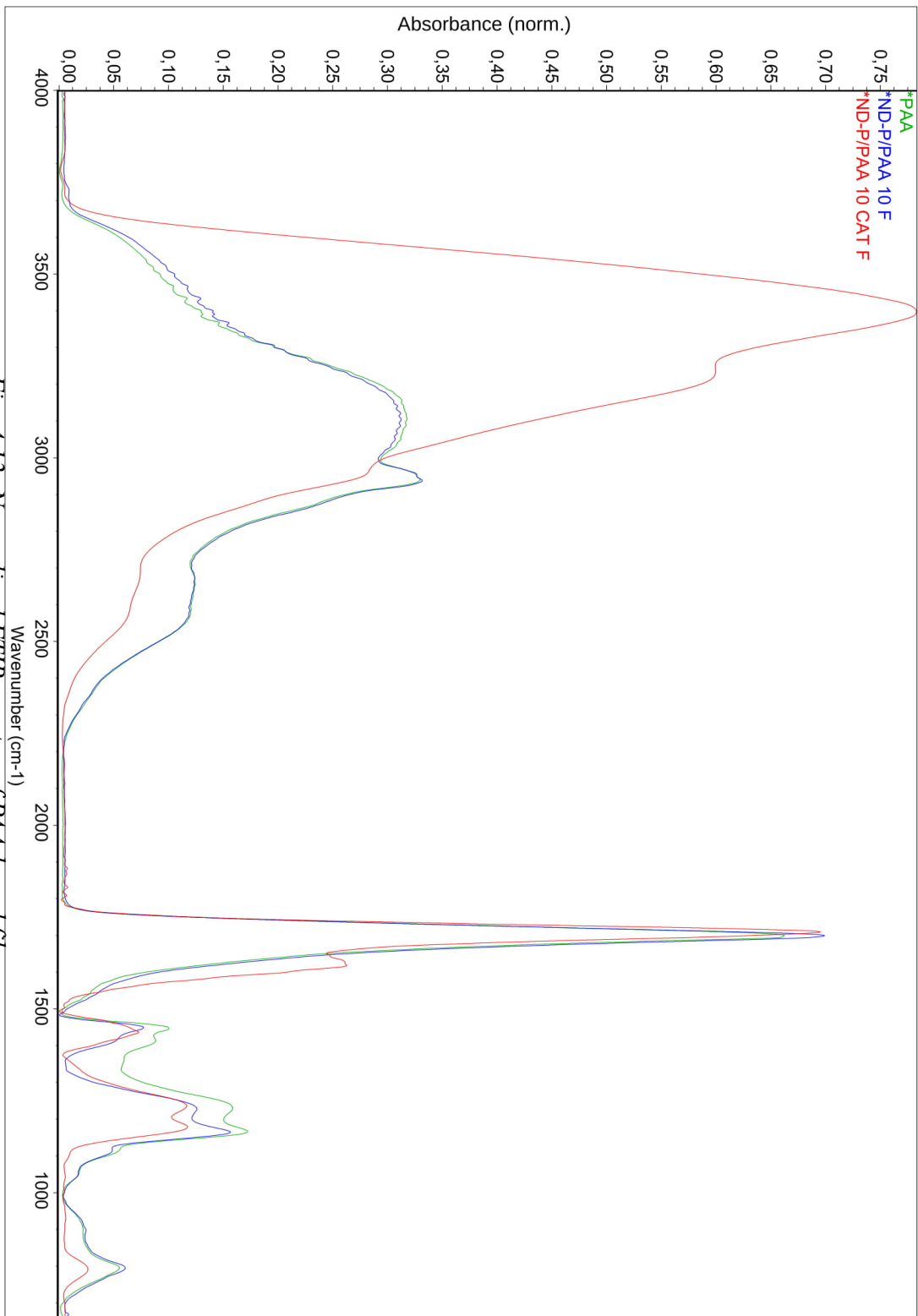


Fig. 4.13: Normalized FTIR spectra of PAA-based films.

There are no significant differences between the spectra of PVA/ND-N films. Apart from the previously mentioned strong bands from water bound to ZnCl_2 , only the bands typical for poly(vinyl alcohol) are visible: a wide and strong band of stretching vibrations of O-H group (3395 cm^{-1}) and C-O bonds ($\sim 1100\text{ cm}^{-1}$) and bands of C-H stretching vibrations originating from the alkyl chain ($2950\text{-}2910\text{ cm}^{-1}$).

The situation is different in the case of PAA/ND-P films. There are visible differences between the recorded spectra. Although it is not easy to identify which bands of C-O and C=O stretching vibrations come from the carboxylic acid and which from the ester (they have absorption bands in a similar range), there are indications that the esterification reaction took place here, also in the situation without the use of a catalyst.

In Figure 4.14, which is a summary of the FTIR spectra of PAA films in the key wavelength range, one can observe a clear change of two bands in the spectra of the mentioned films – bands at 900 and 1410 cm^{-1} . These bands are responsible for the bending vibrations of the OH group and prove its presence in the carboxyl group. These bands are the strongest in the spectrum of the PAA film, weaker in the spectrum of the PAA film with the addition of nanodiamond (ND-P/PAA 10 F), and practically absent in the spectrum of the film to which the catalyst was added (ND-P/PAA 10 CAT F).

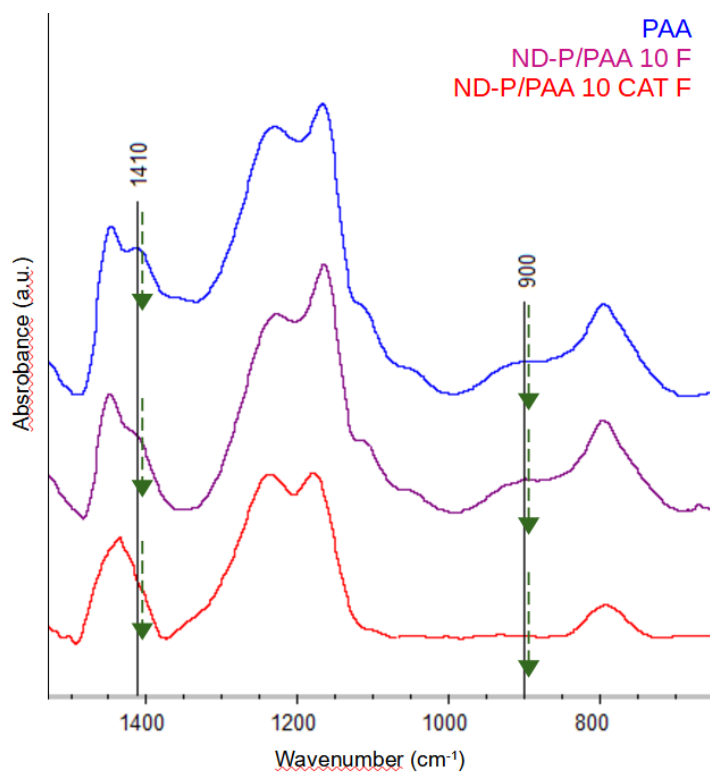


Fig. 4.14: Relevant bands change in the FTIR spectra of PAA-based films: 1410 cm^{-1} and 900 cm^{-1} . There is a weakening of the bands associated with the -OH group on the carboxyl carbon.

This proves the reaction of the carboxyl group in the films ND-P/PAA 10 F and ND-P/PAA 10 CAT F. As a result of this reaction, the -OH bond of the R¹-C(O)-OH carboxyl group is replaced by the -O-R² bond forming thus the ester group R¹-C(O)-O-R² (R¹ and R² are alkyls derived from poly (acrylic acid) and nanodiamond, respectively). This reaction is called esterification. Figure 4.15 shows the scheme with the mechanism of esterification catalyzed by Lewis acid – zinc chloride.

The reaction took place between the carboxyl groups of the polyacrylic acid and the hydroxyl groups on the surface of the nanodiamond. This reaction takes place in an acidic environment. In the case of the ND-P/PAA 10F film, the reaction went poorly. It can be seen that some of the carboxyl groups have reacted, but their presence is still visible.

The situation is different in the case of the ND-P / PAA 10 CAT F film in which the incoming reaction was catalyzed by Lewis acid (ZnCl₂). The complete disappearance of the 900 cm⁻¹ band and the weakening of the 1410 cm⁻¹ band relative to the same band were observed in the spectra of the ND-P/PAA 10 F and PAA films. This proves that the carboxyl groups of the poly (acrylic acid) react at a very advanced level.

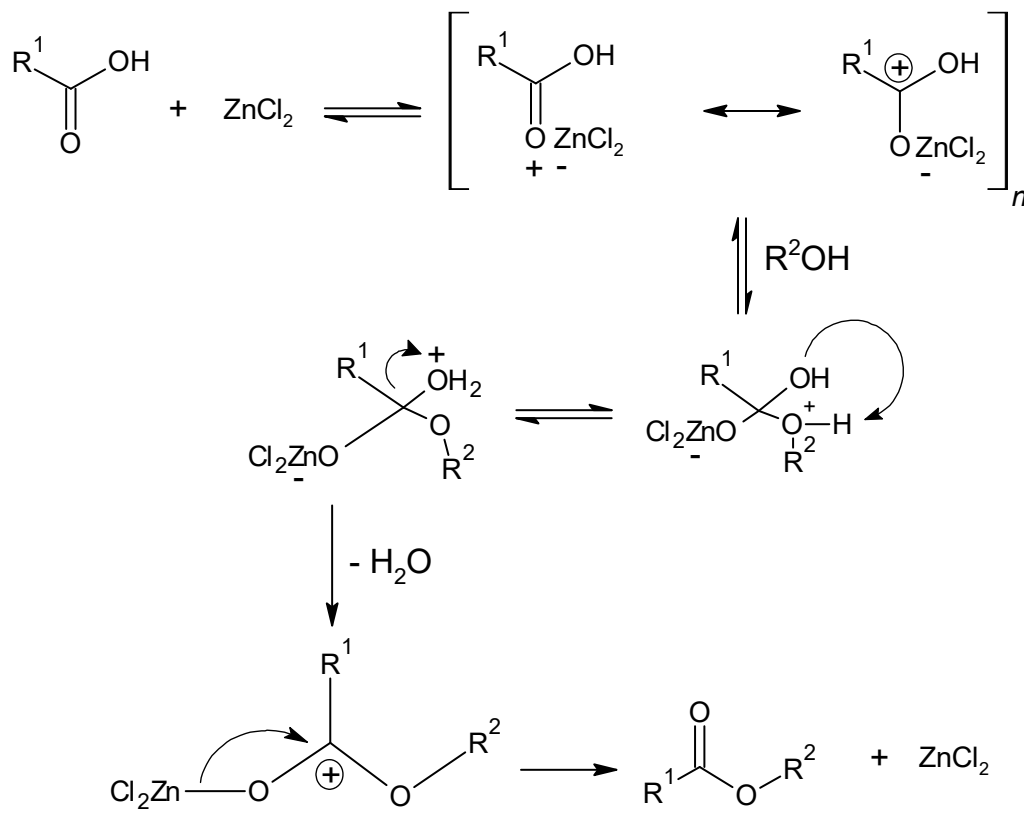


Fig. 4.15: The mechanism of zinc chloride-catalyzed esterification.

Moreover, the obtained result proves the legitimacy of using a Lewis acid, which is ZnCl_2 , to catalyze the reaction in an aqueous medium. Despite the fact that zinc chloride is a hygroscopic compound that binds water molecules (which in such a hydrated state its ability to accept electrons is blocked, and thus it loses the properties of Lewis acid), it is possible to carry out the reaction by removing water from the reaction system while dehydrating zinc chloride. Thus, it can be presumed that the reaction takes place when the solvent (water) is completely removed and zinc chloride is dehydrated at high temperature, when the substrate – poly (acrylic acid) is melted. Additionally, water is removed at high temperature and will be a by-product of esterification. Thanks to this, the equilibrium of the reaction is not maintained and the reaction goes towards the obtained products – according to Le Chatelier's principle.

The strong 3397 cm^{-1} band visible in the spectrum in Fig. 4.13 indicates the continued presence of water bound to the zinc chloride.

It is suspected that the ND-N/PVA system failed to react for two main reasons:

1. The probability of a catalytic reaction

As shown in the scheme in Fig. 14.5, the catalytic reaction takes place at the carboxylic carbon atom. In the case of the ND-N/PVA system, the carboxylic carbon atom is on the surface of the nanodiamond. The probability of a reaction act (meeting of the carboxylic carbon with zinc chloride), and then of the thus activated carbocation (very unstable) with the hydroxyl group of polyvinyl alcohol, is quite low due to the low concentration of ND compared to the polymer concentration.

2. Steric effects

There is a steric hindrance because a relatively large functional group (activated carbocation) would get onto the secondary carbon atom with an attached hydroxyl group on the PVA hydrocarbon chain. The lack of easy access makes it difficult to react.

4.4.2 Surface morphology

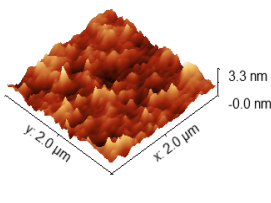
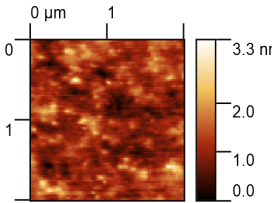
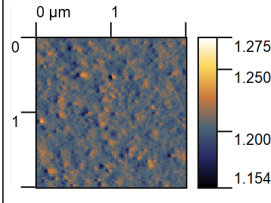
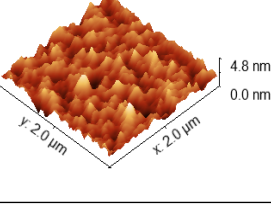
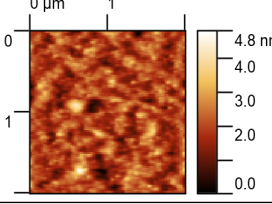
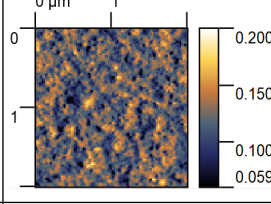
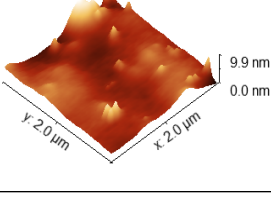
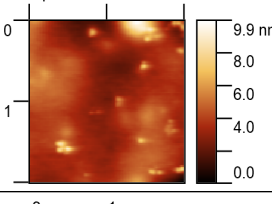
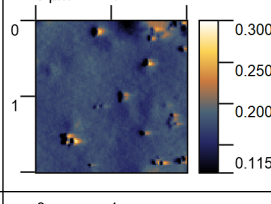
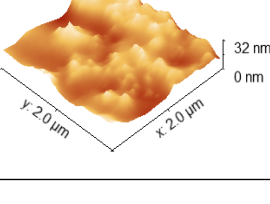
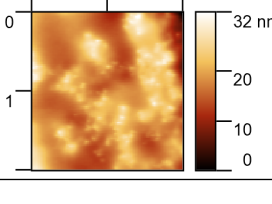
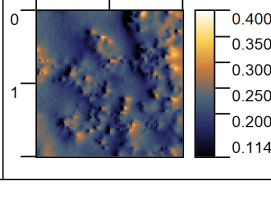
Evaluation of surface morphology of composite films coated on microscope slide was performed using an atomic force microscopy (AFM). A JPK Nanowizard III microscope in non-contact mode was used. The Lock-in amplifier filtered out weak signals accompanied by strong noise. The collected data were subsequently processed in Gwyddion 2.56 software. This technique was used to determine the surface roughness parameter, NDP grain size analysis and NDP surface coverage. In addition, three-dimensional models of the surface of the tested samples were made in nanometric resolution. Due to the size of nanodiamond particles, the size of the scanned area on the sample surface was 20x20 μm and 2x2 μm .

In order to be able to observe nanodiamonds on the tested surface, the Lock-in technique was used. This technique consists in AC modulation to detect small AC signals hidden in a noisy environment. More precisely, the technique of Amplitude Modulation Atomic Force Microscopy (AM-AFM) with Phase imaging, which is an addition to AM-AFM, were used to perform the high compositional contrast images, where the different phases are clearly distinguished.

AFM images obtained with the topography imaging (height projection) were the basis for determining the parameters describing the surface roughness, and the images taken by Phase imaging Lock-in technique were the basis for grain analysis. In these images, the higher amplitude (in volts) indicates the presence of nanodiamond particles, and the lower amplitude – the signal coming from the polymer.

Table 4.13 summarizes the taken topography and phase AFM images of the four types of tested coatings.

Tab. 4.13: AFM Topography images and Phase images of prepared coatings.

Coating	Image type		
	Topography (height) image (3D projection)	Topography (height) image	Lock-in phase image
ND-N/PVA 10 F			
ND-N/PVA 100 F			
ND-P/PAA 10 F			
ND-P/PAA 100F			

Surface topography

Table 4.14 shows the roughness parameter of samples' surfaces. The data was obtained from topography imaging.

Among the measured surface roughness parameters were Mean roughness (Arithmetical mean height, Sa) and Maximum height (Sz). Arithmetical mean height expresses, as an absolute value, the difference in height of each point compared to the arithmetical mean of the surface. It is used to evaluate general surface roughness. Maximum height is the sum of the largest peak height value and the largest pit depth value within the examined area.

Tab. 4.14: Surface roughness of prepared coatings.

Roughness parameter	Sample			
	ND-N/PVA 10 F	ND-N/PVA 100 F	ND-P/PAA 10 F	ND-P/PAA 100F
Sa [nm]	0.823	0.916	4.809	8.1004
Sz [nm]	6.670	10.367	41.863	61.228

Polymer coatings with nanodiamonds obtained on microscope slides are characterized by roughness at the nanometer level, while PVA-based coatings are less rough than PAA coatings. In the case of PVA coatings, the average roughness is below 1 nm, while the roughness of PAA coatings is in the order of a few nanometers. This difference is well shown by the Sz parameter – Maximum Height, which defines the difference in height between the deepest point and the highest point. The difference between PVA and PAA coatings is several dozen nanometers.

The amount of nanodiamond introduced in the coating affects the surface roughness – coatings with more of it are rougher. This difference is clearly visible in the case of ND-P/PAA 10F and 100F films, where the mean roughness increases by nearly 70%. Interestingly, in the case of ND-N/PVA 10 F and 100 F films, the difference is small and amounts to only 11%.

The increase in roughness is a logical consequence of the increased amount of nanodiamond directly on the surface, which is the main cause of unevenness on the surface.

Nevertheless, these values are not high and the nanometric structure of the coating has been retained in all coatings verified in this regard.

Particle analysis

The AFM images obtained from phase imaging (Lock-in technique) was used in the analysis of nanodiamond particles located on the coatings surfaces. Marking the particles in the image was performed using *Watershed segmentation* algorithm. The obtained data on the size and distribution of nanoparticles on the surface of the coatings are presented in Table 4.15.

Tab. 4.15: Size and distribution of nanodiamond particles on the surface of prepared coatings.

Sample	ND-N/PVA 10 F			ND-N/PVA 100 F			ND-P/PAA 10 F			ND-P/PAA 100F		
	No.	1	2	3	1	2	3	1	2	3	1	2
Coverage [%]	1.730	0.731	1.387	4.528	5.671	7.893	1.572	1.077	0.764	3.658	3.189	2.655
	1.28 ±0.41			6.0 ±1.4			1.14 ±0.33			3.17 ±0.41		
Mean particle size [nm]	24.899	23.651	24.456	25.124	25.878	27.282	36.785	33.163	32.053	33.456	32.690	30.959
	24.3 ±0.5			26.1 ±0.9			34.0 ±2.0			32.4 ±1.0		
Mean particle area [nm ²]	689.102	606.713	654.965	724.661	781.307	906.740	1618.22	1309.94	1211.06	1772.66	1580.83	1311.68
	650 ±34			804 ±76			1380 ±173			1560 ±190		

As could be expected, in the case of coatings with more nanodiamonds (ND-N/PVA 100 F and ND-P/PAA 100 F), the degree of surface coverage of nanodiamonds is greater than for coatings with less nanodiamonds (ND-N/PVA 10 F and ND-P/PAA 10 F). However, the level of coverage, i.e. the amount of nanodiamond on the surface, does not match the content in the total volume of the polymer coating formed. The volumetric content of nanodiamonds in the ND-N/PVA 10 F and ND-P/PAA 10 F coatings is 0.36% and 0.43%, respectively, with the nanodiamond surface coverage levels in these coatings being 1.28% and 1.14%, respectively. This indicates a greater chance of nanodiamond particles on the surface than inside the coating, which is a very favorable phenomenon for the usefulness of such a coating, since only nanodiamonds on the surface and in direct contact with the stored food are of functional importance.

It looks a bit less impressive in the case of coatings with higher nanodiamond content – ND-N/ PVA 100 F and ND-P/PAA 100 F. These coatings contain 3.48% and 4.18% by volume of nanodiamonds, respectively. And the level of surface coverage by nanodiamonds is 6.0% and 3.17%, respectively. Unfortunately, in the case of the ND-P/PAA 100 F coating, the level of coverage indicates an uneven distribution of the nanodiamond in the volume of the coating to the detriment of its appearance on the surface.

On the other hand, the content of nanodiamond in the coating does not affect the size of the particles formed – carboxylated nanodiamond in polyvinyl alcohol forms particles of approx. 25 nm, and hydroxylated nanodiamond in polyacrylic acid forms particles of approx. 33 nm.

4.5 Characterization of coated plastics

4.5.1 Free surface energy and wettability of plastic substrate

The sessile drop technique was used for evaluation of plastic substrate free surface energy (FSE), before and after plasma surface treatment. Activation of the compound surface increases its wettability by polar liquids, e.g., aqueous solutions and suspensions. As a result, the solid-liquid contact area is greater and the adhesion higher. Through this test, the effectiveness of the surface activation of the polypropylene film with cold plasma was assessed.

The procedure was based on the European Standard EN 828. The Owens, Wendt, Rabel and Kaelble (OWRK) method was adopted to FSE determination [73]. The See System E device by AdveX Instruments was used for the tests. The device was equipped with light source, hi-res camera and was supported by dedicated software for taking pictures of the drops and determining the contact angles by analysis their contour. Water and diiodomethane were used as test liquids. Their surface tension, disperse and polar proportion are presented in Table 4.16.

Tab. 4.16: Surface tension and its components of used test liquids. [74]

Designation of the test liquid	Surface tension [mN/m]	Disperse proportion [mN/m]	Polar proportion [mN/m]
Water	72.8	22.1	50.7
Diiodomethane	50.8	50.8	0

The measurement procedure was as follows: The tested LDPE film (plasma treated or non-modified) was stuck to a microscope slide with dimensions of 76×25 mm with double-sided tape. The whole was placed on the adjustable instrument's sample carrier. The lighting, the image acquisition and analysis system were switched on. The sample carrier was adjusted so that the image transmitted from the attached camera clearly showed the edge of the sample at which the drops would be dosed. The micropipette was used for dosing 3 μ L of test liquid drops. When the drop hits the surface, a picture is taken, the software calculates the right and left contact angles between the liquid and the surface and calculates the mean value. Each test liquid was dosed 5 times per sample. The results with contact angles are shown in Table 4.17 and Figure 4.16.

Tab. 4.17: Contact angles of test liquids on non-modified and plasma treated LDPE film.

Sample	No.	Test liquid			
		Water		Diiodomethane	
		Contact angle [°]	Mean contact angle [°]	Contact angle [°]	Mean contact angle [°]
Non-modified LDPE film	1	94.55	96.0 ±1.3	55.61	56.8 ±3.1
	2	96.7		57.1	
	3	94.3		51.53	
	4	96.44		59.31	
	5	97.8		60.24	
Plasma treated LDPE film	1	49.09	56.5 ±4.7	33.13	31.9 ±2.1
	2	56.92		32.4	
	3	62.99		27.71	
	4	52.51		32.78	
	5	53.49		33.4	

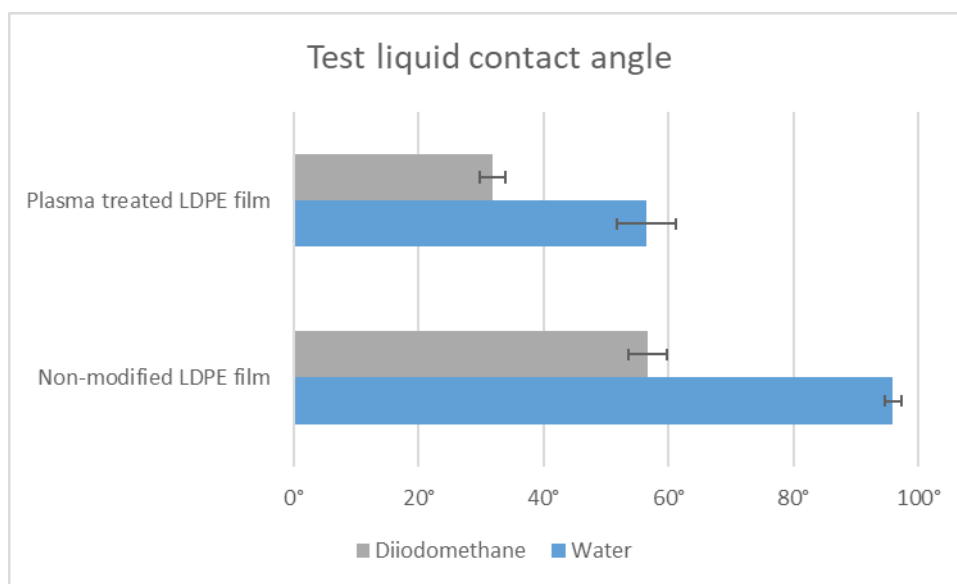


Fig. 4.16: Contact angles of test liquids on non-modified and plasma treated LDPE film.

For the determination of the surface free energy, the term $\frac{(1+\cos(\theta)) \cdot \sigma_L}{2\sqrt{\sigma_L^D}}$ is plotted against the term $\frac{\sqrt{\sigma_L^P}}{\sqrt{\sigma_L^D}}$

where

- θ are the measured and averaged contact angles for the individual liquids;
- σ_L are the total surface tension of the liquids;
- σ_L^P and σ_L^D are the polar and the disperse proportions of the total surface tensions.

Based on the plotted two points in the Cartesian coordinate system, the slope of the line (coefficient m) and its y -intercept (coefficient b) were calculated. The square of the slope (coefficient m) is equal to the polar proportion of the solid body surface energy σ_S^P , while the square of coefficient b is equal to the disperse proportion σ_S^D . The sum of these two proportions is the total surface energy of the solid body σ_S .

The test was carried out on both non-modified and plasma treated film. The results are presented in Table 4.18 and visually in the column chart in Figure 4.17, where it is clearly visible how the share of individual proportions changes in the total surface free energy.

Tab. 4.18: Surface free energy and its proportions of treated and untreated LDPE film.

Sample	Surface free energy [mN/m]	Disperse proportion [mN/m]	Polar proportion [mN/m]
Non-modified LDPE film	31.3	30.4	0.9
Plasma treated LDPE film	57.1	43.4	13.6
Increase after treatment	82.4%	42.8%	1410%

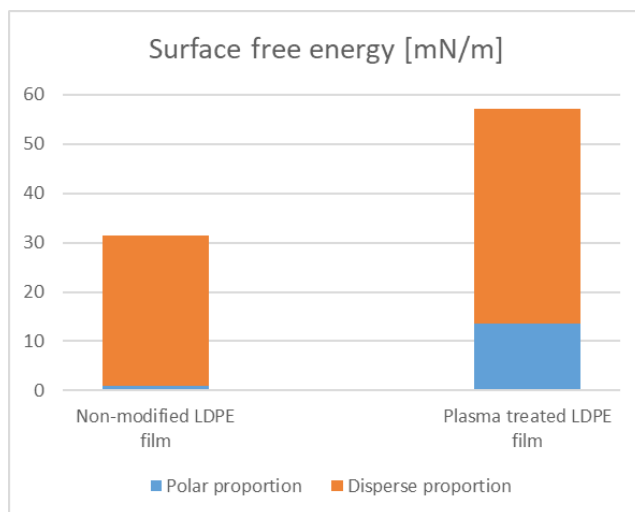


Fig. 4.17: Share of individual proportions in the total surface free energy of LDPE film.

The wettability of LDPE film (both non-modified and after plasma treatment) by film-forming solutions used in this work for the production of antioxidant coatings was also verified. The contact angle measurement procedure was the same as for wetting with water and diiodomethane. The results from this test are shown in Table 4.19 and in column chart in Figure 4.18.

Tab. 4.19: Contact angles of film-forming suspensions/solutions on non-modified and plasma treated LDPE film.

Liquid	Contact angle				
	Non-modified LDPE film		Plasma treated LDPE film		change
		Std Dev		Std Dev	
PAA 1% _{aq}	74.1	± 4.3	58.5	± 4.6	21%
PVA 1% _{aq}	70	± 10	40.5	± 6.2	42%
ND-P/PVA 10 S	48.5	± 6.4	39.3	± 2.1	19%
ND-P/PVA 100 S	40.6	± 0.7	36.4	± 3.4	10%
ND-P/PAA 10 S	79.3	± 6.3	51.0	± 5.8	36%
ND-P/PAA 100 S	84.3	± 5.1	53.6	± 2.8	36%
ND-N/PVA 10 S	78.0	± 9.6	42.5	± 1.9	46%
ND-N/PVA 100 S	73.9	± 7.3	43.7	± 2.7	41%
ND-N/PAA 10 S	87.5	± 3.0	59.4	± 6.6	32%
ND-N/PAA 100 S	80.3	± 9.9	54.2	± 3.6	32%

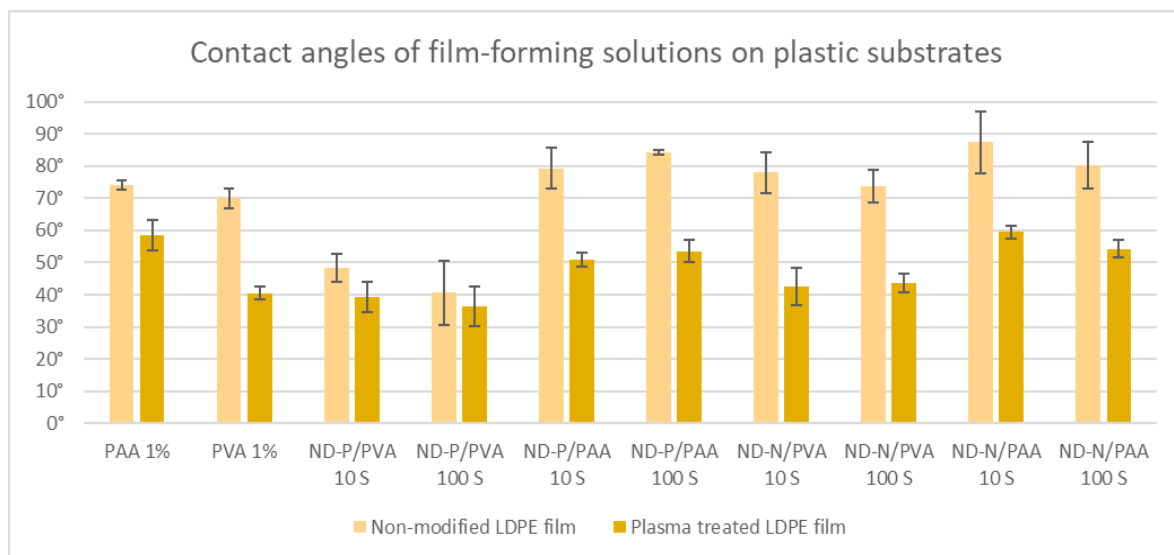


Fig. 4.18: Contact angles of film-forming suspensions/solutions on non-modified and plasma treated LDPE film presented in column chart.

Plasma treatment

Plasma activation allowed to lower the surface free energy of the polyethylene substrate. After activation, the distilled water contact angle of the plastic surface decreased from 96° to approx. 57° and the diiodomethane contact angle from 57° to 32°. The total surface free energy increased as a result of activation from 31.3 mN/m to 57.1 mN/m, which is over 82% increase. Although the share of the dispersion component in the surface free energy is greater than the polar component, the increase in this component by as much as 1410% meant that it no longer had a marginal share in the surface free energy. Its contribution became significant and had a significant impact on the increase in SFE after plasma activation. This proves the introduction of heteroatoms into the aliphatic polyethylene chains as a result of ionization, increasing the polarity of the polymer material.

The dispersion component is related to the interaction of London dispersive forces (LDF), which are a kind of induced dipole-induced dipole intermolecular interaction, which are characteristic of non-polar compounds that do not have a constant dipole moment. Dispersion interactions are based on an instantaneous change in electron density. Ionized air and oxygen radicals contribute to changes in the density of the electron cloud of hydrocarbon chains. The electrons are not permanently located in the molecule, which results in the formation of temporary dipoles.

Nevertheless, in the case of wetting the surface with aqueous suspensions and adhesion to polar polymers (such as PAA and PVA), the polar component is mainly important. According to the equation of the OWRK theory

$$W_A = 2(\sqrt{\sigma_1^D \cdot \sigma_2^D} + \sqrt{\sigma_1^P \cdot \sigma_2^P}) \quad (4.1)$$

the work of adhesion is influenced only by the same interactions (dispersion-dispersion or polar-polar) and not the dispersion-polar combination.

According to the quoted equation (4.1), an increase in the polar component by 1410% in the plasma-activated polyethylene material contributes to at least almost 4-times greater adhesion to another polar phase.

LDPE film wettability

Plasma activation of the LDPE film surface allowed to achieve lower contact angles by film-forming suspensions based on PVA and PAA. Lower contact angles, i.e. better wettability, enable more efficient coverage of the surface of the plastic foil and ensure higher higher adhesion of coatings formed after evaporation of the solvent – water.

It is particularly important because suspensions with the addition of a functionalized nanodiamond are characterized by a contact angle that is even higher, even by several degrees, than that of pure polymers. The exceptions are ND-P/PVA 10 S and 100 S suspensions, which are unstable and the test of their wettability did not give a reliable result.

The divergence of the contact angles of the tested liquids on the untreated LDPE substrate was from 70° to even 90°. After plasma activation, the contact angle of the LDPE surface with suspensions decreased by an average of 36%! After this treatment, the contact angles were between 40° and 60°. Suspensions based on the PVA solution wetted the substrate more than those based on PAA. This is reflected in the surface pan of these suspensions – it is greater in suspensions based on PAA solution. There was no unequivocal effect of the nanodiamond concentration in the suspension on the surface wettability.

4.5.2 Films adhesion

The adhesion of the thin PAA and PVA coatings to the base material – LDPE packaging film was evaluated in scratch-test on a Bruker UMT TriboLab instrument. Due to the lack of adhesion of the thin films to the untreated plastic substrate, tests were carried out on samples in which the substrate was treated with cold atmospheric plasma. The loading force increased linearly from 2 to 10 N along a path of 5 mm during 30 seconds. The speed of the sample displacement relative to the tip was about 170 $\mu\text{m/s}$ and the speed of loading about 0.27 N/s. The measured values of the critical load L_{c1} (force at which the first layer break occurs) and L_{c3} (critical load at which complete tearing of the layer occurs) are given in Table 4.20 and presented in column chart in Fig. 4.19. The magnitude of the critical load at which the layer breaks was evaluated using an optical microscope. Furthermore, records of the course of normal force, coefficient of friction and acoustic emission were monitored.

Tab. 4.20: Scratch-test critical loads of prepared coatings on plasma-treated LDPE film.

Coating			Lc ₁ [N]	Lc ₃ [N]
Polymer	Nanodiamond	ND conc. in polymer matrix		
PVA	-	-	5.14	5.73
	ND-P	10 mg/1 g	2.99	4.15
		100 mg/1 g	2.59	3.71
	ND-N	10 mg/1 g	2.62	3.78
		100 mg/1 g	2.72	3.40
PAA	-	-	3.17	5.20
	ND-P	10 mg/1 g	2.77	3.61
		100 mg/1 g	3.04	3.65
	ND-N	10 mg/1 g	2.46	2.89
		100 mg/1 g	2.34	3.00

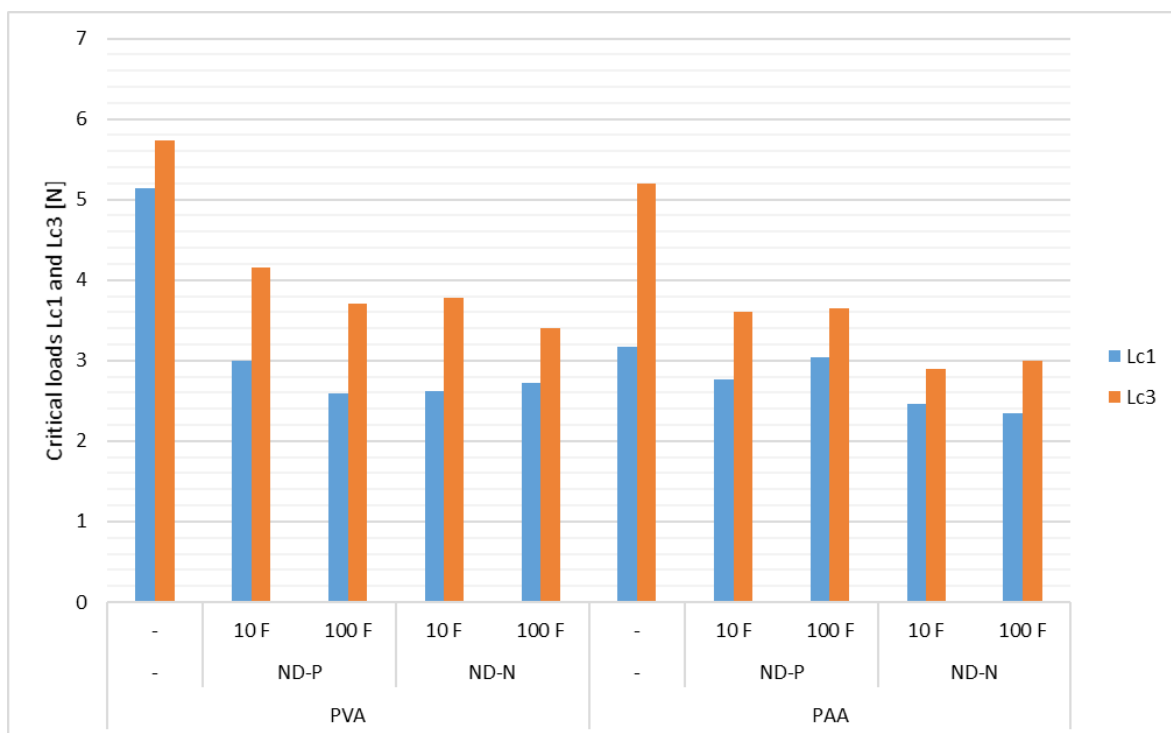


Fig. 4.19: Scratch-test critical loads of prepared coatings on plasma-treated LDPE film.

Coatings made of pure PVA and PAA polymers without the addition of nanodiamonds have the highest adhesion to LDPE film. The addition of nanodiamonds has a significant negative effect on adhesion – in extreme cases it reduces it by 40% compared to the coating without the addition of ND. The type of introduced nanodiamond also influences

the adhesion. Layers with carboxylated nanodiamond have lower adhesion to the LDPE film than layers with hydroxylated nanodiamond. In addition, the amount of added nanodiamond also affects the adhesion - more is associated with less adhesion, however, this phenomenon was observed only in the case of a coating with a PVA matrix. In the case of the PAA-based coating, no effect of ND on adhesion was observed.

The reason for this (decrease in adhesion after adding ND) can be found in the chemical mechanism of adhesion rather than in the mechanical one. This is supported by the fact that the type of ND has a more significant influence than its quantity. Moreover, the surface topography using the AFM technique showed that the surface of the layers is quite plain – the roughness is at the nanometer level (which is not conducive to adhesion).

A clue pointing to the influence of the chemical mechanism as the main cause of the adhesion loss may be the contact angle of the film-forming suspensions from which the coatings are obtained on the plasma-activated LDPE film. In the case of PVA-based coatings, a tendency was observed between the pH of film-forming suspensions and the adhesion of the coatings made from them. The highest adhesion is shown by a coating without the addition of ND, obtained from a suspension with a pH = 5.66. The addition of ND increases the pH - the more added ND, the higher the pH). Moreover, a greater increase in pH causes ND-N than ND-P. The higher the pH of the suspensions, the lower the adhesion of the resulting coatings.

The pH of suspensions is closely related to the degree of dissociation of the hydroxyl groups, thus affecting the dipole moment of the carbon atom in the hydrocarbon chain to which the hydroxyl group is attached. This in turn influences the strength of the polar interaction between the dipoles at the interface and ultimately the adhesion.

4.5.3 Coefficient of friction

Like adhesion, the coefficient of friction (CoF) was determined during the scratch test on the Bruker UMT TriboLab device and only concerned the coatings covering the previously plasma-activated LDPE film substrate. CoF values were taken into account when the coatings had not yet been damaged, i.e. until the critical load L_{c1} was reached. Table 4.21 presents the CoF values of individual coatings determined during the scratch-test. Fig. 4.20 shows the results graphically and highlights the CoF limits for packaging films processing.

Tab. 4.21: Coefficient of friction of prepared coatings on plasma treated LDPE film.

Polymer	Coating		Coefficient of friction [-]	Std Dev ±
	Nanodiamond	ND conc. in polymer matrix		
PVA	-	-	0.562	0.008
	ND-P	10 mg/1 g	0.677	0.045
		100 mg/1 g	0.529	0.018
	ND-N	10 mg/1 g	0.636	0.007
		100 mg/1 g	0.509	0.012
	PAA	-	-	0.306
ND-P		10 mg/1 g	0.559	0.017
		100 mg/1 g	0.309	0.006
ND-N		10 mg/1 g	0.578	0.012
		100 mg/1 g	0.502	0.007

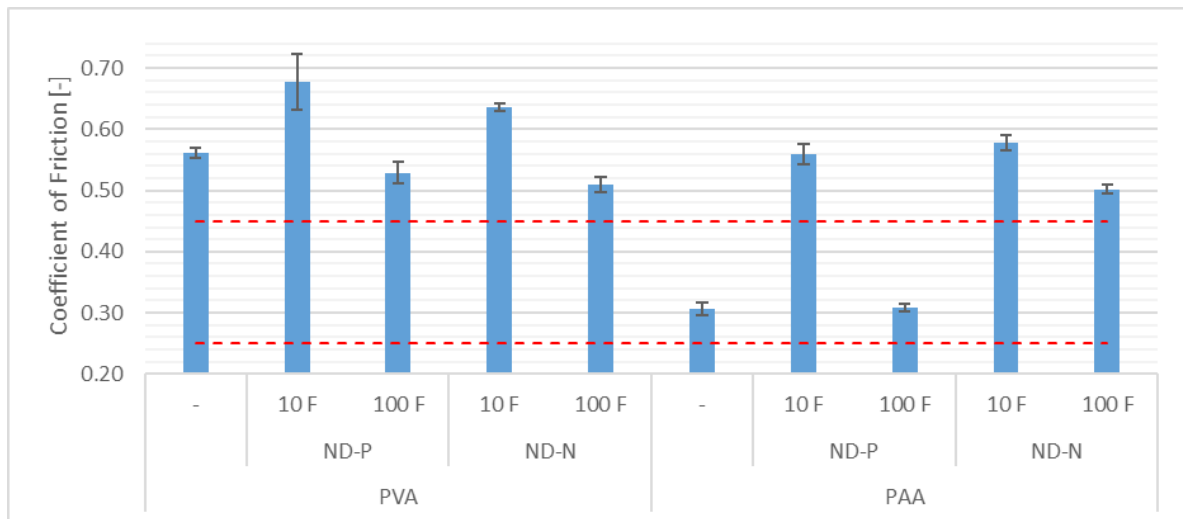


Fig 4.20: CoF values of prepared coatings with highlighted CoF limits for packaging film processing.

As mentioned in the previous chapter, the coefficient of friction of plastic films is a very important parameter for the packaging industry. Too high or too low a value of this coefficient may cause problems on the production line or in film processing. It is assumed that in the processing of packaging films, the material should have a CoF between 0.25 and 0.45. Too low value causes that the slip is too high, and too high value contributes to the lack of film slip on the elements of the processing line.

It turns out, however, that PVA-based coatings are characterized by a high coefficient of friction, which could make processing films with such a coating difficult.

An interesting effect of the addition of ND to the coating on its CoF was observed. A small addition of ND (10 mg per 1 g of polymer) causes a significant increase in CoF, while the addition of more ND (100 mg per 1 g of polymer) reduces it to a level lower than coatings without ND!

A similar phenomenon was observed for PAA-based coatings – an increase in CoF with a low amount of ND, a decrease with a high amount of ND. However, pure PAA coatings have a low CoF of about 0.3, and the addition of a small amount of ND (10 mg per 1 g of polymer) causes a huge increase in CoF.

This is not the case with the ND-P/PAA 100 F coating. The addition of 100 mg of ND-P did not change the CoF with respect to the pure PAA coating – although it would be more appropriate to say that this amount eliminated the increase in CoF associated with the addition of ND.

The nanodiamond is used as a lubricant, e.g. in polymer composite materials [75,76,77]. Therefore, it is reasonable to use more ND in coatings, for example due to the need to reduce the CoF of PVA coatings or to maintain a low CoF of PAA coatings.

4.5.4 Antioxidant properties

Undoubtedly, the most important research proving the usefulness of polymer coatings with functionalized nanodiamond is the evaluation of their antioxidant properties. These properties were verified by measuring the peroxide value of the oil applied to the coatings. The oil had been subjected to a controlled rancid process using UV-C rays.

For this purpose, a test stand was prepared to irradiate the tested surface with UV-C radiation. The stand consists of an aluminum bottomless box casing with dimensions of 22 x 30 x 20 cm (L x W x H) with a mounted 18W UV-C bulb inside which main emission was at 254 nm. A 210 x 297 mm sheet of packaging films covered with a polymer-ND composite coating were stuck to aluminum plates of the same dimensions. In Fig. 4.21 a prepared laboratory stand equipped with a UV-C light source is shown and Fig. 4.22 shows the LDPE packaging film covered with a coating stuck to aluminum plate. Tests were also carried out on uncoated films for comparison purposes. Prior the test, 15 ml of linseed oil was evenly spread over the surface of the film. The plate with the film and oil applied was placed under the stand, completely covering it, as shown in Fig. The UV light was turned

on for 10 or 180 seconds. After that time, the plate with the film was immediately removed from the test-stand and the rancid oil was scraped into a 15 ml conical test-tube.

To determine the degree of rancidity in the tested oils, the determination of the peroxide number in the collected samples was carried out. The test procedure was carried out in accordance with the European Standard EN ISO 3960, and the test samples were prepared in accordance with EN ISO 661.

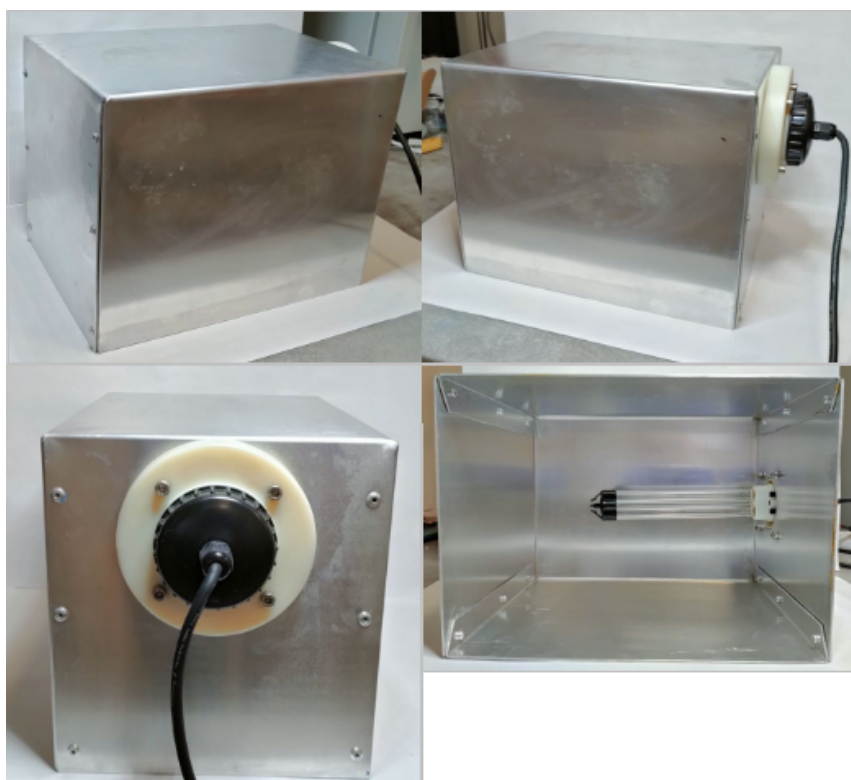


Fig. 4.21: Prepared laboratory stand for exposure to UV-C radiation to carry out a controlled process of linseed oil rancidity on the modified packaging film. Source: photograph by author.



Fig. 4.22: LDPE packaging film covered with ND-P/PAA 100 F coating stuck to aluminum plate. Source: photograph by author.

The method described in the EN ISO 3960 standard is based on the titration determination of the peroxide value where the endpoint of the titration is determined iodometrically (visually). The molecular iodine formed by the oxidation of iodide ions by peroxides is determined iodometrically with a starch indicator by titration with sodium thiosulphate standard solution. In a first step, a fresh 0.01 N sodium sulfate standard solution was prepared by diluting the 0.1 N sodium thiosulfate standard solution with freshly boiled water. Due to limited stability, 0.01 N sodium thiosulfate solution should be prepared daily. The next step is to determine the titre of the prepared solution (factor determination). For this purpose, a small amount of potassium iodate (approx. 0.3 g) was dissolved in freshly boiled water (250 ml) and cooled to room temperature. Then 5 ml of this solution was pipetted and transferred to a 250 ml flask. 50 ml of freshly boiled water, 5 ml of 4 mol/L hydrochloric acid and 0.5 ml of saturated potassium iodide solution (175 g/100 ml) were added. The mixture should be titrated by iodometric method in the presence of starch with previously prepared 0.01 N sodium thiosulphate solution.

The factor, F , of the 0.01 N sodium thiosulfate solution was calculated using Formula (4.2):

$$F = \frac{m_{KIO_3} \cdot V_1 \cdot 6 \cdot 1000 \cdot w_{KIO_3}}{M_{KIO_3} \cdot V_2 \cdot V_3 \cdot c_{thio} \cdot 100} \quad (4.2)$$

where

- 6 is the equivalent for the titre ($1 \text{ mol KIO}_3 \Leftrightarrow 3 \text{ mol I}_2$);
- V_1 is the volume of the potassium iodate solution, used for the titre determination, in milliliters;
- V_2 is the total volume of potassium iodate solution, in milliliters;
- V_3 is the volume of 0.01 N thiosulfate solution used for the determination, in milliliters;
- m_{KIO_3} is the mass of potassium iodate, in grams;
- w_{KIO_3} is the purity of potassium iodate, in g/100 g;
- M_{KIO_3} is the molecular mass of potassium iodate, (214 g/mol);
- c_{thio} is the concentration of the sodium thiosulfate standard solution, in moles per litre (0.01 mol/L).

Having determined the factor of the sodium thiosulphate solution, it is possible to proceed to the determination of the peroxide value in the collected samples. 5.0 g of sample are needed to perform the test. However, if the expected peroxide value is less than 1, 10.0 g of the sample should be used. The taken sample was dissolved in 50 ml of the glacial acetic acid/isooctane solution (volume ratio 3:2) in Erlenmeyer flask. Then 0.5 ml of a saturated solution of potassium iodide was added and stirred for 60 seconds. After opening the flask, 100 ml of deionized water was added and swirled. The liberated iodine was immediately titrated with 0.01 N sodium thiosulfate solution. During titration, the mixture color has changed from yellow orange to pale yellow and, after addition of 0.5 ml of starch solution (1 g/100 ml), from violet to colorless. The titration was stopped when the solution was colorless at least for 30 seconds. The peroxide value, PV, in miliequivalents (meq) of active oxygen per kilogram, was calculated using the Formula (4.3)

$$PV = \frac{(V - V_0) \cdot c_{thio} \cdot F \cdot 1000}{m} \quad (4.3)$$

where

- V is the volume of sodium thiosulfate solution used for the determination, in milliliters;
- V_0 is the volume of the sodium thiosulfate standard solution used for the blank test, in milliliters;
- c_{thio} is the concentration of the sodium thiosulfate solution, in moles per liter;
- m is the mass of the test portion, in grams;
- F is the factor of the 0.01 N sodium thiosulfate solution.

The list of prepared samples and obtained results are presented in Table 4.22 and on graph in Fig.4.23. During the research, commercially available linseed oils of the same brand were used. Each time the oil was freshly opened prior to testing and its peroxide value was the reference. As can be seen from the presented results, the same commercial product can be characterized by a different degree of rancidity and had different initial peroxide value. For this reason, normalization was carried out and the PV increases in relation to the reference points are presented in Table 4.23 and on graph in Fig. 4.24. These results show

the increase in the Peroxide Value in relation to the reference sample – oil not exposed to UV radiation.

The highest increase in the Peroxide Value was observed in the UV-irradiated oil on the unmodified LDPE film, with 180 seconds this value increased by 22.65 meq. In the oil on PVA and PAA coatings without nanodiamant, the PV increased by 10.78 and 12.01 meq, respectively. In the case of the oil on PVA and PAA coatings with the addition of nanodiamonds, the PV increase was the lowest and after 180 seconds of UV irradiation it ranged from 2.06 to 2.47 meq. A similar behavior was observed with 10 seconds of UV irradiation. However, in the case of coatings with more nanodiamonds (100 mg / 1 g of polymer), due to the low initial PV and the small increase difference, the rancid phenomenon was not observed and it is suspected that they are not fully reliable.

Tab. 4.22: Peroxide Values of tested linseed oils on prepared coatings without (ref) and after UV irradiation in certain time.

Sample	Exposure time [s]	Peroxide Value PV [meq]	Std Dev \pm
Non-modified	ref	5.67	0.15
	10	9.15	0.17
	180	28.32	0.44
PVA	ref	5.67	0.15
	10	8.13	0.19
	180	16.45	0.01
ND-N/PVA 10 F	ref	5.67	0.15
	10	7.4	0.07
	180	8.14	0.03
ND-N/PVA 100 F	ref	1.1	0.15
	10	0.88	0.14
	180	3.2	0.15
PAA	ref	5.67	0.15
	10	7.47	0.12
	180	17.68	0.01
ND-P/PAA 10 F	ref	5.67	0.15
	10	8.09	0.05
	180	7.73	0.14
ND-P/PAA 100 F	ref	1.1	0.1
	10	1.1	0.1
	180	3.5	0.1

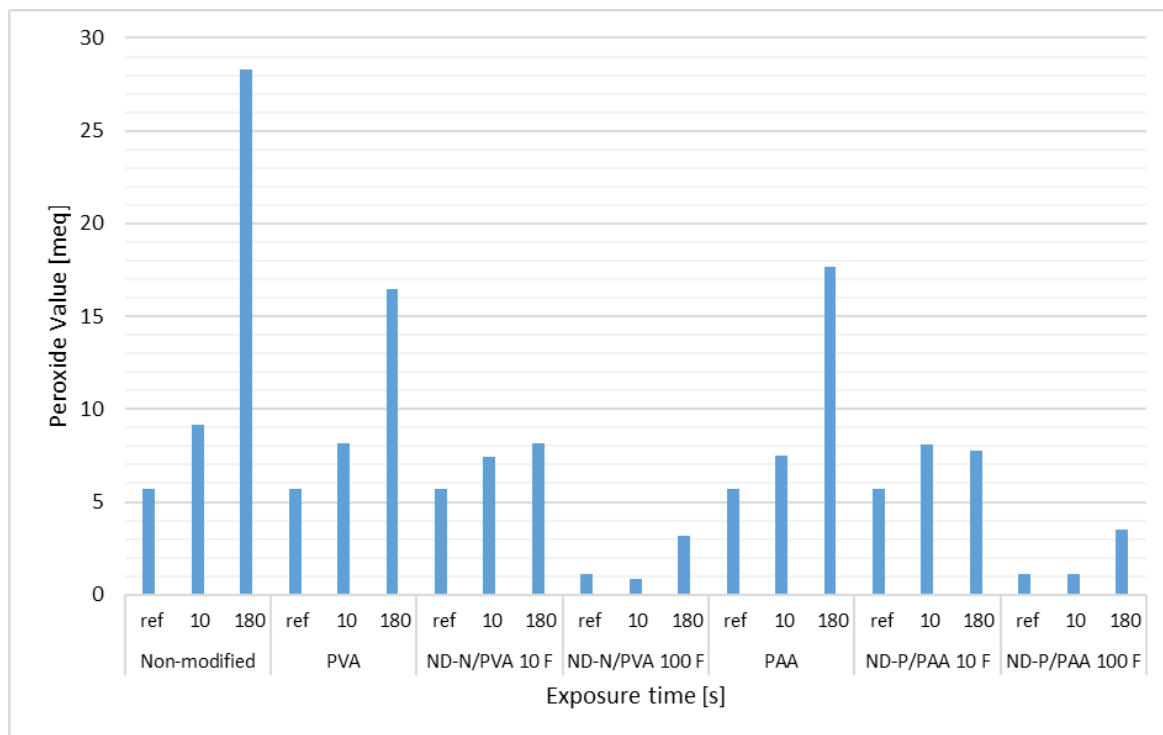


Fig. 4.23: Peroxide Values of tested linseed oils on prepared coatings without (ref) and after UV irradiation in certain time.

Tab. 4.23: Peroxide Values increase of tested linseed oils on prepared coatings after UV irradiation in certain time.

Sample	Exposure time [s]	Peroxide Value increase ΔPV [meq]
Non-modified	10	3.48
	180	22.65
PVA	10	2.46
	180	10.78
ND-N/PVA 10 F	10	1.73
	180	2.47
ND-N/PVA 100 F	10	-0.22
	180	2.1
PAA	10	1.8
	180	12.01
ND-P/PAA 10 F	10	2.42
	180	2.06
ND-P/PAA 100 F	10	0
	180	2.4

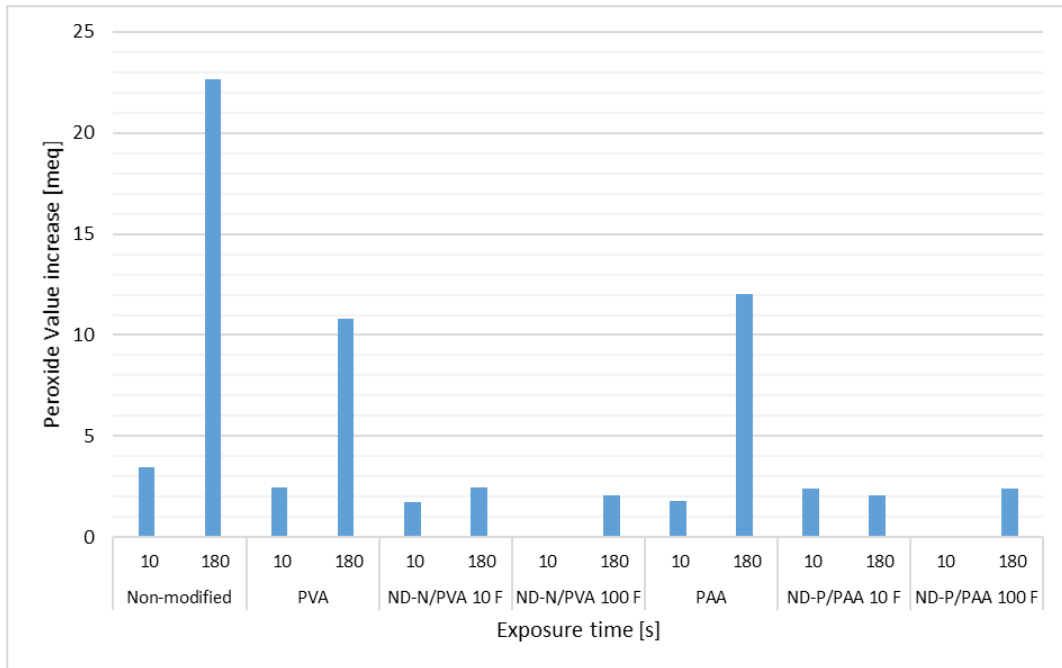


Fig. 4.24: Peroxide Values increase of tested linseed oils on prepared coatings after UV irradiation in certain time.

The observed reduced degree of oil rancidity on pure PVA and PAA coatings in relation to the LDPE substrate results from the fact that these polymers absorb more UV radiation. The absorbed radiation does not catalyze the fatty acid oxidation reaction. [57]

The effect of these coatings can be compared to a sunscreen, as their action is based on an organic chemical filter mechanism. [61,78]

The addition of functionalised nanodiamonds to PVA and PAA coatings significantly inhibits the rancidity process. It is especially noticeable with 180 seconds of UV irradiation – the addition of a small amount of nanodiamond (10 mg per 1 g of polymer) to the PVA coating contributed to a 4 times smaller increase in the peroxide number, and to the PAA coating almost 6 times!

The addition of more nanodiamonds to polymer coatings (100 mg per 1 g of polymer) does not improve their anti-rancidity properties – the peroxide number in the case of 180 s UV irradiation is similar to the smaller amount of nanodiamond (10 mg per 1 g of polymer) in the coating.

5 Summary and conclusion

The protection of food against deterioration is a key issue in terms of preventing its wastage and the problem of short-term consumption. Various concepts related to the so-called active packaging to prevent spoilage in so many ways are developed worldwide. As part of this study, an innovative approach to coating standard packaging films was proposed, making them active packaging with antioxidant properties. This was done in such a way that the production process is not harmful to the environment, and the coatings can be biodegradable under certain conditions. Moreover, the produced coatings are harmless to the user and do not react with fatty foods.

The matrix of the produced coatings are water-soluble and biodegradable polyvinyl alcohol (PVA) and polyacrylic acid (PAA). These substances are not classified as hazardous or harmful to health. Due to the fact that they are water-soluble polar polymers, their processing does not require the use of harmful organic solvents (especially VOCs) and they are resistant to oils and fats, so direct contact with stored fatty food does not adversely affect their condition. The selection of polymers with appropriate molecular weights allows for obtaining solutions (and in the next stage – suspensions) characterized by low viscosity, thanks to which mixing, homogenization and casting are not distorted. The whole processes run smoothly without much energy expenditure. It is particularly important because the solutions of these polymers are the basis for the film-forming suspensions obtained in the subsequent steps, from which, after pouring and evaporating water, coatings with antioxidant properties are prepared.

Detonation nanodiamond was used as a component with antioxidant properties in the produced coatings. The nanodiamond particles used in the research had a functionalised surface as a result of hydroxylation or carboxylation. On the one hand, the functional groups on the surface of the diamond activate its free radical scavenger potential, and on the other hand, they ensure a high absolute value of the Zeta potential, preventing the particle aggregation and sedimentation, thanks to which the produced film-forming suspensions are characterized by high stability. Due to the chemical nature of the functional groups on the surface of nanodiamond particles (protonated hydroxyl or deprotonated carboxyl groups), these particles have a positive (ND-P) or negative (ND-N) Zeta potential, respectively. The value of the potential is closely related to the pH of the

suspension in which the particles are present – too high or too low a pH may reduce the absolute value of the Zeta potential, which will result in particle aggregation and make the produced film-forming suspensions unstable. In the course of the conducted works, it was possible to obtain stable suspensions, both based on PAA and PVA, characterized by different concentrations of nanodiamonds.

The obtained film-forming suspensions would be cast on the surface of a standard packaging film made of LDPE. In order to ensure the required wettability of the aqueous suspensions on the non-polar film and sufficient adhesion of the coating produced after evaporation of the water, plasma activation of the LDPE surface had to be performed. Plasma surface activation, also called plasma treatment, was performed using cold atmospheric plasma generated by piezoelectric material based on lead zirconium titanate with co-fired copper electrodes. As a result of plasma treatment, polar heteroatoms are introduced into the structure of the polymer, increasing its surface free energy. As a result, the contact angle is lowered and the suspension better covers the surface of the film. As it turns out, plasma activation of the surface is a necessary process to perform, otherwise there is no adhesion at all between the LDPE film and the produced PVA/PAA coatings with the nanodiamond.

The coatings with nanodiamonds produced on plastic film and glass were subjected to a series of tribological tests and a microscopic examination of the surface topography. Research carried out with the use of atomic force microscopy has shown that during the formation of a thin composite film (coating), the nanodiamond does not aggregate and the formed nanodiamond clusters (grains) have nanometric sizes ranging from 24 to 34 nm and their surface area is on average from 650 to 1560 nm². Moreover, coatings with a small amount of nanodiamond particles show an above-average presence of nanodiamond particles on the surface in relation to their content in the entire volume. It is a very desirable phenomenon and is crucial for the antioxidant functionality of the coatings.

Scratch-test of PVA/PAA coatings on LDPE film showed that the addition of nanodiamonds has a negative effect on adhesion, but does not reduce it dramatically to an unacceptable level. On the other hand, nanodiamond has a significant impact on the coefficient of friction (CoF) of the produced coatings. PVA/PAA coatings have a naturally high CoF, which is unacceptable for the processing of packaging films. The nanodiamond

has the properties of a lubricant and its addition of a large amount can reduce the CoF to the appropriate level (between 0.25 and 0.45).

It was also checked whether it was possible to incorporate the functionalized nanodiamond into the polymer with covalent bonds that would be formed as a result of the esterification reaction. In order for the esterification reaction to take place, a polyvinyl alcohol (containing hydroxyl groups attached to hydrocarbon chain) with a carboxylated nanodiamond and a polyacrylic acid (containing carboxyl groups attached to hydrocarbon chain) with a hydroxylated nanodiamond were selected. Lewis acid – ZnCl_2 was used as a reaction catalyst. The progress of the reactions was verified by making the FTIR spectrum of the prepared coatings. The reaction took place only in the PAA–hydroxylated nanodiamond system, however, the analysis of vibration bands from the polymer carboxylic groups indicates that the reaction was very advanced. This confirmed the possibility of incorporation of the hydroxylated nanodiamond with a covalent bond with the polymer matrix and carrying out the esterification reaction with Lewis acid, even in an aqueous environment – of course under strictly defined temperature conditions enabling water removal (i.e. water as solvent and as formed by-product) from the reaction system.

The test verifying the functionality of the coatings in terms of antioxidant properties was the peroxide value (PV) determination of linseed oil spread on the film with the coatings subjected to a controlled rancidity process. The PV is one of the rancidity degree indicators in a high-fat products. The spread oil was irradiated with UV-C radiation at various times (10 or 180 seconds). The test confirmed the effectiveness of the coatings. The PVA and PAA polymers have UV radiation absorbing properties, and the functionalized nanodiamond has free radical scavenging properties. In case of 180 seconds UV irradiation in the oil spread over the composite coatings, there was an 11 times lower PV increase compared to the oil spread over the unmodified standard packaging film.

As a result of this study, it was possible to develop a method of obtaining polymer coatings with the addition of nanodiamonds on the packaging film with excellent anti-rancid properties. Due to the use of polar polymers as a matrix, the coatings are resistant to oils and fats. The nanodiamonds on the surface of these coatings are well dispersed and maintain their nanostructure. The aqueous suspensions from which the coatings are prepared turned out to be stable – there is no aggregation and sedimentation of

nanoparticles. They can be stored for a long time since preparation. Moreover, these suspensions do not require harmful organic solvents for preparation. They are safe for health and the environment. The coatings are characterized by satisfactory adhesion to the polyethylene packaging film and, due to the addition of an appropriate amount of nanodiamond, the correct coefficient of friction, thanks to which they can be mechanically processed on the packaging processing lines and welded. As part of further research works related to the development of antioxidant food packaging, it is planned to use a copolymer of polyethylene and polyvinyl alcohol as a polymer matrix. This polymer does not require any harmful organic solvents for processing, and is resistant to water. Thanks to this, the coatings will find a wider application in other food products, not only in high-fat products. In addition, it is planned to conduct more extensive research on polymer-nanodiamond suspensions and determine their stability depending on the pH, concentration and size of nanoparticles. This task will be quite a challenge as the commonly used Zeta potential testing devices measuring with the Dynamic Light Scattering (DLS) technique cannot cope with dissolved polymers of high molecular weight. However, the challenge is worth the effort to develop more optimal active packaging coatings that will prevent spoilage and food waste.

References

- [1] SPADA, Alessia; CONTE, Amalia; DEL NOBILE, Matteo Alessandro. The influence of shelf life on food waste: A model-based approach by empirical market evidence. *Journal of cleaner production*, 2018, 172: 3410-3414.
- [2] SUN, S. K., et al. Impacts of food wastage on water resources and environment in China. *Journal of Cleaner Production*, 2018, 185: 732-739.
- [3] FAO. *Food wastage footprint: Impacts on natural resources*. FAO, 2013.
- [4] YILDIRIM, Selçuk, et al. "Active packaging applications for food." *Comprehensive Reviews in Food Science and Food Safety* 17.1 (2018): 165-199.
- [5] DOMÍNGUEZ, Rubén, et al. Active packaging films with natural antioxidants to be used in meat industry: A review. *Food Research International*, 2018, 113: 93-101.
- [6] VERA, Paula; CANELLAS, Elena; NERÍN, Cristina. New antioxidant multilayer packaging with nanoselenium to enhance the shelf-life of market food products. *Nanomaterials*, 2018, 8.10: 837.
- [7] LUZI, Francesca; TORRE, Luigi; PUGLIA, Debora. Antioxidant Packaging Films Based on Ethylene Vinyl Alcohol Copolymer (EVOH) and Caffeic Acid. *Molecules*, 2020, 25.17: 3953.
- [8] MITURA, Katarzyna. Antioxidant properties of bioactive food packaging with nanodiamonds. *Engineering of Biomaterials*, 2017, 20.
- [9] MITURA, Katarzyna A.; ZARZYCKI, Paweł K. Biocompatibility and toxicity of allotropic forms of carbon in food packaging. In: *Role of Materials Science in Food Bioengineering*. Academic Press, 2018. p. 73-107.
- [10] MITURA, Katarzyna, et al. Bioactive food packaging with nanodiamond particles manufactured by detonation and plasma-chemical methods. In: *Food Packaging*. Academic Press, 2017. p. 295-328.
- [11] MITURA, Stanisław. Nanodiamonds. *Journal of Achievements in Materials and Manufacturing Engineering*, 2007, 24.1: 166-171.
- [12] NIEMIEC, Tomasz, et al. The effect of diamond nanoparticles on redox and immune parameters in rats. *Journal of Nanoscience and Nanotechnology*, 2011, 11.10: 9072-9077.
- [13] DOLMATOV, Valerii Yu. Detonation-synthesis nanodiamonds: synthesis, structure, properties and applications. *Russian Chemical Reviews*, 2007, 76.4: 339.
- [14] MITURA, Katarzyna, et al. Interactions between carbon coatings and tissue. *Surface and Coatings Technology*, 2006, 201.6: 2117-2123.
- [15] ADACH, Kinga; FIJALKOWSKI, Mateusz; SKOLIMOWSKI, Janusz. Antioxidant effect of hydroxylated diamond nanoparticles measured in soybean oil. *Fullerenes, Nanotubes and Carbon Nanostructures*, 2015, 23.12: 1024-1032.
- [16] MOREIRA, Felismina TC, et al. Synthesis of molecular biomimetics. In: *Biomimetic Technologies*. Woodhead Publishing, 2015. p. 3-31.
- [17] ACHMATOWICZ-SZMAJKE, TERESA, JANICKI, STANISŁAW, FIEBIG, ADOLF and SZNITOWSKA, MAŁGORZATA, 2014, *Farmacja stosowana*. Warszawa : Wydawnictwo Lekarskie PZWL.
- [18] TADROS, TH. F, 2012, *Dispersion of powders in liquids and stabilization of suspensions*. Weinheim : Wiley-VCH.

- [19] BIRDI, K.S. Introduction to Surface and Colloid Chemistry Recent Advances and General Remarks. In: BIRDI, K.S. (ed.). Handbook of surface and colloid chemistry. CRC press, 2015.
- [20] IUPAC Compendium of Chemical Terminology *Gold Book* Version 2.3.3,
- [21] JONES, Richard G.; UNION INTERNATIONALE DE CHIMIE PURE ET APPLIQUÉE. POLYMER DIVISION. Compendium of polymer terminology and nomenclature: IUPAC recommendations, 2008. Cambridge: Royal Society of Chemistry, 2009.
- [22] PIGOŃ, Krzysztof, et al. *Chemia fizyczna: Podstawy fenomenologiczne*. Wydawnictwo Naukowe PWN, 2013.
- [23] KRALCHEVSKY, P.A., DANOV, K.D. Chemical Physics of Colloid Systems and Interfaces. In: BIRDI, K.S. (ed.). Handbook of surface and colloid chemistry. CRC press, 2015.
- [24] FERMIN, D.; RILEY, J. Charge in Colloidal Systems. In: COSGROVE, Terence. Colloid science. Blackwell publishing limited, 2005.
- [25] MATUSIAK, Jakub; GRZĄDKA, Elżbieta. Stability of colloidal systems-a review of the stability measurements methods. *Annales Universitatis Mariae Curie-Skłodowska, sectio AA-Chemia*, 2017, 72.1: 33.
- [26] ADAIR, J. H.; SUVACI, E.; SINDEL, J. Surface and colloid chemistry. In: BUSCHOW, KH Jürgen, et al. Encyclopedia of materials. Science and technology, 2001.
- [27] LAGALY, Gerhard; SCHULZ, Oliver; ZIMEHL, Ralf. *Dispersionen und Emulsionen: eine Einführung in die Kolloidik feinverteilter Stoffe einschließlich der Tonminerale*. Springer-Verlag, 2013.
- [28] ENDER, Volker. *Praktikum Physikalische Chemie: 25 Versuche für das Grundpraktikum, zur Grenzflächenchemie und zur Wasseraufbereitung/ Springer Spektrum*, 2015.
- [29] HUNTER, Robert J. *Zeta potential in colloid science: principles and applications*. Academic press, 2013.
- [30] WILLIAMS, P.M. Zeta Potential. In: DRIOLI, Enrico; GIORNO, Lidietta (ed.). *Encyclopedia of membranes*. Springer, 2018.
- [31] BURSA, Stanisław. *Chemia fizyczna*. Wydawnictwo Uczelniane Politechniki Szczecińskiej, 1972.
- [32] BASIŃSKI, Antoni. *Chemia fizyczna*. Warszawa : PWN, 1966.
- [33] KUJAWSKA, MONIKA. Wykłady z chemii. *Dydaktyka.polsl.pl* [online]. [Accessed 22 January 2021]. Available from: http://dydaktyka.polsl.pl/rg5/slaczka/chem_V_W12.html
- [34] KUMAR, Ajeet; DIXIT, Chandra Kumar. Methods for characterization of nanoparticles. In: *Advances in nanomedicine for the delivery of therapeutic nucleic acids*. Woodhead Publishing, 2017. p. 43-58.
- [35] "Film-Forming Material." *The Great Soviet Encyclopedia*, 3rd Edition. 1970-1979. The Gale Group, Inc. 15 Jan. 2021. Available from: <https://encyclopedia2.thefreedictionary.com/Film-Forming+Material>.
- [36] "пленкообразующий материал". In: КАБАНОВ, В.А.(Ed.) *Энциклопедия полимеров*. Том 2. Л - Полинозные волокна, 1974.
- [37] NAGARKAR, Rigved; PATEL, Jatin. Polyvinyl alcohol: A comprehensive study. *Acta Scientific Pharmaceutical Sciences*, 2019, 3.4: 34-44.

- [38] SAINT-AUBIN, Karell, et al. Dispersion and film-forming properties of poly (acrylic acid)-stabilized carbon nanotubes. *Langmuir*, 2009, 25.22: 13206-13211.
- [39] BRIGGS, David; RANCE, Derek G.; BRISCOE, Brian J. Surface properties. In: ALLEN, G.; BEVINGTON, J.C. *Comprehensive Polymer Science: the Synthesis, Characterization, Reactions & Applications of Polymers.*, 2, 707-732, Pergamon Press, 1989.
- [40] ZHANG, J. Work of Adhesion and Work of Cohesion. In: WANG, Q. Jane; CHUNG, Yip-Wah. *Encyclopedia of tribology*. Springer, 2013.
- [41] GRUNDKE, K. Characterization of polymer surfaces by wetting and electrokinetic measurements—contact angle, interfacial tension, zeta potential. In: STAMM, Manfred. (Ed.) *Polymer surfaces and interfaces. Characterization, Modification and Applications*; Springer: Berlin, Germany, 2008.
- [42] DILLINGHAM, GILES. Why One Contact Angle Fluid is All You Need to Control Your Process. *Btglabs.com* [online]. [Accessed 22 January 2021]. Available from: <https://www.btglabs.com/why-one-contact-angle-fluid-is-all-you-need-to-control-your-process>
- [43] RECYŃSKA, KATARZYNA. Zwilżalność powierzchni. AGH [online]. 2015. [Accessed 22 January 2021]. Available from: <http://home.agh.edu.pl/~kmr/instrukcje/zwilzalnosc.pdf>
- [44] Learn corona processing. KASUGA [online]. [Accessed 22 January 2021]. Available from: <https://www.ekasuga.co.jp/study/corona/>
- [45] MITURA, S., et al. Nanocrystalline diamond, its synthesis, properties and applications. *Journal of Achievements in Materials and Manufacturing Engineering*, 2006, 16.1-2: 9-16.
- [46] MITURA, Katarzyna, et al. Interactions between carbon coatings and tissue. *Surface and Coatings Technology*, 2006, 201.6: 2117-2123.
- [47] MITURA, Katarzyna, et al. Haemocompatibility of non-functionalized and plasmachemical functionalized detonation nanodiamond particles. *Archives of Metallurgy and Materials*, 2015, 60.
- [48] ADACH, K.; SKOLIMOWSKI, J.; MITURA, K. Chemiczna modyfikacja nanoproszków diamentowych wytwarzanych metodą detonacyjną. *Elektronika: konstrukcje, technologie, zastosowania*, 2011, 52.11: 84-86.
- [49] MOCHALIN, Vadym N., et al. The properties and applications of nanodiamonds. *Nature nanotechnology*, 2012, 7.1: 11-23.
- [50] MOCHALIN, Vadym N.; GOGOTSI, Yury. Nanodiamond–polymer composites. *Diamond and Related Materials*, 2015, 58: 161-171.
- [51] REINA, Giacomo, et al. Chemical functionalization of nanodiamonds: opportunities and challenges ahead. *Angewandte Chemie*, 2019, 131.50: 18084-18095.
- [52] OZAWA, Masaki, et al. Preparation and behavior of brownish, clear nanodiamond colloids. *Advanced Materials*, 2007, 19.9: 1201-1206.
- [53] GIBSON, N., et al. Colloidal stability of modified nanodiamond particles. *Diamond and Related materials*, 2009, 18.4: 620-626.
- [54] ZHANG, Yinhang, et al. A critical review of nanodiamond based nanocomposites: Synthesis, properties and applications. *Composites Part B: Engineering*, 2018, 143: 19-27.

- [55] JABEEN, Saira, et al. A review on polymeric nanocomposites of nanodiamond, carbon nanotube, and nanobifiller: Structure, preparation and properties. *Polymer-Plastics Technology and Engineering*, 2015, 54.13: 1379-1409.
- [56] MORIMUNE, Seira, et al. Poly (vinyl alcohol) nanocomposites with nanodiamond. *Macromolecules*, 2011, 44.11: 4415-4421.
- [57] MURPHY, Brian, et al. Oxford IB Diploma Programme: Chemistry Course Companion. Oxford University Press-Children, 2014.
- [58] KIM, Ho-Joong, et al. Diamond nanogel-embedded contact lenses mediate lysozyme-dependent therapeutic release. *ACS nano*, 2014, 8.3: 2998-3005.
- [59] PADAYATTY, Sebastian J., et al. Vitamin C as an antioxidant: evaluation of its role in disease prevention. *Journal of the American college of Nutrition*, 2003, 22.1: 18-35.
- [60] THOMAS, A. Fats and Fatty Oils. In: ULLMANN, Fritz. (Ed.) *Ullmann's Encyclopedia of Industrial Chemistry*. Wiley-VCH Verlag GmbH & Co. KGaA, Weinheim, 2012.
- [61] LIN, Qianyu, et al. UV Protection and Antioxidant Activity of Nanodiamonds and Fullerenes for Sunscreen Formulations. *ACS Applied Nano Materials*, 2019, 2.12: 7604-7616.
- [62] HOLT, Katherine B., et al. Redox properties of undoped 5 nm diamond nanoparticles. *Physical Chemistry Chemical Physics*, 2008, 10.2: 303-310.
- [63] OHL, DANIELLE. What is coefficient of friction (COF), and why is it important in packaging?. Viking Masek [online]. 2020. [Accessed 22 January 2021]. Available from: <https://vikingmasek.com/packaging-machine-resources/packaging-machine-blog/what-coefficient-friction-cof-and-why-it-important-packaging>
- [64] Coefficient of Friction (COF) Flair Flexible Packaging. Flairpackaging.com [online]. [Accessed 22 January 2021]. Available from: [http://www.flairpackaging.com/pages/home/resources/packaging_101/CoefficientofFriction\(COF\)/1](http://www.flairpackaging.com/pages/home/resources/packaging_101/CoefficientofFriction(COF)/1)
- [65] HARE, Brian A.; MOYSE, Allan; SUE, Hung-Jue. Analysis of scratch-induced damages in multi-layer packaging film systems. *Journal of Materials Science*, 2012, 47.3: 1389-1398.
- [66] KÜCÜKPINAR, Esra; LANGOWSKI, Horst-Christian. Adhesion Aspects in Packaging. *Journal of adhesion science and technology*, 2012, 26.20-21: 2317-2324.
- [67] KRAWCZYK-KŁYS, Iwona; JARUGA, Izabella. Właściwości adhezyjne powierzchni. *TECHNOLOGIA I JAKOŚĆ WYROBÓW*, 28.
- [68] MITTAL, K. L. The role of the interface in adhesion phenomena. *Polymer Engineering & Science*, 1977, 17.7: 467-473.
- [69] ALI, Z. I., et al. Thermal stability of LDPE, iPP and their blends. *Thermochimica acta*, 2005, 438.1-2: 70-75.
- [70] LDPE Chemical Compatibility Chart. Calpaclab.com [online]. [Accessed 22 January 2021]. Available from: <https://www.calpaclab.com/ldpe-chemical-compatibility-chart/>
- [71] SDBS-2708. SDBSWeb. Sdbs.db.aist.go.jp [online]. National Institute of Advanced Industrial Science and Technology (AIST), 1999. [Accessed 22 January 2021]. Available from: <https://sdbs.db.aist.go.jp/sdbs/cgi-bin/landingpage?sdbno=2708>

- [72] SDBS-2709. SDBSWeb. Sdbs.db.aist.go.jp [online]. National Institute of Advanced Industrial Science and Technology (AIST), 1999. [Accessed 22 January 2021]. Available from: <https://sdbs.db.aist.go.jp/sdbs/cgi-bin/landingpage?sdbno=2709>
- [73] Determination of the surface energy of a solid. Dataphysics-instruments.com [online], [Accessed 22 January 2021]. Available from: <https://www.dataphysics-instruments.com/knowledge/understanding-interfaces/solid-surface-energy/>
- [74] Surface Tension Components and Molecular Weight of Selected Liquids. Accudynetest.com [online], [Accessed 22 January 2021]. Available from: https://www.accudynetest.com/surface_tension_table.html
- [75] NEITZEL, Ioannis, et al. Tribological properties of nanodiamond-epoxy composites. *Tribology letters*, 2012, 47.2: 195-202.
- [76] LEE, Jung-Yeob; LIM, Dae-Soon. Tribological behavior of PTFE film with nanodiamond. *Surface and Coatings Technology*, 2004, 188: 534-538.
- [77] CHOU, Chau-Chang; LEE, S. H. Rheological behavior and tribological performance of a nanodiamond-dispersed lubricant. *Journal of materials processing technology*, 2008, 201.1-3: 542-547.
- [78] SERPONE, Nick; DONDI, Daniele; ALBINI, Angelo. Inorganic and organic UV filters: Their role and efficacy in sunscreens and suncare products. *Inorganica chimica acta*, 2007, 360.3: 794-802.

List of Figures

Fig. 3.1: Schemes of the dispersed phase particles.	12
Fig.3.2: Long range electrostatic repulsion forces and short range van der Waals attraction forces.	13
Fig. 3.3: The potential energy of interactions between two particles of the dispersed phase.	14
Fig. 3.4: Diagram showing the ionic concentration and potential difference.	15
Fig. 3.5: The dependence of the Zeta potential on pH.	15
Fig. 3.6: Young's force balance giving the equilibrium contact angle.	18
Fig. 3.7: Introduction of polar functional groups into polymer chain in surface layer of polymeric material.	20
Fig. 3.8: Paths of chemical functionalization of nanodiamond surface.	21
Fig. 3.9: Functionalization of: (a) carboxyl and (b) hydroxyl groups on Nds.	22
Fig. 3.10: The dependence of the Zeta potential on the pH of the ND colloidal suspension in the case of: (a) Positive Zeta potential; (b) Negative Zeta potential.	23
Fig. 3.11: Schemes of the hydrogen bonding interaction between PVA and ND particles.	24
Fig. 3.12: Scheme of chain reaction occurring during oxidative rancidification – oxidation of double bonds.	25
Fig. 3.13: Graphs comparing the scavenging potentials of aqueous suspensions of the ND in comparison to * $p < 0.05$, ** $p < 0.01$, *** $p < 0.001$ M DPPH.	26
Fig. 4.1: Packaging film used in experiments (made by Plastmoroz, Poland): (a) Packaging film roll; (b) outer side; (c) inner side.	28
Fig. 4.2a: DSC curve of first heating stage.	29
Fig. 4.2b: DSC curve of cooling stage.	29
Fig. 4.2c: DSC curve of second heating stage.	30
Fig. 4.3: Results of the viscosity measurement carried out on a rotational viscometer at a defined share rate of 1000 s ⁻¹ at room temperature of 4% aqueous solutions: polyacrylic acid with a molecular weight of 345,000 (blue) and polyvinyl alcohol with a molecular weight of 25,000 (orange).	31
Fig. 4.4: Raman spectra of carboxylated (ND-N, blue) and hydroxylated (ND-P, red) nanodiamond powders formed after evaporation of water from suspensions.	33
Fig. 4.5: Prepared PVA-based suspensions.	35
Fig.4.6: Prepared PAA-based suspensions.	36
Fig. 4.7: Reaction schemes for esterification of: (a) hydroxylated nanodiamond (ND-P) with poly(acrylic acid); (b) carboxylated nanodiamond (ND-N) with poly(vinyl alcohol).	38
Fig. 4.8: pH values of prepared film-forming suspensions/solutions.	40

Fig. 4.9: Mean values of suspensions/ solutions surface tension determined by Du Noüy ring method (blue) and Pendant drop method (orange).	44
Fig. 4.10a: FTIR spectrum of pure PVA film (without ND, without catalyst).	46
Fig. 4.10b: FTIR spectrum of ND-N/PVA 10 F film (with ND, without catalyst).	47
Fig. 4.10c: FTIR spectrum of ND-N/PVA 10 CAT F film (with ND and catalyst).	47
Fig. 4.11a: FTIR spectrum of pure PAA film (without ND, without catalyst).	48
Fig. 4.11b: FTIR spectrum of ND-P/PAA 10 F film (with ND, without catalyst).	49
Fig. 4.11c: FTIR spectrum of ND-P/PAA 10 CAT F film (with ND and catalyst).	49
Fig. 4.12: Normalized FTIR spectra of PVA-based films.	51
Fig. 4.13: Normalized FTIR spectra of PAA-based films.	52
Fig. 4.14: Relevant bands change in the FTIR spectra of PAA-based films: 1410 cm ⁻¹ and 900 cm ⁻¹ .	53
Fig. 4.15: The mechanism of zinc chloride-catalyzed esterification.	54
Fig. 4.16: Contact angles of test liquids on non-modified and plasma treated LDPE film.	61
Fig. 4.17: Share of individual proportions in the total surface free energy of LDPE film.	62
Fig. 4.18: Contact angles of film-forming suspensions/solutions on non-modified and plasma treated LDPE film presented in column chart.	63
Fig. 4.19: Scratch-test critical loads of prepared coatings on plasma-treated LDPE film.	66
Fig 4.20: CoF values of prepared coatings with highlighted CoF limits for packaging film processing.	68
Fig. 4.21: Prepared laboratory stand for exposure to UV-C radiation to carry out a controlled process of linseed oil rancidity on the modified packaging film.	70
Fig. 4.22: LDPE packaging film covered with ND-P/PAA 100 F coating stuck to aluminum plate.	70
Fig. 4.23: Peroxide Values of tested linseed oils on prepared coatings without (ref) and after UV irradiation in certain time.	74
Fig. 4.24: Peroxide Values increase of tested linseed oils on prepared coatings after UV irradiation in certain time.	75

List of Tables

Tab. 3.1: Stability behaviour of a colloid depending on zeta potential.	16
Tab. 4.1: Specification of used polymer compounds.	31
Tab. 4.2: Specification of used nanodiamond suspensions.	32
Tab. 4.3: List of prepared samples of film-forming suspensions.	34
Tab. 4.4: List of prepared samples of polymer-nanodiamond composite coatings.	34
Tab. 4.5: Operating parameters of plasma generator.	37
Tab. 4.6: List of prepared samples of film-forming suspensions containing catalyst (ZnCl ₂).	38
Tab. 4.7: List of prepared samples of polymer-nanodiamond composite coatings made of suspensions containing catalyst (ZnCl ₂).	38
Tab. 4.8: pH values of used initial nanodiamond suspensions.	39
Tab. 4.9: pH values of prepared film-forming suspensions/solutions.	39
Tab. 4.10: Stability of verified suspensions/solutions and their pH.	41
Tab. 4.11: Surface tension of suspensions/solutions determined by Du Noüy ring method.	43
Tab. 4.12: Surface tension of suspensions/solutions determined by the pendant drop method.	44
Tab. 4.13: AFM Topography images and Phase images of prepared coatings.	57
Tab. 4.14: Surface roughness of prepared coatings.	58
Tab. 4.15: Size and distribution of nanodiamond particles on the surface of prepared coatings.	59
Tab. 4.16: Surface tension and its components of used test liquids.	60
Tab. 4.17: Contact angles of test liquids on non-modified and plasma treated LDPE film.	61
Tab. 4.18: Surface free energy and its proportions of treated and untreated LDPE film.	62
Tab. 4.19: Contact angles of film-forming suspensions/solutions on non-modified and plasma treated LDPE film.	63
Tab. 4.20: Scratch-test critical loads of prepared coatings on plasma-treated LDPE film.	66
Tab. 4.21: Coefficient of friction of prepared coatings on plasma treated LDPE film.	68
Tab. 4.22: Peroxide Values of tested linseed oils on prepared coatings without (ref) and after UV irradiation in certain time.	73
Tab. 4.23: Peroxide Values increase of tested linseed oils on prepared coatings after UV irradiation in certain time.	74